Electrochemical in-situ polymerization of graphene oxide/conducting star copolymer nanocomposite as supercapacitor electrode

UNIVERSITY *of the*
WESTERN CAPE

By

Rugia Ali Elgmati

A full thesis submitted in fulfillment of the requirements for the degree of

MAGISTER SCIENTIAE

In the Department of Chemistry, University of the Western Cape.

Cape Town, South Africa

Supervisor: Prof. Emmanuel Iwuoha

Co-supervisor: Dr. Abd Almonam Baleg

May 2017

ABSTRACT

These days there are deep concerns over the environmental consequences of the rate of consumption of energy from non-renewable sources because of the accelerated increase in greenhouse effect. There is, therefore, increasing interest in research activities on renewable energy systems (*e.g*., supercapacitors, batteries, fuel cells and photovoltaic cells) and their materials. Supercapacitor materials have attracted much attention because of their high energy storage capacity, large surface area, high specific power density (watts/kg) and low cost. The development of advanced supercapacitor devices requires active electrode materials with high storage capacity and dispensability. Graphene oxide-dendritic star copolymer nanocomposites are fascinating as electrode materials, both scientifically and technologically, due to their exceptional properties, including light weight and high potential. They are materials of choice in some applications, such as high-frequency electronics and energy storage. In this research project, a new graphenated conducting dendritic star copolymer nanocomposite was successfully synthesized via in-situ polymerization of a dendritic star copolymer with graphene oxide (GO). Chemical oxidative polymerization of pyrrole and pyrrole-functionalized poly(propylene imine) dendrimer (PPI-2Py) with additional pyrrole monomer (Py) and GO afforded the graphenated-first generation poly(propylene imine)-co-polypyrrole star copolymer (GO-G1PPI-co-PPy). GO-G1PPI-co-PPy was then characterized using Fourier transform infrared spectroscopy (FTIR), thermo gravimetric analysis (TGA), X-ray diffraction analysis (XRD), high-resolution scanning electron microscopy (HR-SEM) and high-resolution transmission electron microscopy (HR-TEM). FTIR showed that the GO sheets and aromatic polypyrrole rings form GO-G1PPI-co-PPy, indicating that the carboxyl

groups from GO acted as efficient dopants in the polymerization. TGA analysis of the synthesized GO-G1PPI-co-PPy showed that the synthesized nanocomposite had higher thermal stability than the star copolymer. XRD analysis of GO-G1PPI-co-PPy showed the complete coating of PPy between the layered GO. HR-SEM images of the GO-G1PPI-co-PPy nanocomposite films showed densely scattered florets of between 100 nm and 1 μm in diameter attached to the GO surface. The electrochemical behaviour of GO-G1PPI-co-PPy was studied by cyclic voltammetry (CV), constant current charge and discharge (CCCD), and electrochemical impedance spectroscopy (EIS) with a 0.07 cm^2 glassy carbon disk electrode (GCE) in 1 M H_2SO_4. The results showed that the GO-G1PPI-co-PPy electrode material had a mass of 3.2×10^{-3} g and improved capacitance on the GCE. The specific capacitance of the GO-G1PPI-co-PPy/GC electrode was 350 F/g and the charge-discharge current density was 30×10^{-6} A within an electrochemical window of -800 to 460 mV. The specific power of the GO-G1PPI-co-PPy electrodes reached 98 KWh/kg at specific energy values of 40 Wh/kg in a three-electrode cell. These values were higher than those for G1PPI-co-PPy, which could only reach 103 F/g, ~48 KWh/kg and 23 Wh/kg. Indications are, therefore, that the incorporation of GO into the G1PPI-co-PPy matrix had a pronounced effect on the electrical conductivity and electrochemical capacitance of the GO-G1PPI-co-PPy nanocomposite.

KEYWORDS

Graphenated-first generation poly(propylene imine)-co-polypyrrole

Graphene oxide

Poly(propylene imine)-co-polypyrrole

Nanocomposite

Electropolymerization

Cyclic voltammetry

Electrochemical impedance spectroscopy

Galvanostatic charge-discharge

Supercapacitors

Supercapacitor cells

Specific capacitors

Specific energy

Specific power

DECLARATION

I declare that "Electrochemical in-situ polymerization of graphene oxide/conducting star copolymer nanocomposite as supercapacitor electrode" is my own work, that it has not been submitted before for any degree or examination at any other university, and that all the sources I have used or quoted have been indicated and acknowledged by complete references.

Rugia Ali Elgmati

Signature:  Date: May 2017

DEDICATION AND ACKNOWLEDGEMENTS

In the name of Allah, the most Gracious and the most Merciful.

Praise be to Allah the Almighty, for thee (alone) we worship and thee (alone) we ask for help. Praise also is upon Muhammad S.A.W. who guided and led us to the right path.

First and foremost, I would like to my very sincere gratitude goes to all my family-I thank my parents (dear mother and dear father) for your love, constant daikm, support and encouragements, and my husband (Salem), extend my thanks and great appreciation to him and my children (Mohamed and Aestbrq) whose presence gladdened my life. I am also indebted to my lovely brothers and sisters in Libya for giving me the strength and support throughout my studies and especially during those hard and discouraging moments in the history of our nation.

I would like to acknowledge and thank the University of the Western Cape for granting me an opportunity to study in my all-time favourite institution. I would like to thank my supervisor, Prof Emmanuel Iwuoha for guiding me all the way and for giving me the opportunity to be part of the SensorLab research group and my co-supervisor Dr Abd Almonam Baleg for your support, advice and mentorship. My appreciation also goes to SensorLab senior researchers and colleagues especially Dr Milua Masikini, Meryck Ward and Lindsay Wilson and all my friends. Thank you all for your great support and friendship. You have indeed been great. Last but not the least, I thank Kassim Badmus, who stood with me throughout the journey of writing this thesis.

TABLE OF CONTENT

LIST OF FIGURES

LIST OF SCHEMES

LIST OF TABLES

LIST OF ABBREVIATIONS

GO-G1PPI-co-PPy	Graphenated-first generation poly(propylene imine)-co-polypyrrole
CP	Conducting polymer
CPs	Conducting polymers
PPI-2Py	Functionalized dendrimer
G1PPI-co-PPy	First generation poly(propylene imine)-co-polypyrrole
GO	Graphene oxide
G1PPI	First generation poly(propylene imine)
PPI	Poly(propylene imine)-co-polypyrrole
PPy	Polypyrrole
PANI	Polyaniline
PEDOT	Poly(3,4-ethylene-dioxythiophene)
2-Py	2-Pyrrole aldehyde
CV	Cyclic voltammetry
ΔEp	Difference in potential peak potentials
GCE	Glassy carbon electrode
EIS	Electrochemical impedance spectroscopy
R_{ct}	Charge transfer resistance
R_s	Solution resistance
Z''	Imaginary impedance

Z’	Real impedance
SC	Specific capacitance
Hz	Hertz
C	capacitance
ECs	Electrochemical capacitors
EDLC	Electrochemical double layer capacitor
Cdl	Double layer capacitance
SCs	Supercapacitors
EDLCs	Energy double layer capacitance
FT-IR	Fourier transform infrared spectroscopy
^{1}H NMR	Proton nuclear magnetic resonance spectroscopy
HR-SEM	High-resolution scanning electron microscopy
HR-TEM	High-resolution transmission electron microscopy
TGA	Themo gravimetric analysis
XRD	X-ray diffraction
DCM	Dichloromethane
$CDCl_3$	Deuterated chloroform
A	Ampere
M	Molarity
m	Mass
F	Farads
CA	Chrono Amperometry

Q	Charge
n	Number of electrons
*e*V	Electron volts
v	Scan rate
Ω	Ohm
η	Coulombic efficiency
Ω	Frequency
∞	Infinity

CHAPTER ONE

INTRODUCTION

1.1- Summary

This chapter covers the research background; supercapacitors and their brief history are introduced. The objectives of this work are stated. The research framework and investigations are also outlined in this chapter.

1.2- Background

Advancements in scientific research output, industrialization, commercialization, and access to good medical facilities and nutrition have contributed significantly to the current high world population growth and energy demands. By the year 2050 the world population would have reached 9 billion (World Economic and Social Development, 2013) [1]. The majority of people will be living in urban settlements with modern facilities. Subsequently, there will be an increase in energy consumption and, by extension, higher pressure on the already saturated energy demand. An international energy agency (WEO, 2007) projected that 55% more energy will be needed by the year 2030 [2]. North America and the Middle East have been identified as the leaders in energy consumption in the term of burning fossil fuels. There is increasing generation of carbon dioxide, methane and other greenhouse gases as a resulting of fossil fuel burning. Currently, 86% of the actual energy demand is met with fossil fuels, while the remaining is met from other sources. Energy consumption is a very important modern economics parameter in the determination of a country's growth and development. Improved technology leads to efficient management of energy, but when the available energy decreases it is very difficult to manufacture good materials for sophisticated energy technologies and

hence the efficiency of energy production technologies decreases further. Energy conservation is an important method of energy management. Research efforts are currently intensifying on how to improve energy conservation and maximum energy storage technologies. There has been much interest in energy storage technologies and many efforts directed at the investigation and development of more efficient batteries, fuel cells and supercapacitors. The battery is very popular energy storage device; it converts the stored chemical energy into electrical energy. The battery cell consists of well-arranged electrodes in an electrolyte, which ensures the exchange of ions while the electrons flow through the external circuit. Model electrodes for battery application should be inexpensive, nontoxic, have high energy and power densities, and last long. A battery ensures maximum energy storage, but its life cycle and shelf life are limiting [3].

Fuel cells can provide stored electrical energy while been recharged continuously. Fuel cells efficiently convert hydrogen and oxygen to electrical energy, heat and water. A fuel cell is an energy storage device with near zero emission. The chemical reaction of fuel cell does not degrade over time, and there is no chemical waste disposal issue, unlike in the case of batteries [4]. It is the environmental friendliness of fuel cells that attracted researchers and investors to its development. Despite the opportunities that fuel cells offer, they are currently very expensive to build; it is costly to maintain the hydrogen infrastructure which supplies coast to coast hydrogen fuel to the system. However, the development of alternative technology for fuel storage and a delivery method may take years of scientific research.

Supercapacitors (SCs), also called ultra-capacitors or electrochemical-capacitors are energy storage devices that employ high surface area electrode materials and thin electrolytic dielectrics to achieve greater capacitances when compared to other energy storage devices

such as batteries, fuel cells and conventional capacitors [5]. Supercapacitors have the ability to maintain a greater shelf-life and longer life cycle with their higher power densities, making them the perfect alternative to batteries and fuel cells. The electrochemical capacitor is an electrical energy storage device that has two electrodes immersed in an electrolyte with a separator between the electrodes much like a battery. The electrodes are known to be fabricated from high surface area, porous material having pores of diameter in the manometer range. The surface area of the electrode materials used in these capacitors is large, usually in the range 500-2000 m^2/g [6]. Charge is stored in the micropores at or near the interface between the solid electrode material and the electrolyte. Capacitance of SCs has proven to be a complication when calculated because of its dependent on complex phenomena occurring at the electrolyte/solid interface of the micropores on the electrode. SCs have found application in many areas that exploit SCs advantages to provide resourceful solutions to a variety of emerging energy applications, especially applications that require instant power applications. Such advantages are long lifetime, low impedance, rapid charging and discharging, cost effective energy storage, high energy density, low voltage, linear discharge *etcetera*. Their high power density makes them perfect for the parallel combination with batteries that have high energy density to push against the hybrid energy storage systems [7-8]. SCs have found application in computer systems, uninterruptible power source systems, power conditioners, welders, inverters, automobile regenerative braking systems, power supplies, power back up in laptops, mobile phones, digital cameras and power generators. The main purpose of this work is to develop a high charge storage material that synergistically combines both the characteristics of the electric double layer capacitors (EDLCs) and a pseudocapacitor by synthesis and characterize the supercapacitor using of graphene stabilized dendritic star copolymer nanocomposites. A combination of graphene stabilized dendritic star copolymer

nanocomposites can give higher capacitance and energy storage.

1.3- Problem statement

Presently, as the movement for environmental protection is increasingly dominant and the rapidly increasing oil price is an undeniable reality, this brings in enormous amount of research interest in the development of alternative energy and energy storage/conversion devices with high power and energy densities. New and advanced materials are therefore essential to cope with these new trends for clean and renewable energy. There are several technologies available for the reliable energy storage, like pumped hydroelectric, compressed air, batteries, fuel cell, flow batteries, solar fuels, flywheel, superconducting magnet and capacitor. Among these technologies, electrochemical systems such as high density batteries and supercapacitors have several important advances over the others so become more appealing [9].

Supercapacitors have better reversibility and longer life cycles than batteries, and possess higher energy density as compared with conventional capacitors. Therefore SCs become increasingly important in the fields of power source especially in small scale application like memory protection in several electronic devices. SCs have attracted considerable attention over the past decades because of their higher power density and longer cycle life than secondary batteries and their higher energy density compared to conventional electrical double layer capacitors. To develop an advanced SC device, an active electrode material with high capacity performance is indispensable. From the materials point of view, porous carbon materials, conducting polymers, and transition-metal oxides are fundamental candidates used as SC electrode materials.

Much research has therefore gone into supercapacitors. This is the main reason why supercapacitors are the main focus of this thesis. One of the most powerful aspects of conducting polymers are their ability to be nanostructured through innovative synthetically manipulated transformations, such as to tailor the prepared polymers for more specialized applications. In an era where the dependence on nanotechnology is rapidly proliferating in virtually every aspect of humanity of particular interest is innovative hybrid polymeric-dendrimer.

1.4- Aims and objectives of the study

This study is to prepare and characterize novel conducting dendrimeric star copolymers which have a central poly(propylene imine) (PPI) dendrimer core with conducting polypyrrole chains extending from the core. Polypyrrole (PPy) exhibits good electrical conductivity and high air stability and is a potentially useful conductive polymer. Polypyrrole, one of the most studied conducting polymers has been used in a wide range of technological applications in several areas such as secondary batteries, electrochromic display devices, light-emitting diodes, capacitors, sensors, membranes, and enzyme electrodes therefore we intend exploiting some of its unique features in this study. The ultimate goal is to develop supercapacitors which will provide a superior alternative to lithium ion batteries which are known to multifunction and are not so stable as portable devices. Herein we intend develop a cheap yet stable, portable device capable of storing energy for lengthy periods of time.

The objective of this work is to use graphene-poly(propylene imine)-co-polypyrrole nanocomposites materials to develop flexible and high performance supercapacitor electrode system.

Specific objectives:

- Synthesis of graphene oxide (GO) by modified Hummers method will be using graphite, H_2SO_4 and $KMnO_4$.
- Synthesis of G1PPI-co-PPy star copolymers will be by polymerization PPI-2Py with Py monomer.
- Synthesis of the graphenated conducting dendrimeric star copolymers nanocomposite for supercapacitors by polymerization PPI-2Py with Py monomer/GO.
- Preparation of the electrode of GO-G1PPI-co-PPy nanocomposites will be using electrochemically copolymerize PPI-2Py with Py/GO in H_2SO_4.

To develop and characterize the novel graphenated conducting dendrimeric star copolymers GO-G1PPI-co-PPy based nanocomposites for supercapacitors.

The physical characterization of the graphenated conducting dendrimeric star copolymers GO-G1PPI-co-PPy based nanocomposites by techniques Fourier transform infrared spectroscopy, thermo gravimetric analysis, X-ray diffraction, high- resolution scanning electron microscopy, and high-resolution transmission electron microscopy.

Electrochemical characterization will be performed using chronopotentiometry, cyclic voltammetry and electric conductivity measurements will be done by electrochemical impedance spectrometry.

1.5- Research framework

The first task was to identify the best methods and conditions to prepare the GO. Two batches of GO were to be synthesized using the same method and conditions to ensure that the GO had no impurities and to avoid agglomeration. The GO was then to be functionalized with

dendritic star copolymer have been incorporated on the GO. It also controls the particle size and avoids agglomeration.

The second task was to characterize the physical properties like size and morphologies of graphene oxide and the functionalized graphene oxide using analytical methods. This gives an insight to the electrochemical behavior of the nanostructure and will help to optimize the preparation conditions and to compare the graphene oxide to the graphene oxide-dendritic star copolymer.

The third task was to synthesize palladium nanoparticles/nanocomposites using various synthesis techniques. The prepared nanoparticles and nanocomposites were to be mounted on the graphene oxide-dendritic star copolymer.

The fourth task was to characterize the composite materials using FTIR, TGA, XRD, HR-SEM, and HR-TEM.

The last task was to construct and test SCs electrodes and SC cells using potentiostatic galvanostatic constant current charge-discharge in 3-electrode cell configurations in aqueous electrolyte.

1.6- Thesis outline

Chapter 2: The literature review involves the introduction of SCs *e*.g., EDLC, pseudo capacitive and hybrid supercapacitors. It also involves the main materials used in this work; GO its unique properties and as a material of SCs. Conducting polymers (CPs) also reviewed in this chapter. SCs have many applications and South Africa just like other countries is making use of them. Therefore, applications of SCs in South Africa have also been included in this review chapter.

Chapter 3: The main components of this chapter are the synthesis methods employed to obtain the nanomaterials required and the characterization techniques employed to synthesis the materials. It also outlines the type of materials used.

Chapter 4: This chapter presents and discusses results of the synthesis of graphenated-poly(propylene imine)-co-polypyrrole nanocomposites by discussions of the morphological and electrochemical studies of the materials by HR-SEM, HR-TEM, FT-IR, TGA, XRD, CV, and EIS, characterization of SC cells is discussed.

Chapter 5: Conclusions with a brief discussion of the objectives achieved in relation to the study of graphenated-first generation poly(propylene imine)-co-polypyrrole nanocomposites SCs. Recommendations for possible future work are presented and discussed.

CHAPTER TWO

LITERATURE REVIEW

Electrochemical in-situ polymerization of graphene oxide/conducting star copolymer nanocomposites as supercapacitor electrodes

2.1- Summary

In this chapter a literature reviews of supercapacitors, their advantages over batteries, fuel cells and conventional capacitors**.** And highlighting the materials used for the fabrication of the supercapacitor electrodes, their mechanical, electronic, optical, electrical properties, conductive, *etc*. This chapter also covers the synthesis methods that have been used in literature to produce these materials. We also learn the specific capacitance that these materials give out when they are used in the fabrication of the supercapacitor electrodes.

2.2- Supercapacitors

Supercapacitors, also called ultra-capacitors or electrochemical capacitors, are energy storage devices that employ high surface area electrode materials and thin electrolytic dielectrics to achieve greater capacitances when compared to other energy storage devices such as batteries, fuel cells and capacitors. Batteries are known to maximize the efficiency of energy use. Model electrodes for battery application should have high energy, densities, long life span, and be cost effective and nontoxic [10].

A short life cycle and shelf life are the greatest challenges of battery devices [2, 11]. Conversely, supercapacitors have the ability to maintain a greater shelf life and longer life

cycle with their higher power densities, making them very good alternates to batteries.

The electrochemical capacitor is an electrical energy storage device that has two electrodes immersed in [12]. Good electrodes are usually fabricated from high surface area and porous material with pores diameter in nanometer range. The surface area of the electrode materials used in the capacitors is large; usually in the range 500-2000 m^2/g^3. Charge is stored in the micropores at or near the interface between the solid electrode material and the electrolyte. Capacitance of SCs have proven to be a complication when calculated because of its dependent on complex phenomena occurring at the electrolyte/solid interface of the micropores [13]

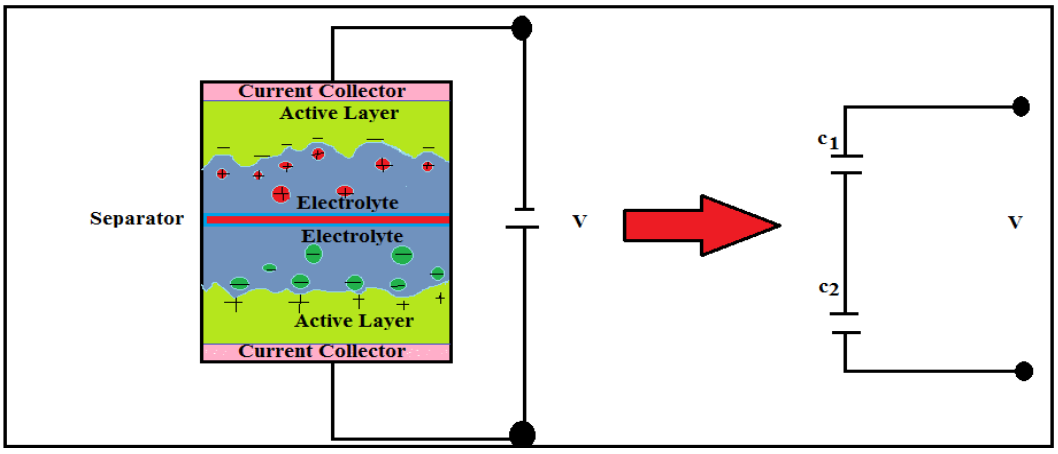

Figure 2.1 Typical schematic representation of the main elements of a supercapacitor [12].

In the electrode, the stored capacitance is directly proportional to surface area, A of one plate and inversely proportional to the distance of separation between the two plates as presented by the equation (2.1) below.

– (2.1)

– – (2.2)

The two attributes of SCs are its high energy and power intensity. The energy, stored in a capacitor is directly proportional to its capacitance, C and is also a factor of potential difference, V (2.2).

The power, P is the energy expended per unit time. To determine the power of a SC one must consider the fact that they are represented as circuits in series with external resistance R in which external components of a SCs current collector, electrodes and dielectric material, has a high contribution to the resistance and the measured power is given by the equation (2.3).

— (2.3)

The performance of supercapacitors compared to conventional capacitors, batteries and fuel cells is demonstrated using a Ragone plot given in Figure 2.2. The Ragone plot demonstrates that supercapacitors have higher specific energy than conventional capacitors, but much lower specific power as compared to them. It also demonstrates that supercapacitors have less specific energy compared to batteries and fuel cells, but attain higher specific power.

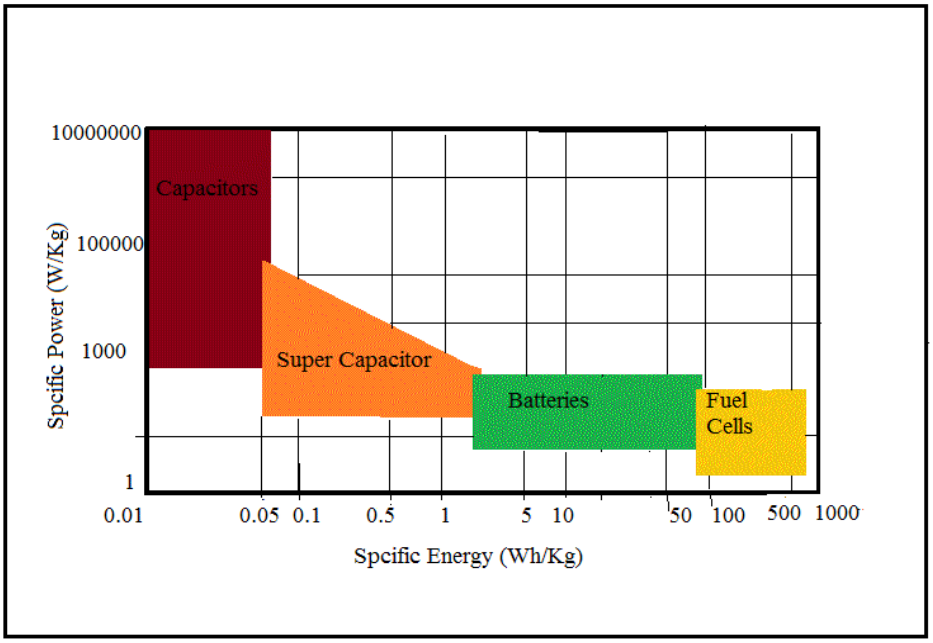

Figure 2.2 Ragone plot [14].

2.3- Types of supercapacitors

Supercapacitors can be divided into three general classes; electrochemical double-layer capacitors, pseudo capacitors, and hybrid capacitors. Each class is characterized by its unique mechanism for storing charge. These are respectively, non-Faradaic, Faradaic, and a combination of the two. Faradaic processes, such as oxidation-reduction reactions involve the transfer of charge between electrode and electrolyte. A non-Faradaic mechanism, by contrast, does not use a chemical mechanism [15]. Rather, charges are distributed on surfaces by physical processes that do not involve the making or breaking of chemical bonds. SCs have found application in many areas that exploit its advantages to provide resourceful solutions to a variety of emerging energy applications, especially applications that require instant power supply. Such advantages are long lifetime, low impedance, rapid charging and discharging, cost effective energy storage, high energy density, low voltage, linear discharge, *etc*. Their high power density makes them perfect

for the parallel combination with batteries that have high energy density to push against the hybrid energy storage systems. SCs have found application in computer systems, Universal power supply systems, power conditioners, welders, inverters, automobile regenerative braking systems, power supplies, power back up in laptops, mobile phones, digital cameras, iPhone and power generators.

2.3.1- Electric double layer capacitance

Similar to conventional electrostatic capacitors, charge storage in electric double layer capacitors is largely electrostatic in nature. Instead of charges accumulating on two conductors separated by a dielectric as in conventional capacitors, forms on the charged electrode, and the other layer comprised of ions forms in the electrolyte giving rise to the double layer formation. The thickness of double layer or the separation of charges is very small, on the order of several Angstroms. An estimate of the specific capacitance of such a double-layer can be obtained using equation (2.4)

(2.4)

where C is the capacitance, A is the surface area, **ε** is the relative dielectric constant of the medium between the two layers (the electrolyte), and δ is the distance between the two layers N (the distance from the electrode surface to the center of the ion layer)

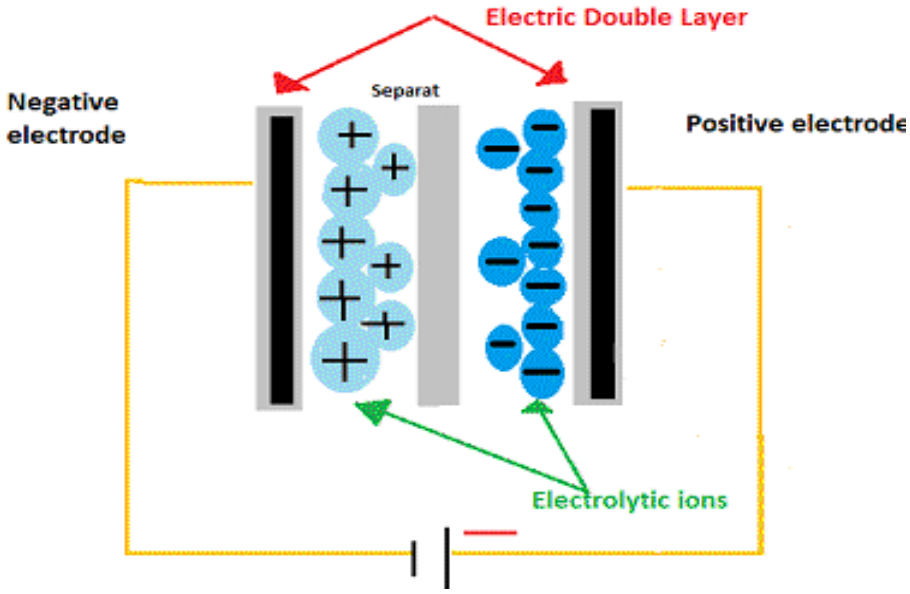

Figure 2.3 Schematic representation of electric double layer supercapacitor [16].

In terms of the charges Δq that are accumulating across electrode electrolyte interphase to extents the potential difference built up across the interphase, ΔV, the double layer capacitance can be expressed as

$$C = \frac{\Delta q}{\Delta V} \quad (2.5)$$

EDLCs are constructed by two electrodes immersed in an electrolyte with an ion permeable separator placed between the electrodes in order to prevent electrical contact, but still allow ions from the electrolyte to pass through. The ions in the pores of the active material create the double layer by diffusion. As a result, at each electrode/electrolyte interface, there is one double-layer present. In addition to the capacitance that arises from the separation of charge, sometimes a small Faradaic contribution to the double-layer capacitance can be made from electrochemical surface reactions (reversible surface quinonoid-type redox reactions or chemisorption's processes) that can occur on the surface of the carbon electrode [17]. Since the thickness of the double layer is very small,

a fraction of a nm, capacitance values of 15-50 μF/cm^2 are possible with the EDLCs. Moreover, by utilizing high surface area of materials (~1000 m^2/g), large capacitances of 150-300 F/g are practically attainable [18]. Since the double layer capacitance does not involve any phase transition mechanism as in batteries, charging-discharging is highly reversible, rapid and hundreds of thousands of cycles are typically achievable with a given element.

2.3.2- Pseudocapacitors

The energy storage mechanism, which involves the effect of the ions flow due to the change in electrochemical state of the material, is called faradic process *e. g*, in batteries the chemical energy is being carried out by flow of ions when the potential is applied across the two electrodes of battery. The capacitance in pseudocapacitor depends on the fast and reversible faradic reactions occurring on the electro active materials of electrode surface at the appropriate potentials which assists in fast charge-discharge rate and high reversibility.

In pseudocapacitor, the charge transfer occurs across the double layer of the electrode and electrolyte interphase, the energy storage mechanism in pseudocapacitors is indirect and to some extent analogous to battery charging and discharging principle. The pseudocapacitance is then calculated by as described in literature [19]. The cause of developing pseudocapacitance depends on the four types of electrochemical reactions (a). It may be developed due to the redox reactions of ions adsorption on the electrode surface from the electrolyte: (b) redox reactions develop due to changes in the oxidation state of transition metals, *e.g.*, RuO_2, MnO_2, and IrO_2 used as the active electrode material; (c) doping of the conducting polymer material also gives rise to reversible redox reaction and

thus build pseudocapacitance; and (d) the self-discharge degradation of the supercapacitor due to irreversible reactions. The charge movements in the above electrochemical faradic reactions are voltage dependent, which is the same to charging-discharging in batteries [19]. Many factors can influence the pseudocapacitance *e.g*., the porosity of materials, particle sizes, conductivity of electrode materials, as well as the surface area of the electrode, packing of electrolyte, design of cell, *etc*. Generally the pseudocapacitance shows 10 times more capacitance than the electric double layer capacitance, on the other hand it has some draw backs *e.g*., lifecycle and reliability of a device [20-21]. During the oxidation and reduction of these materials, the insertion and removal of counter ions from an electrolyte solution to the electrode surface helps in maintaining the charge neutrality. Another important difference between pseudocapacitors and electrochemical double layer capacitors is that the entire mass of the material is used to store charge. In the following sections are the types of capacitor based on pseudocapacitance mechanism are discussed.

2.3.2.1- Types of pseudocapacitors

So far three types of pseudocapacitors are widely known. In the following section these three types are discussed.

(a) Type I

In type I both super capacitor electrodes are fabricated from identical material. Usually the capacitor either is comprised of the same p type conducting polymer, or both electrodes can be made of the same n type conducting polymers and transition metals. This type of pseudocapacitor is called symmetric capacitor. The capacitance in this type of supercapacitor depends on the individual capacitance of each electrode, which is given [22].

Where is the overall capacitance of the cell, which is calculated by adding the individual capacitance of two electrodes in series. Since, both electrodes are alike, so C2, this means that the same amount of charge is utilized by each electrode for doping or non-doping of the electrode materials. However this type of capacitor is limited in capacitance and has a narrow potential window [23]. Besides the window than type I. Configuration of type II supercapacitor is known as an asymmetric device. This device could have the hybrid system based on the composite material consisted of transition metals, *e.g*., RuO_2, IrO_2, MnO_2, Ce_2O_3 and even non-redox carbon materials (activated carbon, graphite, carbon nanotubes, porous carbon, *etc*.) combined with p or n type conducting polymers [23].

(b) Type II

Supercapacitors have greater capacity than type I, using different p, n type polymer electrodes. In this type the capacitance participation and the amount of charge utilized in overall capacitance of each electrode is not the same. Type II is due to higher working cell voltage and shows the increase in energy density and is the most common type in practical use today [24].

(c) Type III

Configuration of the type III is different from type I and type II capacitors, as it is based on two of the same or different conducting polymers with one of the electrodes comprised either of an n type or p type doped polymer. Due to having both electrodes in its doping states, it provides the less resistance, large voltage window and high specific capacitance [25].

2.3.3- Hybrid capacitor

In order to exploit the full advantages of EDLCs and pseudo capacitors improvements in the overall performance of a device, the third type of capacitor was attempted, which is called hybrid capacitor. The hybrid system renders higher power and energy density without sacrificing the cycle stability and life of the device since the energy storage mechanism in hybrid systems depend on both faradic and non-faradic processes. In a hybrid system, electrode configurations are based on either composite electrodes (which are integrated with carbon-based materials, conducting polymer) or metal oxide materials lead the benefit of physical and chemical charge storage mechanisms together in a single electrode [26]. The coupling of carbon based material electrodes with pseudo capacitor electrodes has gained an immense importance due to substantial enhancement in total capacitance of the device.

2.4- Graphene

Graphene is one of the allotropes of carbon with an indefinite large aromatic molecule. It has a single atomic layer of carbon atoms in a sp^2 hexagonal bonding configuration (typical of group IV family).They predominantly form covalent compound by making use of their tetravalent property. Graphene is a basic structural element of all the other allotropes of carbon like charcoal, carbon nanotube, fullerenes, and graphite. The thin atomic size and sp^2 hybridization give graphene it peculiar properties of high conductivity, mechanical strength and heat conduction. The properties and possible applications of graphene based materials depend greatly on their synthesis procedure (mechanically or chemically generated) [27]. Both the mechanical exfoliation and the high-temperature growth techniques can produce high quality graphene with low

throughput but at an high cost [28]. In contrast, the chemically derived approach yields high throughput graphene with graphitic defects at a low cost [28]. An electrochemical performance analysis of mechanically and chemically derived graphene demonstrates that pristine graphene has a lower catalytic activity than graphene oxide or bulk graphite [29]. GO has emerged as the cost effective and mass production precursor of graphene based material. GO consists of a single-layer of GO. It is usually produced by the chemical treatment of graphite through oxidation, with subsequent dispersion and exfoliation in water or suitable organic solvents [30-31]. With respect to its structure, there have been several structural models [32] proposed over the years. These assume the presence of various oxygen containing functional groups in the GO. The oxygen functional groups have been identified as mostly in the form of hydroxyl and epoxy groups on the basal plane, with smaller amounts of carboxyl, carbonyl, phenol, lactone, and quinone at the sheet edges [33]. Currently, the precise atomic structure of GO is still uncertain and remains to be fully elucidated. This is primarily due to the uncertainty pertaining to both the nature and distribution of the oxygen containing functional groups, its nonstoichiometric atomic composition, and the lack of sufficiently sensitive analytical techniques for characterizing the GO structure [34].

Low agglomeration (high dispersal) of GO in different liquid matrixes compare to graphite oxide give it an advantage in the modification of its structure by ceramic or polymer matrix for an enhanced mechanical or electrical property. The intended application of GO will however determine the medium of modification.

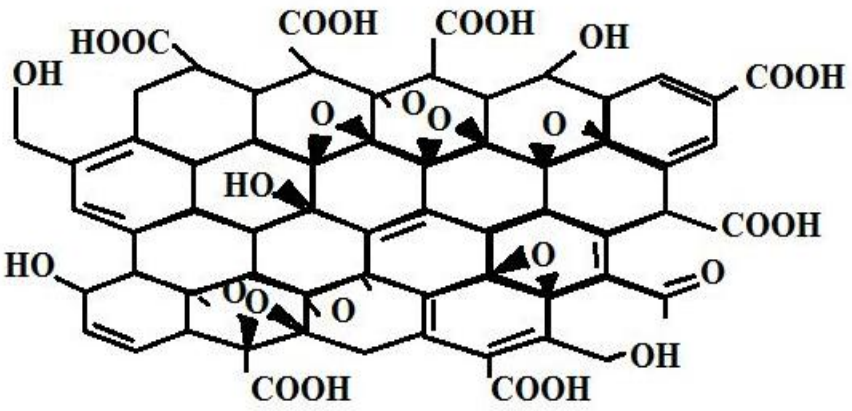

Graphene Oxide

Figure 2.4- Chemical structure of graphene oxide [35].

2.4.1- Synthesis of graphene oxide

The first synthesis of graphene oxide was prepared by the micromechanical cleavage of from highly ordered pyrolytic graphite [34]. In this synthesis method, a layer is peeled off from the graphite using scotch tape and then transferred on to the silicon substrate [36-37]. The common method used for preparation of graphene oxide is the simple and modified Hummers method (graphite, H_2SO_4, $KMnO_2$, H_2O_2) and (KMn_4, $NaNO_3$, H_2SO_4), respectively. The Hummers method [38] uses a combination of potassium permanganate with sulphuric acid. Permanganate is widely used as an oxidant but the active site is the dimanganese heptoxide. The formation of dimanganese heptoxide from potassium permanganate in the presence of a strong acid is as follows:

(2.6)

(2.7)

The simple H_2O_2 Hummers method involves treating graphite with potassium

permanganate and sulphuric acid, with water added and the whole reaction taking place in an ice bath. This is then followed by the addition of hydrogen peroxide whose function is to stop the gas production that comes out of the reaction. The modified Hummers method involves treating graphite with sodium nitrate and sulphuric acid under constant stirring. After an hour potassium permanganate is added into the reaction keeping the temperature less than 20 °C to prevent overheating and the evolution of gases. The mixture is then stirred at 35 °C for 12 h and the resulting solution is diluted by adding 500 mL of water under vigorous stirring. To ensure the completion of reaction with $KMnO_4$, the suspension is further treated with 30% solution (5 mL).The resulting mixture is washed with HCl and H_2O respectively, followed by filtration and drying, graphene oxide sheets were thus obtained [39]. Researchers are attempting to come up with better synthesis methods of graphene oxide and Marcano *et al.* [40] has come up with an improved synthesis method of GO. In their method instead of using the sodium nitrate, increasing the amount of $KMnO_4$, and performing the reaction in a 9:1 mixture of H_2SO_4/H_3PO_4 improves the efficiency of the oxidation process. This improved method provides a greater amount of hydrophilic oxidized graphene material as compared to Hummers' method or Hummers' method with additional $KMnO_4$. The improved method is advantageous over the Hummers method. The protocol for running the reaction does not involve a large exothermic and produces no toxic gas. Moreover, the improved method yields a higher fraction of well oxidized hydrophilic carbon material [40-41].

2.5- Conducting polymers

Among the synthetic polymers, conducting polymers have attracted considerable attention as important polymer materials since the initial discovery of polyacetylene in the late

1970s [43]. Inherently conducting polymers (ICPs) have the conjugated double-bonded backbone that provides the electronic conductivity after doping with suitable dopants. In general, ICPs are semiconductors with versatile properties and various applications. These peculiar characteristics have an impact on the discovery of vast conducting polymers by means of different synthetic methods. Numerous research papers have been published concerning a variety of the synthesis, physical and chemical properties and application of conducting polymers [44]. On the other hand, this study focused on the recent achievements of the synthesis and application of CPs as electrode materials for supercapacitors. Various carbon materials have been considered for supercapacitor electrodes and a great attention now is also focused on conducting polymers. This can be attributed to the fact that carbon materials only possess double-layer capacitance, while metal oxides and conducting polymer also possess Faradaic capacitance. Generally, the Faradaic capacitance is 10-100 times higher than double layer capacitance [45].

Conducting polymers represent a very interesting family of synthetic metals due to a high doping level and a fast electrochemical switching. The possible application of CPs in electrochemical capacitors is dictated by their significant capacitance values [46]. As opposed to activated carbons where only the surface is used for charge accumulation, in CPs, the total mass and volume is involved in charge storage. Figure 2.5 among the electrically CPs, great attention has been given to polyaniline (PANI), polythiophene (PT), poly-(3,4-ethylenedioxythiophene) (PEDOT), and polypyrrole (PPy).

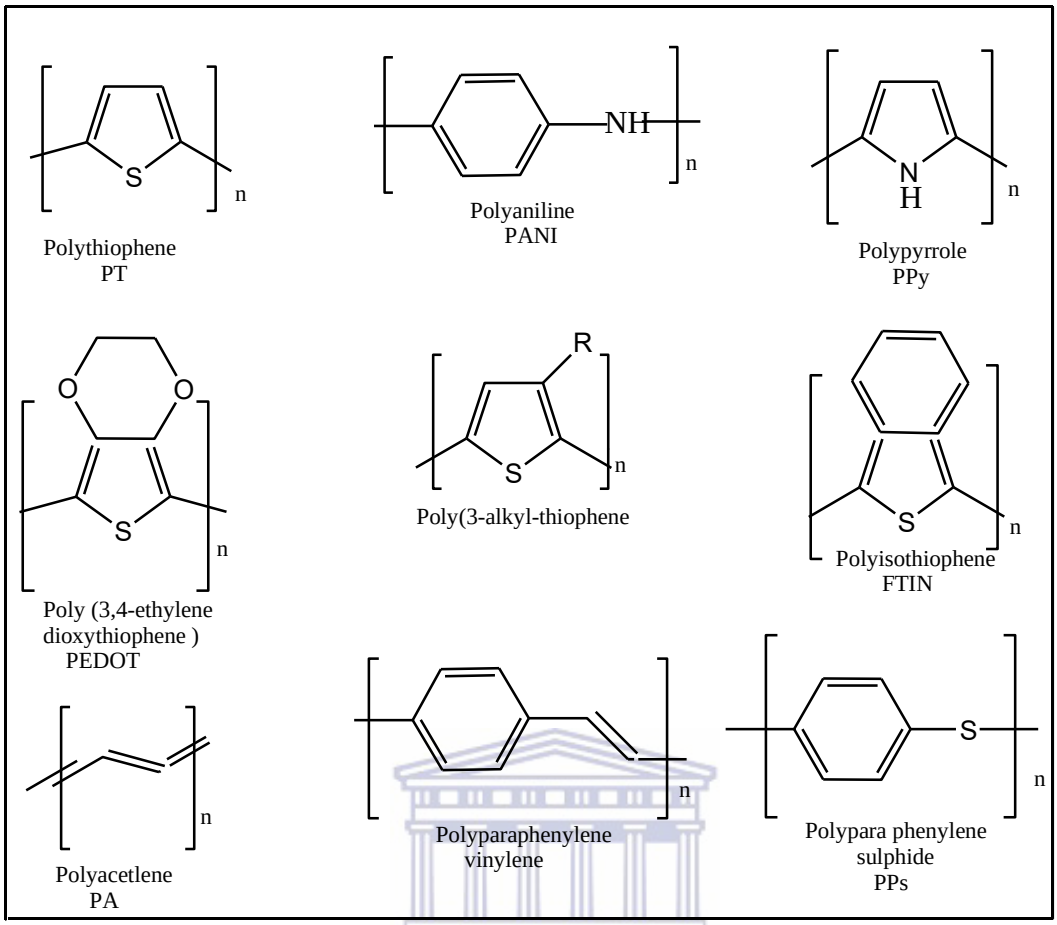

Figure 2.5- Chemical structures of some of conducting polymers [47].

2.5.1- Synthesis of conducting polymers

Conducting polymers can be prepared using chemical and/or electrochemical methods of polymerization. Although the most common method of synthesizing redox conducting polymers is chemical polymerization, both methods have their comparable advantages and disadvantages.

Tables 2.1: Comparable advantages and disadvantages of chemical and electrochemical polymerization of CPs [48]

Polymerization method	Advantages	Disadvantages
Chemical polymerization	-Possibility of large-scale production. -Flexibility of the procedure *i.e*. Postmodification of bulk CPs or options to modify CP backbone covalently. -Simple procedure, does not require complicated electrochemical setup -Aqueous solution can be used as polymerization medium.	-Thin film fabrication. -Relatively poor control of polymer's morphology -Required binder materials in film fabrication
Electrochemical polymerization	-Possibility of thin film synthesis. -No difficulty in the synthesis procedure. -Entrapment of molecules in CPs. -Doping is simultaneous.	-Difficult to remove film from electrode surface. -Post-covalent modification of bulk CPs is difficult. -Requires electrochemical setup.

Various methods are available for the synthesis of conducting polymers [49]. However, the most widely used technique for the synthesis of conducting polymers is the oxidative coupling involving the oxidation of monomers to form action radical followed by the coupling to form di-cations and this repetition finally leads to formation of the polymer. Electrochemical synthesis is rapidly becoming the preferred general method of synthesizing conducting polymers because of its simplicity and reproducibility [50]. Other advantages of electrochemical polymerization reactions are that it can be carried out at room temperature and by varying either potential or current with time, the thickness of the film can be controlled. Electrochemical synthesis can be used to prepare free standing, homogenous and self-doped films [49]. The electrochemical synthesis of

conducting polymer is an electro-organic process rather than an organic electrochemical one because much emphasis is on the electrochemical process rather than organic synthesis. Electrochemical techniques employed in the polymerization of conducting polymers on the electrode surface are; pulse, galvanostatic, potentiostatic or sweeping techniques [51]. However, potentiodynamic techniques are preferred because of the homogenous film produced and strong adherence of the film to the electrode surface [50].

2.5.1.1-Electrochemical oxidation polymerization of conducting polymers

The electrochemical preparation of conducting polymers is usually carried out through oxidative polymerization of their corresponding monomers by constant current, constant potential, or CV in a potential range. The electropolymerization is performed in an electrolyte solution which contains solvent, electrolyte salt, and the monomer. There are many factors influencing the electropolymerization processes, such as solvents, supporting electrolyte salts, concentration of the monomers, and pH value of the electrolyte solutions, as well as polymerization potential, current, temperature, *etc*. Among these factors, the polymerization potential of the monomers is the most important. Lists the oxidation polymerization potentials of the most important monomers pyrrole, aniline, and thiophenes [50-51]. The lower oxidation polymerization potentials of pyrrole and aniline make the electropolymerization of polypyrrole and polyaniline easier, and it can be performed in aqueous solutions.

2.5.1.2- Chemical polymerization of conducting polymers

The chemical oxidation preparation of conducting polymers is performed in solution by using oxidants such as $FeCl_3$ and ($(NH_4)_2S_2O_8$), *etc*., and it is easy to enlarge the

production scale with the chemical polymerization. Chemical polymerization is the most important method for the preparation of polyaniline, and it can also be used to produce conducting PPy.

Conducting polymers can store charges not only in the EDLCs but also through the rapid faradic charge transfer (pseudocapacitance). As a result, the specific capacitance of CP electrodes is higher than that of EDLCs based on carbon electrodes [53]. However, one of the drawbacks for CPs as supercapacitor electrodes is their poor cycling stability because CPs is usually brittle and weak in mechanical strengths. Coupling CPs to a carbon material has been shown to be an effective approach to improving the cycling stability of the CPs [54].

2.5.2- Conducting star copolymers

Star copolymers are a class of branched macromolecules that have a central core to which multiple linear polymer chains are attached. The 3D structure with extended conjugated linear polymer chains give star copolymers properties that are different from the typical 2D, linear polymers. Conducting star copolymer materials are particularly useful as coatings because of their spheroidal structure and their ability to pack in three dimensions [55]. The conducting star copolymers are used in their undoped state for applications in which the conductivity requirements are not too high, for example static dissipation, or where the optical property of the polymer coating is of chief importance, for example as a pigment or reflective layer. Materials with conductivities in the range 10^{-6} to 1 S/cm may be suitable for these purposes. Furthermore, the conducting chains, surprisingly, can provide sufficient intermolecular overlap to give solid materials with electrical higher than the corresponding linear, non-star-conducting polymers [56]. For example, nylon-6

with a star structure has a melt viscosity and crystallization halftimes that are substantially reduced by the branching [57]. The regular 3D structure of star copolymer gels combines the properties of hardness and flexibility and is being investigated to make materials that are hard without being brittle [56]. The combination of star copolymer and conducting polymer structures open up an approach to making materials that have the favourable properties of both, *i.e.*, improved process ability and electrical conductivity. Improved process ability results from the spheroidal structure of hyper branched, dendrimeric and starburst polymers. A conducting star copolymer may be constructed in which two or more different conjugated arms radiate from the central core [58]. Doping of the conducting star copolymers to increase the electrical conductivity may be achieved using methods of prior art applicable to the conjugated radiating chain moieties. For conjugated chains based on Py or thiophene units or derivatives there of doping may be achieved by treatment with oxidizing agents such as iodine, ferric chloride, ferric tosylate, gold trichloride, antimony chloride reference. If the polymer side chains are composed of PANI, doping can be achieved by treatment with acid [58-59]. Doping can also be achieved electrochemically by confining the polymer to an electrode surface and subjecting it to an oxidizing or reducing potential in an electrochemical cell. In this way, doped thin films on conducting substrates are obtained. The electrolyte provides a source of charge compensating ions flowing in and out of the film accompanying the oxidation or reduction reaction. Applications of conducting polymers in batteries, supercapacitors and electro chromic displays frequently entail doping of the polymer by such an electrochemical process [32].

2.5.3- Dendritic polymers

Dendritic polymers belong to a new class of synthetic macromolecules possessing a regular branched tree-like structure whose conduction path is along the π-stack [61]. The π-stack are formed in contrast to the traditional conducting polymer where the conducting path is based on alternating the single and double bond p-conjugated organic system [61], Dendritic polymer conductivity is isotropic rather than anisotropic as usually observed in other conductive layered systems because the dendritic structure can form the p-stack in three dimensions. The field of dendrimer has been expanded greatly in recent years due to their justifiable assurance of being used in variety of applications. One of the progress in dendrimer based sensor system is the use of hybrid dendrimer containing encapsulated metal or the preparation of dendritic star copolymer which makes them useful for application in catalysis and electro catalysis [60-61]. The formation of dendritic star copolymer with conducting polymers such as polyaniline, polythiophene and polypyrrole result in lead to the nano structurization of the product due to elongation of the conjugation chain and unhindered π-stacking of the polymer molecule by the dendrimer [62]. It also leads to improved processibility and electrical conductivity of the product [64]. When compared to linear chain polymer, spherical polymers can provide a material with reduced viscosity and melting point, higher solubility and enhanced substrate penetration as coating. Dendrimeric star copolymers are novel type of molecular architectures in which many linear homo or block copolymer chains are attached to a dendrimer core [64-65]. The preparation of dendrimer-star copolymer involves two general processes. The first process involves linking a monofunctional linear polymer onto the dendrimer surface [67], while the other process involves the growth of arm

polymer chain from the surface of dendrimer by 'controlled/living' polymerizations such as anionic polymerization [66], ring-opening polymerization (ROP) [68] and atom transfer radical polymerization (ATRP) [69]. Synthesis of hybrid dendrimer-star copolymer through the reversible star addition-fragmentation transfer (RAFT) polymerization process has been reported by Zheng and Pan [69-70]. Wang and coworkers reported a conducting star-shaped copolymer consisting of a regioregular poly(3-hexylthiopene) arm attached to a polyphenylene dendrimer core [72]. Miller [73] and Tomalia [74]. Reported the conductivity of polyamidoamine dendrimers modified with cationically substituted naphthalene diimides

2.5.4- Poly(propylene imine) dendrimers

Poly(propylene imine) dendrimers stand for "poly(propylene imine)" describing the propylamine spacer moieties which is the oldest known dendrimer type developed initially by Vögtle [75]. These dendrimers are generally poly-alkyl amines having primary amines as end groups, the dendrimer interior consists of numerous tertiary tries-propylene amines. PPI dendrimers are commercially available up to G5. In addition, these dendrimers are also sometimes denoted "DAB-dendrimers" where DAB refers to the core structure, which is usually based on daimio butane [76]. As an alternative name to PPI, POPAM is sometimes used to describe this class of dendrimers. POPAM stands for poly(propylene amine), which closely resembles the PPI abbreviation. The combination of hydrophilicity, highly branched structure and chemical functionality makes poly(propylene imine) dendrimers very interesting building blocks to obtain well-defined amphiphilic superstructures. Dendrimers have gained a growing scientific interest as building blocks in new molecular architectures [76-77].

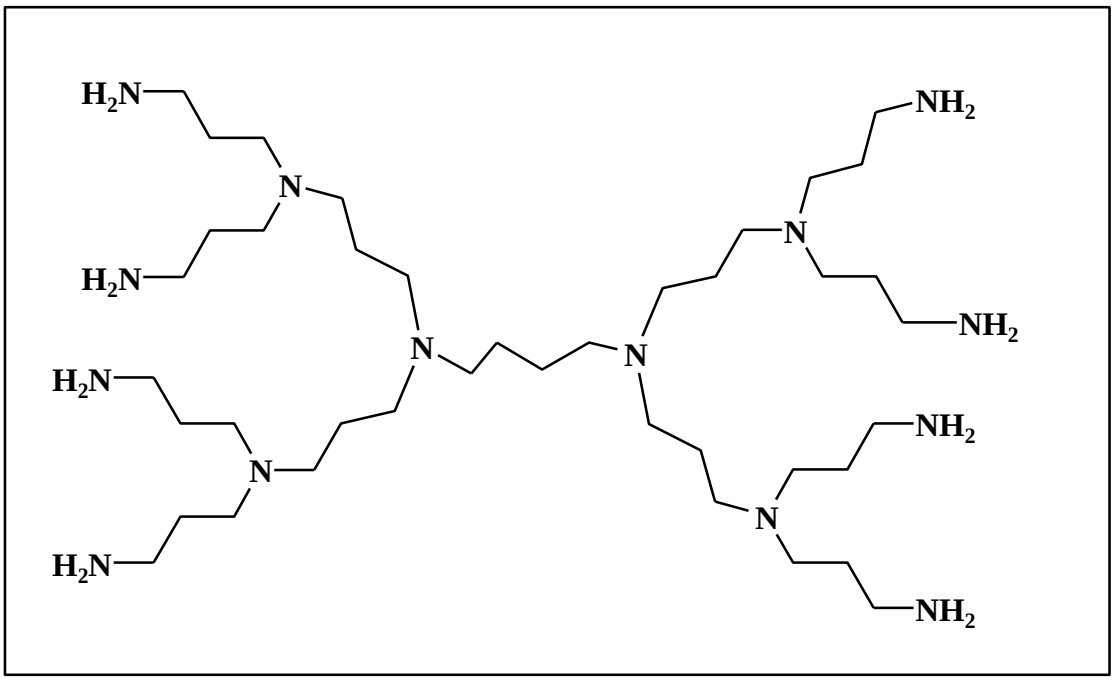

Figure 2.6- Structure of poly(propylene imine) (PPI) dendrimer [79].

The physical and chemical properties of dendrimers are determined by the shape and multiplicity of the core and building blocks and by the size and shape of the end groups, in addition to their chemical [80], it offer us not only the possibility to change the size and molecular weight of the molecule by choosing different generations, but they also allow us to access new molecular structures and self-assembling systems that can be designed to perform one specific function, however the organized structure of dendrimer, ease of modification, and strong adsorption behaviour to a variety of substrates, PPI dendrimers can be used to produce monolayers or stacked film layers, which can be used as sensors to detect hazardous chemical material [81].

Dendrimers are of interest for their unusual physical properties. An important feature of dendrimers is that their viscosity in solution and in melt is lower than that of the linear polymers. Surprisingly, the viscosity decreases with increase in molecular weight, *i.e.*,

higher dendrimers are less viscous [81-82]. The glass transition temperature (Tg) depends on the number of end groups and number of branch points [84]. An increase in the number of end groups lowers the Tg, while Tg is increased with an increasing number of branch points and the polarity of the end groups [85], rheological properties [86], an electrically conducting dendrimer has been reported by Duan *et al.* [87]. The solubility of dendrimers in common solvents, compared to their analogous linear polymers, depends predominantly on the properties of their surface groups [88]. Theoretical studies [89], of the PPI dendrimers have led to predictions of interesting characteristics for the molecule depending on the pH and salt concentrations of the aqueous environment. At low pH and low salt concentration, the interior tertiary amine groups are protonated leading to a repulsion of charges. This charge repulsion results in what is considered an "extended conformation" of the PPI dendrimer. At high pH and high salt concentration, the tertiary amines are no longer protonated, causing a collapse of the dendrimer onto itself [89]. An important property of dendrimers is their tendency to form cationic structures under physiological conditions (pH 7.4), under these conditions, the primary amines on the surface of the dendrimer readily protonate. This creates a polycationic dendrimer with ammonium terminal groups, which leads to a more basic solution [90]. The work described in this dissertation will show, for the first time, that conducting star copolymer can be observed with a modified PPI dendrimer.

2.5.5- Polypyrrole

Polypyrrole exhibits good electrical conductivity and high air stability and is a potentially useful conducting polymer. PPy, one of the most studied conducting polymers and has been in wide range of technological applications in several areas such as secondary

batteries [91-92], electrochromic display devices [93], light-emitting diodes [94], capacitors [95-96], sensors [97], membranes [98], and enzyme electrodes [98-99]. Electrical transport in polymeric materials [68] has become an area of increasing research interest because these materials have great potential for solid state devices. PPy was first synthesized in 1916 where it was prepared by the oxidation of pyrrole to a powder known as "pyrrole black". In 1968 it was first electrochemically deposited [89]. In addition, PPy has been prepared by electropolymerization of Py onto a variety of substrates with promising results [54, 101].

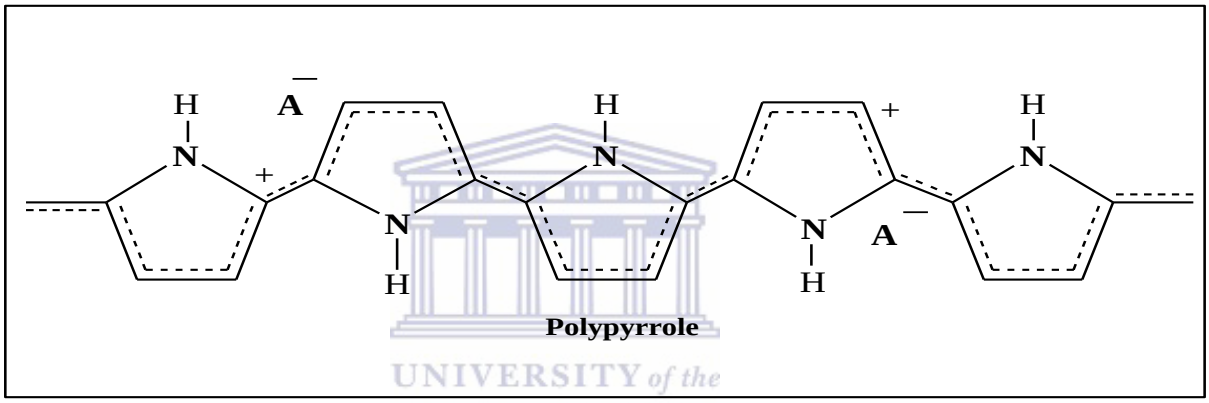

Figure 2.7-PPy with counter ions (A-) to balance charge [55].

PPy (structure seen in Figure 2.7) is an electrodeposited polymer that can be doped with various agents to alter its physical, chemical and electrical properties [102-103]. Additionally, the properties of PPy can be controlled by plating under various conditions [104-105]. As a result of its electro activity, high electrical conductivity and stability it is frequently used in commercial applications such as sensors, batteries, molecular devices and membranes. One of the main advantages of PPy is its stability. Its conductivity decreases only 20% a year in an unprotected environment. It can also withstand temperatures of 100-200 °C, depending on dopant, and is stable in acids [55]. The ability to control the surface properties of PPy, such as wettability and charge density, creates the

potential for modifying tissue interactions with the polymer [106]. The power to alter the properties of PPy through its dopants also adds versatility not seen in other conducting polymers and makes it appealing for biosensor applications. However, PPy itself has rather poor properties in terms of electrochromic behavior [107]. It is common that further enhancement by doping and sensitizing with various dyes is required for good optical properties [108]. Syntheses of conducting star, graft and block copolymers are one of the effective ways to improve the properties of conducting polymers. In order to make them as processable as conventional polymers, several approaches have been developed, one of which is to prepare graft and block copolymers with desired end groups like pyrrole or thiophene [109].

2.6- Nanocomposites

Nanocomposite material has gained tremendous popularity because of their increasingly beneficial application over the microcomposites and monolithic based materials. They are typically nanosized one-dimensional, two-dimensional, three-dimensional or amorphous substances. Their possession of uniquely enhanced properties is as a result of the increased/change in surface area morphology when the diameter of at least one of the substances involved is reduced to nanoscale. The resultant effect of combining suitable nanoparticles is a compound of desired functionalities and drastic improvement in properties such as environmental friendliness, mechanical strength, toughness and electrical or thermal conductivity. Meanwhile, the effectiveness of the nanocomposite is such that the amount of material added is between 0.5 and 5% by weight [110]. Different types of nanocomposites are currently being synthesized for used in a number of fields and applications. Organic/inorganic nanocomposites are very common because of the

typical accessibility to foreign material in inorganic material. Therefore, polymeric organic material can be hosted by a desirable inorganic material to form an interesting hybrid nanocomposite.

Compared with conventional polymer composites, polymer nanocomposites display improved mechanical and tensile strength, reduced scratch and more resistance, higher heat distortion temperature and noise dampening. Problems normally associated with high reinforcement content in composites such as decreased toughness, poor optical clarity and higher melt viscosity are less of an issue in nanocomposite production because a nan reinforcement loading of less than 10 wt% is sufficient to produce high performance polymer nanocomposites.

2.6.1- Nanocomposites of graphene-polymer

Polymer nanocomposites (PNCs) based on carbon nanotubes (CNTs), carbon black and layered silicates have been used for improved mechanical, thermal, electrical, and gas barrier properties of polymers [111]. More recently, the discovery of graphene with its combination of extraordinary physical properties and ability to be dispersed in various polymer matrices has created a new class of PNCs.

Graphene is a two-dimensional, one-atom-thick planar sheet of sp^2 bonded carbon atoms arranged in a hexagonal manner [112], have drawn the attention of researchers because of their astonishing electronic, thermal, and mechanical properties [113]. They have high strength and good conductivity of heat and electricity [114]. It has been viewed as the building block of all other graphitic carbon allotropes of different dimensionality. For example, graphite three dimensional (3D) carbons allotrope is made of graphene sheets

stacked on top of each other and separated by 3.37 Å. The zero-dimensional carbon allotrope, fullerenes (buck balls), can be envisioned to be made by wrapping a section of graphene sheet. The one dimensional carbon allotropes, CNTs and nanoribbons, can be made by rolling and slicing graphene sheets, respectively [115].

2.6.2- Synthesis of graphene-polymer nanocomposites

The dispersion of graphene and its derivatives in polymer is the most important factor for the fabrication of graphene-PNCs [116]. However, functionalize graphene before mixing it with polymer or use of surfactants during mixing is very important for the achievement of good dispersion of graphene sheets into polymer matrix. Since GO could be seen as graphene sheets with functionalized groups, such as carbonyls (=O) or hydroxyl (–OH), many researchers used GO mixing with the polymer before reducing the GO to graphene thermally or chemically during processing [7]. Xu *et al*. reported an efficient method to prepare nylon -6-(PA6-) graphene (NG) composites with improved drafting between graphene and polymer chains by in situ polymerization of caprolactam in the presence of GO. The GO used was thermally reduced to graphene simultaneously during the polycondensation [7, 117]. Stankovich *et al*. prepared a graphene nanosheets/polystyrene (GNS/PS) nanocomposite by solution-phase mixing of the exfoliated phenyl isocyanate-treated graphite oxide sheets with polystyrene, followed by their chemical reduction, [116-118]. Weiling Wang *et al.* [119] obtained GNS by direct sonication using organic solvent/ surfactants which could assist dispersion during mixing Essentially, graphene-polymer nanocomposite have been developed using three strategies: (a) Solution mixing, (b) Melt mixing and (c) In situ polymerization.

Furthermore, graphene is an especially unique conductor with single atomic layer

thickness and the high electrical conductivity of graphene (~6000 S/cm) [120], so a significant change in electrical conductivity of polymers can be achieved with little incorporation of graphene. Graphite/polymer composites are also electrically conductive; however, the low aspect ratio of graphite makes this material not as desirable as graphene/polymer nanocomposites. This is because the low ratio of graphite provides a smaller number of effective particles than graphene for the reinforcement of polymers [121].

a- Solution mixing (solution intercalation)

Solution mixing method has been widely used as an effective technique for fabrication of graphene/polymer and graphene or modified graphene layers are allowed to swell [122]. Graphene or modified graphene can be dissolved easily in a suitable solvent, using water or an organic solvent, *e.g.*, acetone ($(CH_3)_2CO$), chloroform ($CHCl_3$), tetrahydrofuran (THF), dimethyl formamide (DMF) or toluene, owing to the weak forces that stack the layers together. The polymer then adsorbs onto the delaminated sheets and when the solvent is evaporated, the sheets reassemble, sandwiching the polymer to form the nanocomposites [123]. This strategy can be used to synthesize epoxy [122, 124], polyvinyl alcohol (PVA), polyvinyl fluoride (PVF) polyethylene (PE), polymethylmethacrylate (PMMA), polymethylmethacrylate (PEMA), polyurethane (PU) [111, 124] of nanocomposites, but solvent removal is a critical issue [122]. Due to the oxygen functional groups, GO can be directly mixed with water soluble polymers such as PVA. Zhao *et al.* [126]. Therefore, a relatively large number of solvent molecules need to be desorbed from the filler to accommodate the incoming polymer chains [122]. The main advantage of this method is that it allows the synthesis of intercalated nanocomposites

based on polymers with low or even no polarity [116]. The solvent is removed completely by evaporation or distillation and the polymer material containing the fillers is then molded to give shape to the composite. Although the solution mixing approach generally leads to better particle dispersion than melt mixing process, slow solvent evaporation often induces particle reaggregation. In addition, the use of large amounts of solvent and the associated environmental pollution have prevented.

b- Melt mixing

Melt mixing is a typical method for the preparation of high thermoplastic graphene-PNCs [116]. It is environmental friendly because the method is free from toxic solvent [127], it is also economical and suitable for mass production. In this technique, no solvent is required and graphene or modified graphene is mixed with the polymer matrix in the molten state. It can also be used in conventional methods, such as extrusion and injection molding. However, it disadvantages includes inefficient dispersion of graphene in the polymer matrix especially at higher filler loadings due to increased viscosity of the composites. The technique may also cause graphene buckling and even rolling or even shortening of graphene sheets during mixing due to strong shear forces resulting in reducing its aspect ratios which is not favourable for better dispersion [122, 125-128].

c- In situ polymerization

In this method, homogeneously dispersed graphene or its derivatives in a polymer nanocomposites is prepared without a prior exfoliation step [116, 127]. The uniformly dispersed graphene nanosheets in solvent such as epoxy, PMMA, Nylon 6, PU, poly(butylene terephthalate) (PBT) and PANI, *etc.* can be mixed with a monomer (and/or

oligomer) solution with an initiator (*e.g*., photo initiators and thermal initiators). After the initiator is dissociated by radiation or thermal energy [130]. The mixing of monomers into the layered structure of graphite, during in situ polymerization, increases interlayer spacing and exfoliates graphene platelets producing well-dispersed graphene in polymer matrix after polymerization [122]. It was found that the in situ polymerization process is not suitable because makes possible the covalent bonding between the functionalized sheets and polymer matrix via various chemical reactions During polymerization, however, the viscosity usually increases, which may reduce the process ability of nanocomposites [131]. Compared with melt and solvent mixing methods, in situ polymerization can provide enhanced dispersion properties and also better compatibility between graphene and the polymer through the introduction of additional functional groups on the graphene (or its derivatives) surfaces. In situ polymerization should be performed in the solution state to address the elimination of residual solvents. However, this method requires monomer unites and lot of reagent for the polymerization procedure, and thus less applicable in the case of naturally existing polymers [111].

CHAPTER THREE

EXPERIMENTAL

3.1- Summary

This chapter describes the methods and procedures employed to synthesize the materials used in the design of the graphenated-first generation poly(propylene imine)-co-polypyrrole nanocomposites included here are the characterization techniques of the materials (FT-IR, TGA, XRD, HR-SEM and HR-TEM) and electrochemical (CV, EIS and charge-discharge).

3.2- Reagents

Natural graphite powder (microcrystal grade 9.9995%) (Metal base) UCP-1-M grade, "F" purity was purchased from Alfa Aesar South Africa and used for the preparation of graphene oxide (GO) by a modified Hummers method. Graphene-star copolymer, poly(propylene imine) dendrimer (SyMO-Chem, Eindhoven, Netherlands) 2-pyrrole 2-carboxaldehyde (2-Py), lithium perchlorate, ammonium persulfate, dichloromethane (DCM), methanol, chloroform, hydrochloric acid (≥32%) and sulphuric (Sigma-Aldrich, South Africa. The buffer components disodium hydrogen phosphate (Na_2HPO_4), potassium dihydrogen phosphate, potassium chloride (Sigma Aldrich, South Africa) all chemicals were of analytical reagent grade and were used without further purification. The pyrrole monomer (Py) was distilled prior to use. Ultrapure water (resistivity 18.2 MΩ cm), was used as reagent water for aqueous solution preparation and purified by a Milli-QTM system (Millipore). Analytical grade argon and nitrogen gases were purchased from Afrox, South Africa. Alumina polishing pads and powder (0.05, 0.3 and 1.0 μm) were obtained from Buehler, Illinois, USA and Sulfuric acid 95-97%, Fluka.

3.3- Synthesis of graphene oxide

The GO was prepared by modified Hummers method. Concentration of H_2SO_4 (500 mL) was added into a 250 mL in dry clean conical flask and stirred filled with graphite (2 g) at room temperature for 0.5 h. The flask was then cooled to (0 °C) in an ice bath, for half an hour, followed by slow addition of Potassium permanganate ($KMnO_4$) (7 g) and it was then allowed to warm to room temperature. The temperature was then raised to 35 °C with a water bath for 2 h, and the mixture was then stirred with a Teflon-coated magnetic stirring bar (stirring rate: 800 rpm) for 2 h. The reaction mixture was cooled with an ice bath, followed by addition of excess purified H_2O (17.4 MΩ) to the mixture. H_2O_2 (30 wt% in water from Aldrich) was then added until gas evolution ceased. Filtration afforded brown powder GO which was washed by purified H_2O/HCl mixed solvent (9/1 volume ratio) 3 times, followed by suction drying for 12 h filtering and then drying in the vacuum at 25 °C 12 h [132].

3.4- Synthesis of generation one pyrrole functionalized (PPI) dendrimer

The generation one PPI-2Py synthesis was carried out by condensation (n reaction of PPI with 2-pyrrole aldehyde. A reaction mixture of poly(propylene imine) generation one dendrimer (1 g, 3.15 mmol)/2Py generation (1.2 g, 12.625 mmol) in 500 mL dry methanol (CH_3OH) was magnetically stirred under a positive pressure of (N_2 gas) 48 h in a 100 mL three-necked round-bottom flask. The CH_3OH was removed by rotary evaporation and the residual oil was dissolved in 50 mL DCM; the organic phase was then washed with water (50 mL) 6 times to remove unreacted monomer. The DCM was removed by rotary evaporation and yielded the desired product as orange oil. The methanol used above is a slight modification of that reported by Smith *et al.*[133].

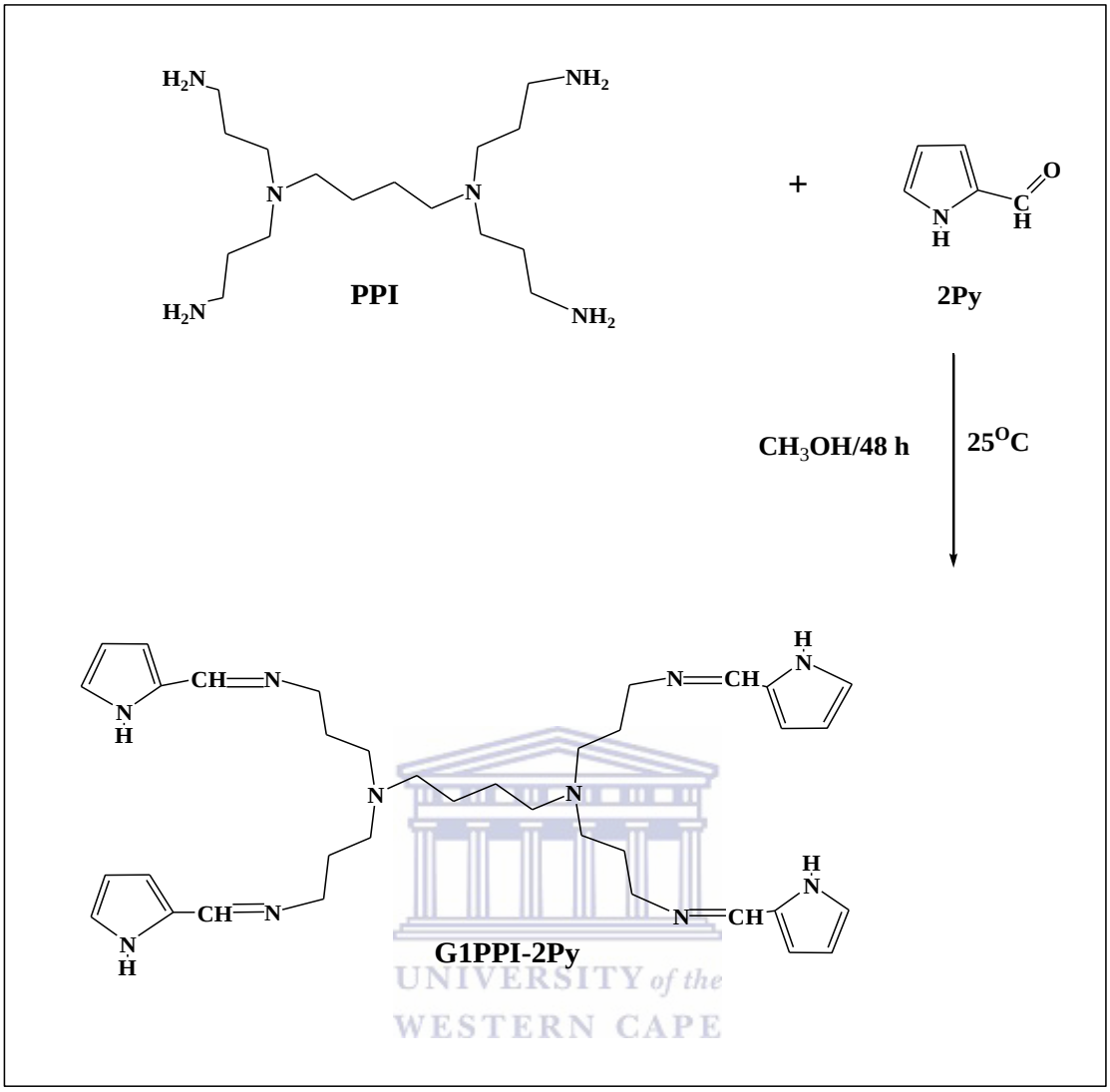

Scheme 3.1-Functionalized generation one poly(propylene imine) dendrimer [89].

3.5- Synthesis of generation one poly(propylene imine-co-polypyrrole)

The generation one poly(propylene imine-co-polypyrrole) G1PPI-co-PPy polymer was synthesized by reacting Functionalized dendrimer (PPI-2Py) with Py using ($(NH_4)_2S_2O_8$) as an oxidant via chemical oxidative copolymerization, yielding conducting star copolymers with polypyrrole. PPI-2Py (0.1 g, 0.16 mmol) of PPI-2Py and Py (0.4 mL, 5.065 mmol) were dissolved in 20 mL of chloroform with stirring. Then the solution of ($(NH_4)_2S_2O_8$) (0.265 g, 11.62 mmol) 0.265 g (11.62 mmol) of ($(NH_4)_2S_2O_8$) in 20 mL of distilled water was slowly added to the above solution. The polymerization reaction was carried out at 25 °C for 1 h and them terminated by pouring CH_3OH into the reaction flask. The resultant G1PPI-co-PPy powder was filtering and drying in a vacuum oven at 45 °C for 12 h. The product yield was 0.154 g (33%) and this method was adapted from literature with slight modification [89]. The same experimental procedure was used prepare homo-polymer PPy except that PPI-2Py was not added to the reaction mixture.

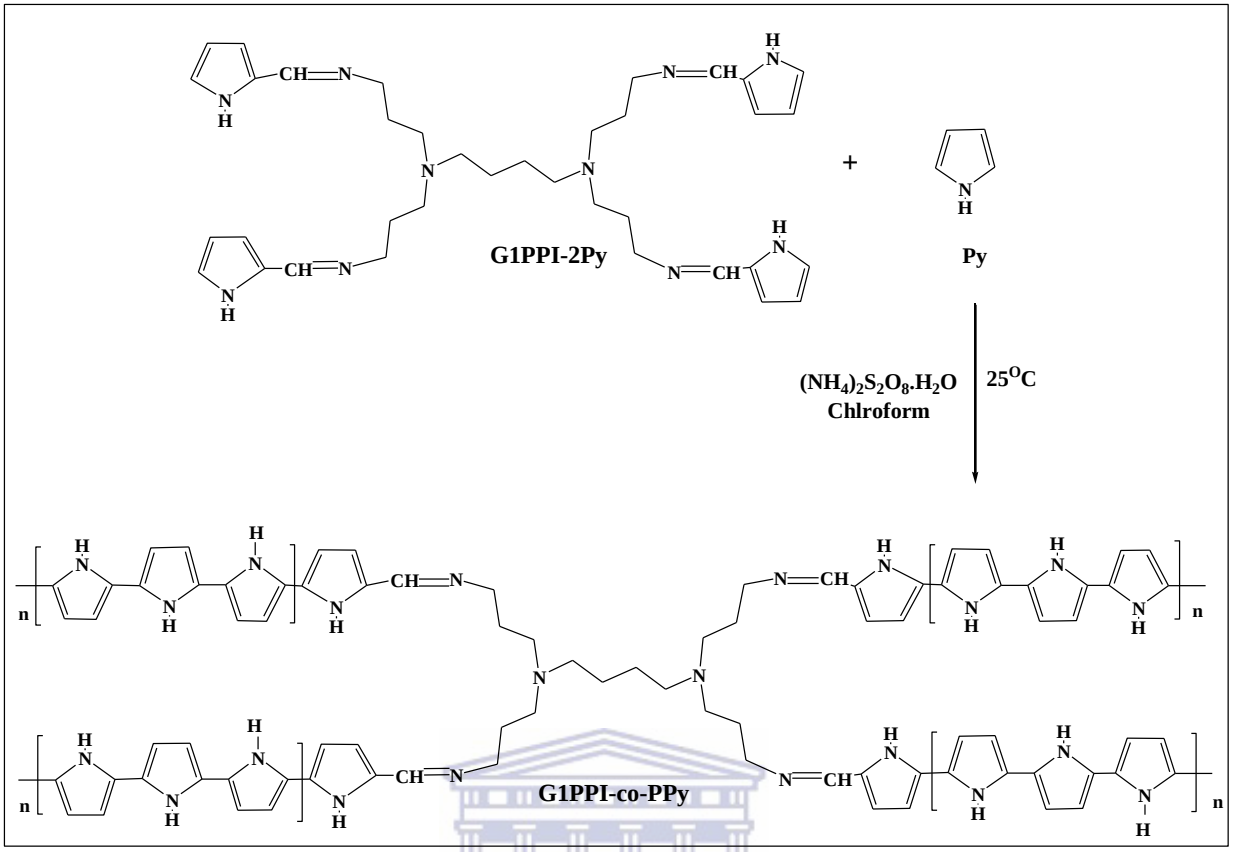

Scheme 3.2- Synthesis of poly(propylene imine)-co-polypyrrole [89].

3.6- Synthesis of graphenated-generation one poly(propylene imine)-co-polypyrrole (GO-G1PPI-co-PPy)

In atypical synthesis of GO-G1PPI-co-PPy nanocomposite, firstly, the required amount of graphite oxide was dispersed into Deionized water by ultra-sonication for 2 h to form uniform exfoliated GO solution. Secondly, G1PPI-co-PPy was synthesized by reacting PPI-2Py with Py using ($(NH_4)_2S_2O_8$) as an oxidant via chemical oxidative copolymerization, yielding conducting star copolymers with polypyrrole. Approximately (0.1 g, 0.16 mmol) of PPI-2Py and (0.4 mL, 5.065 mmol) Py were dissolved in 20 mL of chloroform with stirring. Approximately 0.265 g (11.62 mmol) of ($(NH_4)_2S_2O_8$) in 20 mL of distilled water was slowly added to the above solution into the GO solution under stirring. Thirdly, the

polymerization reaction was carried out at 25 °C for 1 h and them terminated by pouring CH_3OH into the reaction flask. Finally, the resultant GO-G1PPI-co-Py black powder was filtering and drying in a vacuum oven at (60 °C) for 12 h.

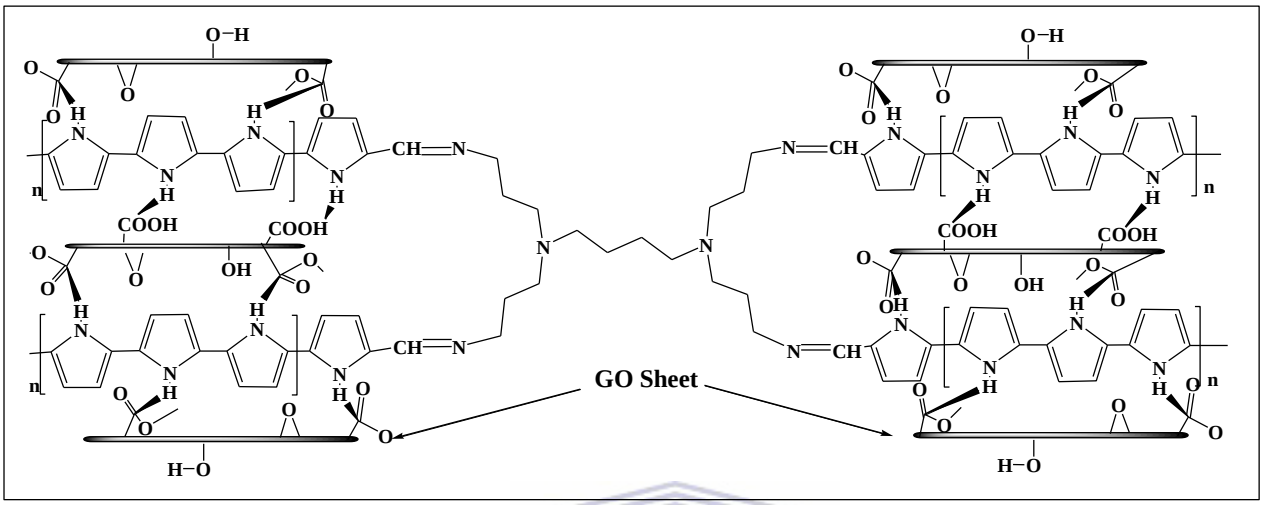

Figure 3.1- Schematic of the synthesis of graphenated-poly(propylene imine)-co-polypyrrole

3.7- Preparation of the electrode materials

3.7.1- Preparation of the electrode poly(propylene imine)-co-polypyrrole

For the preparation of electrode, 5 µL (5 mg/mole) f PPI-2Py was drop coated on surface of a GCE (0.017 cm^2 diameter) and allowed to dry under a blanket of (N_2 g) for 2 h. Then the electrode was transferred to an electrochemical cell containing 5 mL of 1 M H_2SO_4 aqueous solution as supporting electrolyte containing 70 µL of Py. Electrochemical polymerization was achieved CV (+460 mV to -800 mV).

3.7.2- Preparation of the electrode graphenated-poly(propylene imine)-co-polypyrrole

To prepare GO-G1PPI-co-PPy, 5 mL (5 mg/mole) of G1PPI-2Py was drop coated onto the surface of GCE electrode and allowed to day under a blanket of N_2 gas. The GO/Py

composite was prepared separately by adding the synthesized GO (10 mg) into supporting electrolyte of 5 mL (1 M H_2SO_4) aqueous solution and then solicited for 15 min using an ultrasonic bath to acquire a homogeneous solution. 70 µL of Py was then added to the solution and mixed to the dispersion. The mixed solution was once again ultrasonic for 15 min. To ensure homogeneous dispersion, the solution was electrochemically deposited on the electrode coated with G1PPI-2Py. The CV was performed for 60 cycles at an applied potential of (+460 mV to -800 mV) at a scan rate 50 mV/s to achieve GO-G1PPI-co-PPy.

3.8- Preparation of the electrode for the supercapacitor cells

Supercapacitor cells were built by three-electrode cell configuration. The electrolyte was 1 M H_2SO_4 solution, platinum plate counter and GCE modified that were after 60 cycle by polymerized working electrodes respectively and the Ag/AgCl electrode in 3 M NaCl was used as the reference electrode. However, the shape and size of the cells is less important for the development of supercapacitors.

3.9- Instrumentation

3.9.1- Proton Nuclear Magnetic Resonance Spectroscopy

Proton nuclear magnetic resonance (^{1}H NMR) (200 MHz) (Varian Gemini XR200 spectrometer) was used to determine the proton signals. For this study, the NMR spectra were recorded at 25 ^oC using $CDCl_3$ as the solvent, and tetramethylsilane as internal standard.

3.9.2- Fourier Transforms-Infrared Spectroscopy

Fourier transform infrared spectroscopy is a powerful tool that determines the functional groups of materials. The IR portion of the spectrum gives information regarding the

vibrational and rotational motion of atoms in molecules. This technique is known to excite - molecules to higher energy by absorbance of infrared radiation and the energy of absorbed IR radiation increases with amplitude of the vibrational motion of bonds in molecules [134]. The technique is widely used for qualitative analysis and in this study FT-IR has been used to investigate the presence of the amide groups on star copolymer once the star copolymer was functionalized with graphene oxide. The bonding interactions before and after star copolymer was functionalized with graphene oxide were also investigated. FT-IR spectra were recorded on a PerkinElmer Spectrum 100 FT-IR spectrometer. The chemically prepared star copolymer material was analyzed in powder form. The electrochemically prepared star copolymer material was prepared by electrode position on the surface of a coated GCE and then gently scraping from the electrode surface. The spectra were directly recorded in the region 400-4000 cm^{-1}, without mixing with KBr.

3.9.3- Thermo gravimetric Analysis

Thermo gravimetric analysis is a technique in which the mass of a substance is monitored as a function of temperature or time as the sample specimen is subjected to a controlled temperature program in a controlled atmosphere [135]. This can be very useful to investigate the thermal stability of a material. TGA was carried out using a PerkinElmer, Model TGA-7 instrument and the weight of each sample was less than 10 mg. The most common method used in TGA is to continuously weigh a sample on a sensitive balance while heating the sample in the presence of air or an inert gas. As the temperature increases, mass loss occurs due to evaporation of water or solvent, decomposition, or reaction of the material. The mass measurements are collected over a range of temperatures and processed by a computer. A thermo gram is produced, which is a plot of mass loss versus temperature. Mass loss occurs

in steps, based on the temperature at which the material leaves the sample pan.

3.9.4- X-ray diffraction

X-ray diffraction is a crystallinity technique for studying the crystal structure of a material and it is the only method that permits the direct identification of any crystalline material based on their unique crystal structure. In XRD analysis, X-rays of known Wavelength are passed through a sample to be identified in order to identify the crystal structure. The wave nature of the X-rays means that they are diffracted by the lattice of the crystal to give a unique pattern of peaks, or 'reflections', at differing angles and of different intensity (just as light can be diffracted by a grating of suitably spaced lines).

3.9.5- High-Resolution Scanning Electron Microscopy

High Resolution-Scanning Electron Microscopy (HR-SME) images were taken with a Hitachi S3000N scanning electron microscope at an acceleration voltage of 20 kV at various magnifications. Small amounts of the materials (in powder form) were placed on copper grids. An aliquot of 2 μL of each sample were drop coated on the copper grids and dried for two days at room temperature. The samples on the grids were coated with gold using a SC7640 Auto/Manual high resolution super coater (Quorum Technology Ltd., England) at a voltage of 2 kV and plasma current of 25 mA for one minute. HR-SEM images uses electrons rather than light to form an image of objects such as fractured metal components, foreign particles and residues, polymers and biological samples, among others. It uses a focused beam of high energy electrons to generate a variety of signals at the surface of solid specimens. The signals derive from electron sample interaction and reveal information about the sample including external morphology (texture), chemical composition, crystalline

structure and orientation of materials making up the sample. HR-SEM was used to study the morphology of graphene oxide, G1PPI-co-PPy and GO-G1PPI-co-PPy nanocomposite. The morphology of G1PPI-co-PPy as conducting polymer will provide information about where the graphene oxide can be incorporated into the G1PPI-co-PPy structure to form the GO-G1PPI-co-PPy nanocomposite. The morphology of graphene oxide will confirm the successful synthesis of graphene layers and whether they can be entrapped by the expected clustered structure of the G1PPI-co-PPy. GO-G1PPI-co-PPy morphology will confirm the formation of a nanocomposite with GO incorporated onto the clustered structure of G1PPI-co-PPy.

3.9.6- High-resolution transmission electron microscopy

HR-TEM images were taken using Tecnai G2 F20X-Twin MAT 200 kV field emission transmission microscope from FEI (Eindhoven, Netherlands). HR-TEM image is a technique used to study the internal structure of a material. Not only is it used to study the internal structure it is also used to study various characteristics of a material HR-TEM is used to study the shape, orientation, particle size, size distribution and lattice parameters of a material. HR-TEM image provides a direct link in the internal structure and its irregularities at the atomic scale and offers resolution to the Angstrom level as well as enabling the information to be obtained on the atomic packing rather than just the morphology of the sample. The technique uses phase contrast resulting from an interference of several beams and determines whether the particle that makes the specimen are dispersed or agglomerated. However the technique is limited in high magnification imaging which requires high electron dose where by the specimen needs to be relatively insensitive. For graphene oxide independent nanosheets are observed and these should be wider in thickness and also flat. In this study HR-TEM was

used to confirm the size and shape, distribution and morphology of synthesized materials, *i.e.*, GO, functionalized graphene oxide and the functionalized graphene oxide-star copolymer nanocomposites.

3.10- Electrochemical techniques

Electrochemical techniques are used to interrogate the redox properties of the biosensors and their prospective platform components at the electrode surface which occur when a potential is applied. From the redox behaviour of different materials under different conditions, various parameters such as rate constant, diffusion coefficient, formal potential, film thickness, sensitivity, detection limits, surface concentration, solution resistance, charge transfer resistance and process reversibility can be determined. However, the main limitation of voltammetric techniques is that the species under investigation must be either reducible or oxidizable in the range where both the electrode and the electrolyte are electrochemically inert.

3.10.1- Cyclic Voltammetry (CV)

Cyclic voltammograms were recorded with computer interfaced to BASi Epsilon (BASi® Corporate Headquarters 2701 Kent Avenue West Lafayette, IN 47906 USA) using a 10 mL electrochemical cell with a three electrodes set up the electrodes used in the study were sketch of a cell setup.(1) glassy carbon working electrode (A = 0.071 cm^2) from, (2) platinum wire from Sigma Aldrich acted as counter electrode and (3) Ag/AgCl from BAS kept in (3 M NaCl) was the reference electrode and 1 μm, 0.3 μm and 0.05 μm fine alumina micro polishing pads were obtained from Buehler, LL, USA and were used for polishing the glassy carbon electrode before modification.CV is a simple and direct electro analytical technique

used to clarify the kinetics of electrochemical reactions taking place at the electrode surface [136]. CV provides information on the thermodynamics of redox processes and the kinetics of heterogeneous electron-transfer reactions. It is useful in a comprehensive characterization of nanophase electro catalysts. CV can also be used in solution to understand reaction intermediates as well as obtaining the stability of reaction products [89]. It can also be used to study the electron stoichiometry of the system, the diffusion coefficient of the analyte and the reduction potential (which can be used as an identification tool). Advantages of this technique include its broad accessibility due to its low cost and the accessibility to extensive theory for electrochemist as well as other field of specialists. However this technique has some drawbacks which includes; difficulties in determining the mechanism of two or more closely spaced charge transfer reactions. In this study CV was used to determine the electrochemical activity of GO-G1PPI-co-PPy and G1PPI-co-PPy whereby there was an observed increase in current with an increase in applied potential and was used for the testing of the biosensor and determination of the analyze of interest.

3.10.2- Electrochemical impedance spectroscopy (EIS)

Electrochemical impedance spectroscopy measurements of electrochemically prepared of the modified GC working electrode were performed in a solution containing 1 M H_2SO_4 and the same three-electrode cell arrangement. The electrolyte for CV was measured with CH Instruments, Inc. Electrochemical work station, 600 E Potentiostat 3700 Tennison Hill Drive Austin, TX 78738-5012 USA. The results are then plotted in the form of Nyquist plots at perturbation amplitude of 10 mV and within the frequency range from 1000 kHz to 100 mHz at room temperature. EIS is based on applying an alternating current (AC), potential (E) of a small amplitude (perturbation), and obtaining an AC current signal (I) in which the

impedance (Z) can be obtained. These analyses allow for the characterization of the double layer interface of the electrodes and the physicochemical processes at various time constants, simplifying electron transfer at high frequency and mass transfer at low frequency. Results obtained from EIS are usually fitted using equivalent circuits of resistors and capacitors such as the Randles circuit model [137]. EIS data is either represented as the Nyquist plot; which is the plot of the real impedance (Z') versus the imaginary impedance (Z'') or the Bode plot; where the modulus of the impedance (log /Z/) and the phase angle Ψ between the AC potential and the AC current as a function of the frequency (log ω) are plotted. The Nyquist plot provides visual insights into the system dynamics at the electrochemical interface. The plot consists of a semicircle at high frequency which describes the electron transfer process at the electrode interface (charge transfer resistance) and a linear region at lower frequencies known as the Warburg impedance which arises from mass transfer limitations and can be used to calculate apparent diffusion coefficients. The Bode plot shows frequency independent plots which represent the behaviour of resistive, capacitive or diffusive processes [133-134].

3.10.3- Galvanostatic charge-discharge technique

Charge-discharge technique is a standard technique used to test the performance and cycle life of capacitors and batteries. This technique used was a Voltalab PGZ402 instrument (Radiometer Analytical, France). The system is capable of switching between charge and discharge automatically according to the cut off potentials set. Normally, charge and discharge are conducted at constant current until a set voltage is reached. The charge (capacity) of each cycle is measured and the capacitance. Both are plotted as a function of cycle number. This curve is called the capacity curve. In practice, charge is commonly called capacity. The capacitance values were calculated using the equation (2.2).

Since long cycle life is important to supercapacitors, the charge-discharge technique was employed to examine the service life of the electrode nanomaterials this study was run at a current density of a 9.3×10^{-3}A/g for 100 cycles and at the same potential window of CV.

CHAPTER FOUR

RESULTS AND DISCUSSION

4.1 Summary

The synthesis of GO-G1PPI-co-PPy nanocomposites was done through polymerization using G1PPI-co-PPy and GO. FTIR, TGA, X-ray, HR-SEM and HR-TEM were used in the characterization and identification of the resulting nanocomposite. Electrochemical characterization of bare GCE, G1PPI-co-PPy and GO-G1PPI-co-PPy nanocomposites were also done using CV, EIS and charge-discharge. The result of this analysis shows that a GO/Conducting polymers polymer nanocomposite with good electrochemical properties and cycling performance was synthesized.

4.2- Physical characterization

4.2.1- Fourier Transform-Infrared Spectroscopy

The FTIR was employed to investigate the bonding interactions in pure graphene oxide, of G1PPI-co-PPy and GO-G1PPI-co-PPy nanocomposites. In the spectrum of GO Figures 4.1 the peaks at 3318, 1724, 1599, 1417 and 1061 cm^{-1} were assigned to the O-H stretching, C=O (carbonyl) stretching, C–O stretching and O–H bending vibrations respectively. This supports the fact that Graphene oxide is a highly absorptive material as verified by its ability to become a gel like solution [135-137].

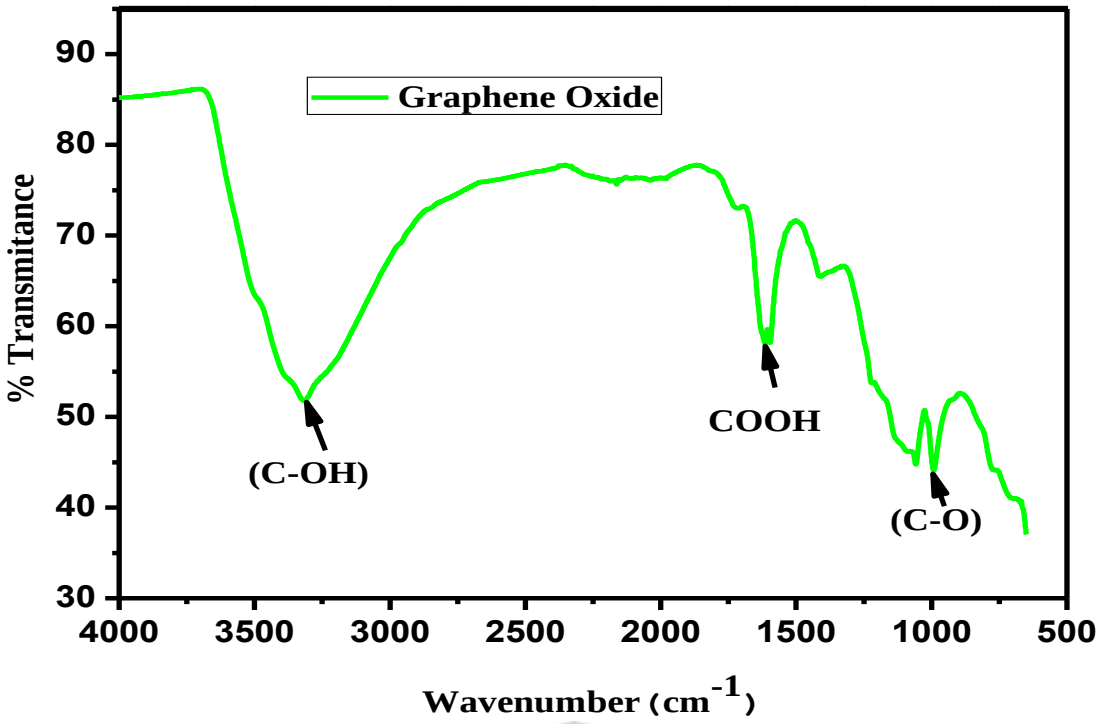

Figure 4.1- FTIR spectrum of GO.

Copolymerization of GO with G1PPI-co-PPy results in change of peaks in FT-IR. The alteration in the peak of carbonyl groups reveals that the graphene has been oxidized. The polar groups, especially the surface hydroxyl groups, result in the formation of hydrogen bonds between graphene and water molecules; this further explains the hydrophilic nature of graphene oxide. The intensity of these peaks decreased significantly, and some of the peaks almost disappeared, Figure (4.2).

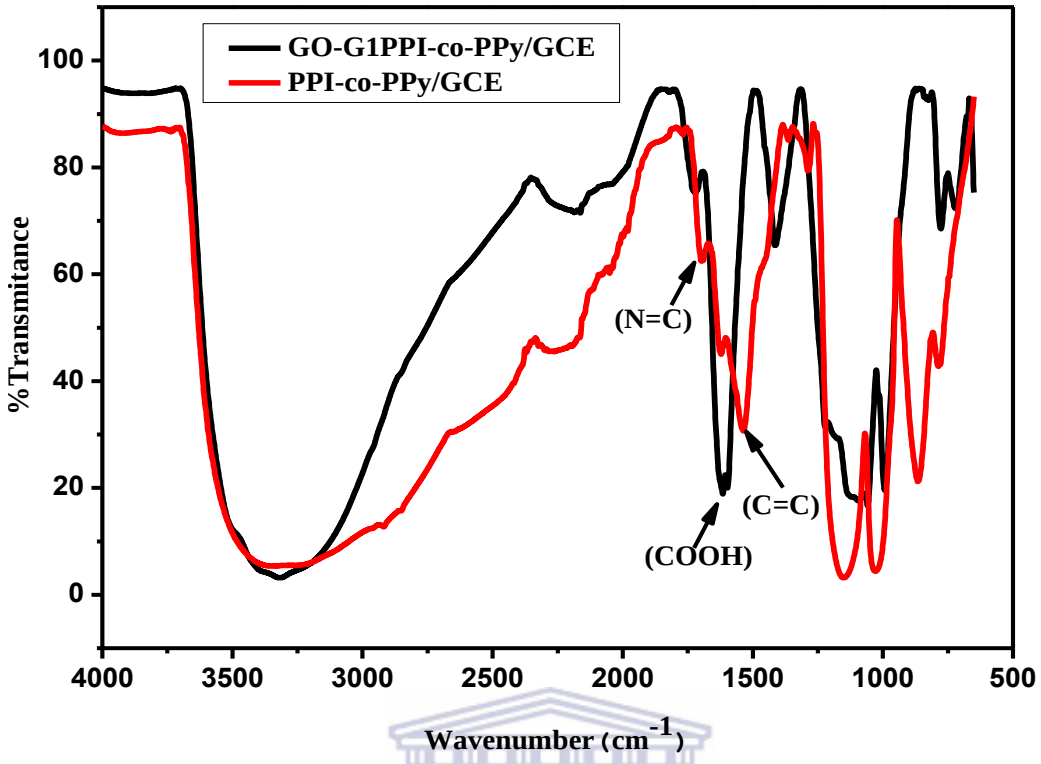

Figure 4.2- FTIR spectroscopic analysis of G1PPI-co-PPy and GO-G1PPI-co-PPy nanocomposites.

In the G1PPI-co-PPy spectra the bands due to PPy at 1522, 1145, 1027 and 845 cm^{-1}, whereas the sharp N=C band in PPI-2Py now appears at 1704 and 1617 cm^{-1}. The intense absorption at 775 cm^{-1}, ascribed to the out-of-plane C–H bending at α position of the Py. This is an evidence of the polymerization from C–H at α position of Py moiety of the functionalized dendrimers, and conversion to G1PPI-co-PPy via α–α coupling. The sharp absorption peak at 1043 cm^{-1} corresponds to the N-H deformation [55]. The peaks at 1286 cm^{-1} and 1626 cm^{-1} are related to the C–C stretching vibration and C=C stretching mode of the Py ring, respectively. However, for GO-G1PPI-co-PPy nanocomposites peak due to the COOH group has been downshifted 1617 cm^{-1} which is probably due to the π-π interactions and hydrogen bonding between the GO sheet and aromatic polypyrrole rings from G1PPI-co-PPy, indicating that the carboxyl groups from GO acted as efficient dopants in the

polymerization.

4.2.2- Thermo gravimetric Analysis

The Thermo gravimetric analysis is a plot of weight loss versus temperature for GO, G1PPI-co-PPy and GO-G1PPI-co-PPy nanocomposite. The experiment was performed at a heating rate of 10 °C/min under N_2 the atmosphere. The results are as shown in Figure 4.3 (c). The plot of GO weight lost against temperature change shows a 26% lost at 200 °C as a result of the release of absorbed water, and a further rapid 16% weight loss from 200 to 300 °C which is attributed to the thermal decomposition of instable oxygen-containing functional groups that yield CO, CO2 or water. The weight loss of GO at 700 ˚C is about 55%. This result corresponds with published article on TGA of GO [141]. The TGA result of synthesized GO-G1PPI-co-PPy nanocomposite as shown Figure 4.3 demonstrated a relative stability compare to the reactant materials (GO and G1PPI-co-PPy). (a) The weight loss near 169 °C is probably due to removal of the oxygen- containing functional groups (*e.g.*, COOH, OH). After 250 ˚C, major weight loss occurred due to decomposition of the Py from the composite. Finally at 469 °C, almost 24% weight loss for GO, G1PPI-co-PP nanocomposite was observed.

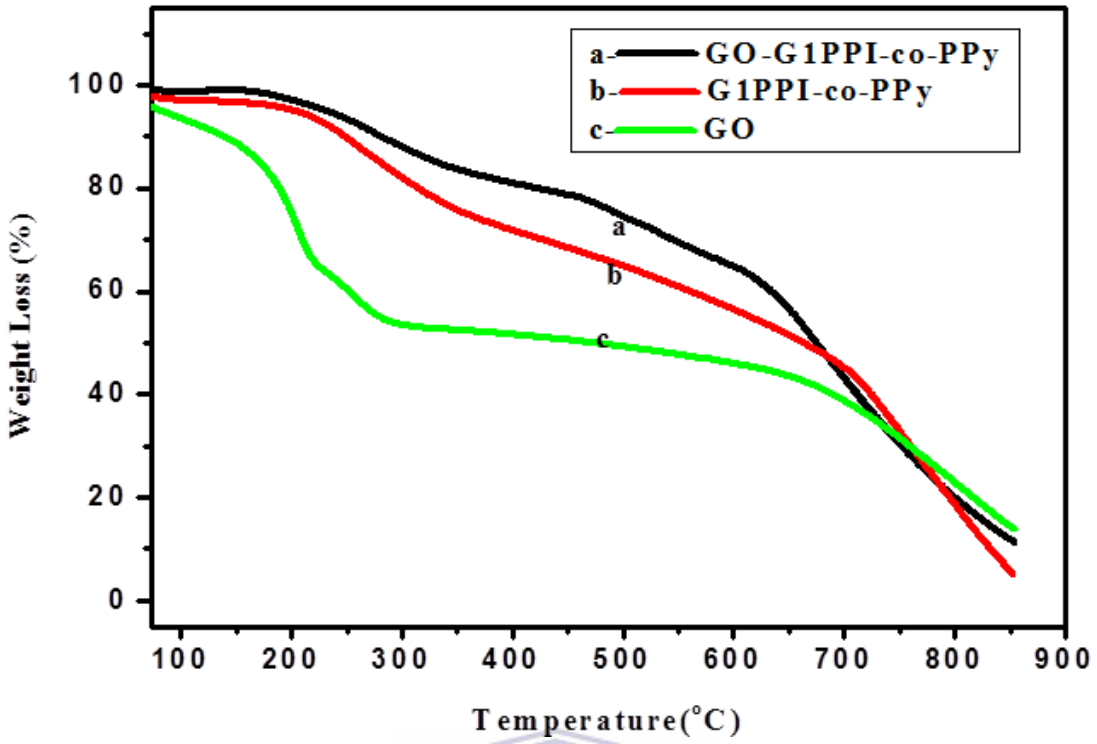

Figure 4.3- TGA curves obtained at 10 °C/min under N_2 for GO, G1PPI-co-PPy and GO-G1PPI-co-PPy nanocomposites.

4.2.3- X-ray Diffraction Analysis

X-ray diffraction spectra of GO, G1PPI-co-PPy and GO-G1PPI-co-PPy nanocomposite are as presented in Figure 4.4. The GO shows an intense and sharp peak centered near 10^o of the GO sheets. This value is larger than the d-spacing of pristine graphite 20, as a result of the introduction of oxygenated functional groups. [138-140]. The broad peak centered at 24° is peculiar to G1PPI-co-PPy and it is corresponded to the scattering from bare polymer chains at the interplanar spacing [55]. In the case of the GO-G1PPI-co-PPy nanocomposites, the peak is also situated at 24^o almost the same as that of G1PPI-co-PPy which was ascribed to the diffraction peak of G1PPI-co-PPy [55]. Additionally, the peak ascribed to GO within these nanocomposites disappeared, illustrating the complete coating of PPy between the layered GO [142].

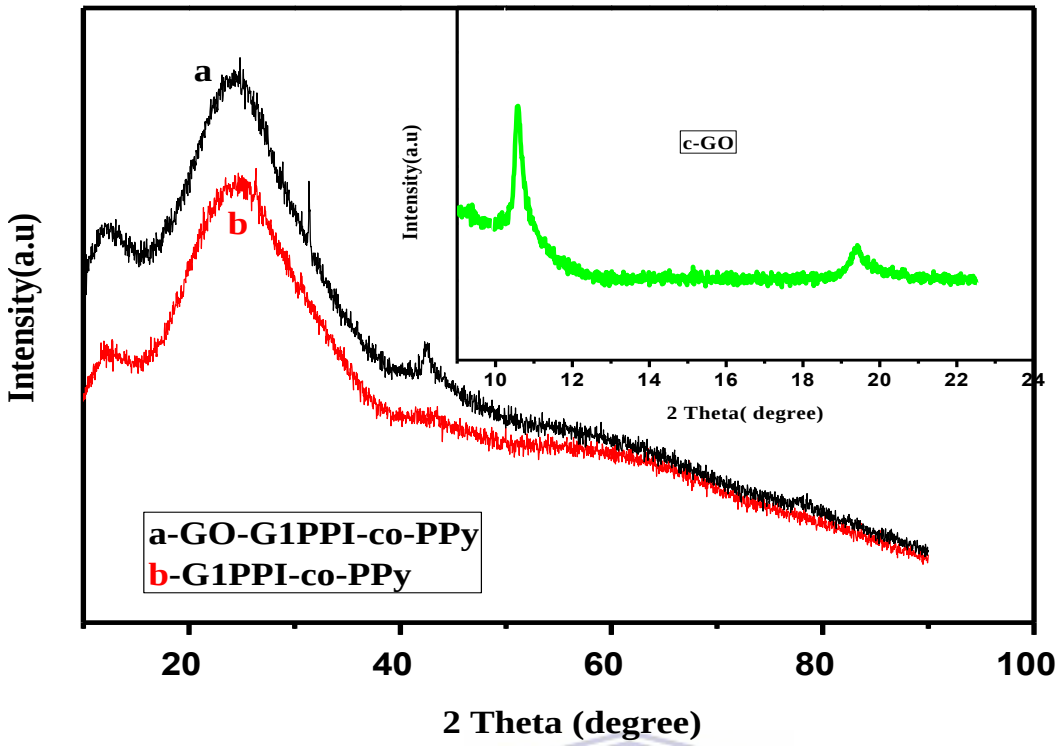

Figure 4.4- X-ray study of GO, G1PPI-co-PPy and GO-G1PPI-co-PPy nanocomposites.

4.2.4- High-resolution scanning electron microscope (HR-SEM)

The HR-SEM images for (a, b) GO, (c, d) G1PPI-co-PPy and (e, f) GO-G1PPI-co-PPy nanocomposites. In Figures 4.5 (a to f).The GO showed a well exfoliated folding sheets of GO and closely associated [144-145]. The G1PPI-co-PPy, morphology resembles densely clustered florets, whereas the chemically prepared exhibits a dense growth of whelk-like helixes. Figure 4.5 (e, f), revealed G1PPI-co-PPy with diameters ranging 100 nm and 1 µm resembles densely scattered florets attached to the graphene oxide surface, particularly along the edges of the stacked nanosheets with a thickness of several nm. This suggests that the compatibility between G1PPI-co-PPy and GO is sufficient to obtain nanosized dispersion without an additional surface treatment. The GO-G1PP-co-PPy scattered on the GO surface might be an indication of good capacitive behaviour.

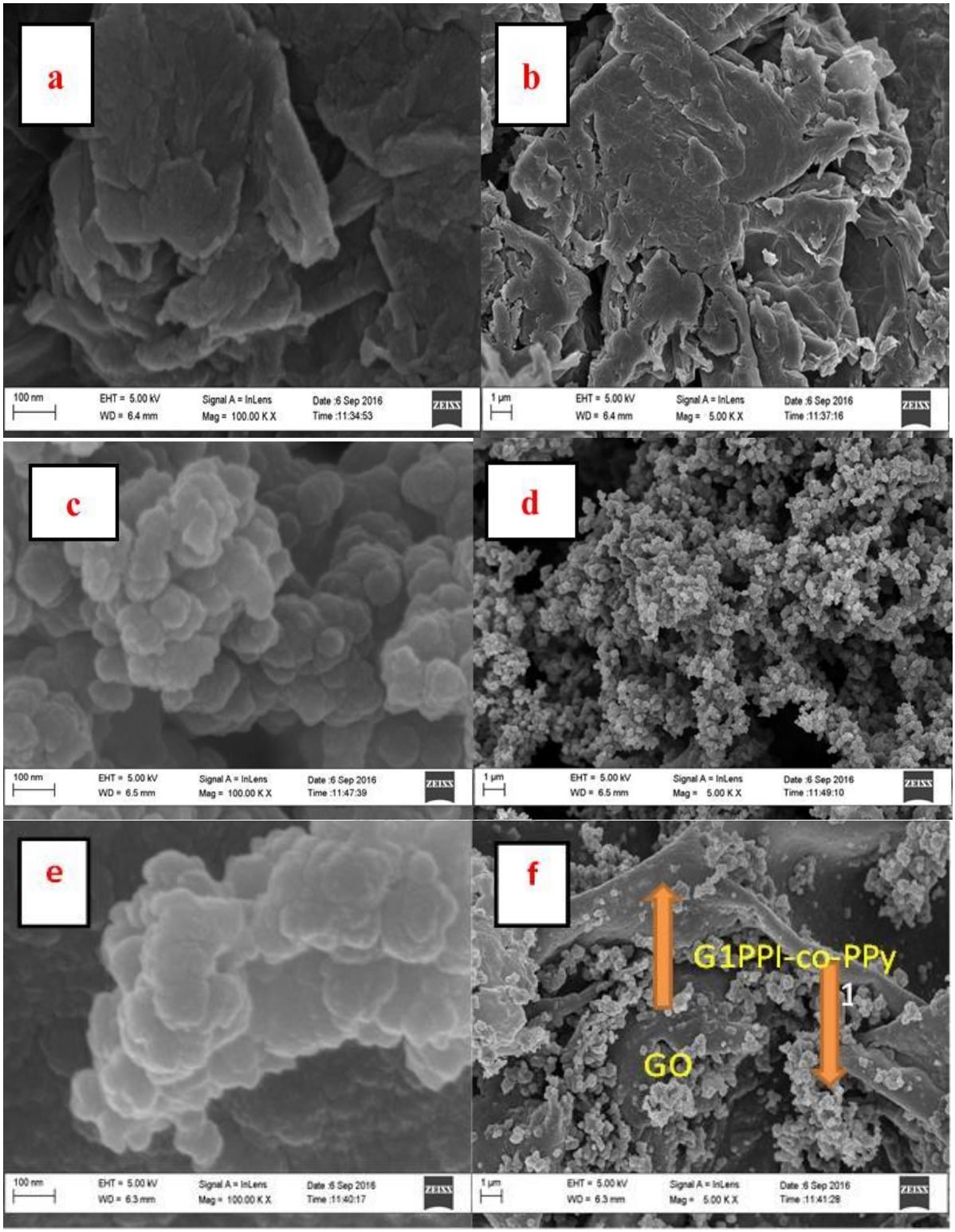

Figures 4.5 HR-SEM images: (a, b) GO, (c, d) G1PPI-co-PPy and (e, f) GO-G1PPI-co-PPy nanocomposites.

4.2.5- High-resolution transmission electron microscopy

The HRTEM images for GO, G1PPI-co-PPy and GO-G1PPI-co-PPy nanocomposites at various magnification. in Figure 4.6 (a, b), GO showed a transparent wrinkled surfaces of silky sheets and an entangled folding edges can also be observed [140-141]. Revealed the elemental composition of GO acquired from HR-TEM of GO, of oxygen atom of -OH and -COOH groups on GO layer surface facilitated the further oriented aggregation of action radical of carbon [146]. Figure 4.6 (c, d), shows the HR-TEM image of G1PPI-co-PPy. The electron diffraction pattern in Figure 4.6 (c, d), indicates the G1PPI-co-PPy is amorphous structure. Figure 4.6 (e, f), shows the HR-TEM image of GO-G1PPI-co-PPy nanocomposites. The GO-G1PPI-co-PPy nanocomposite has pronounced edges, which may be attributed to the embedment of single-layer and multi-layer GO in composite matrix. The electron diffraction pattern in Figures 4.6 (e, f), confirms that the composite contains the components with crystal structure, such as single-layer and multi-layer GO. It also shows the existence of large amount of oxygen containing functional groups O-H, C=O, C-O CO2 on the surface of GO sheets on the surface of GO sheets. Also that edge of GO-G1PPI-co-PPy nanocomposites includes ordered structure, which may be the embedded GO in nanocomposite. An indication of successful polymerization for prepared GO-G1PPI-co-PPy nanocomposites by GO with G1PPI-co-PPy composites.

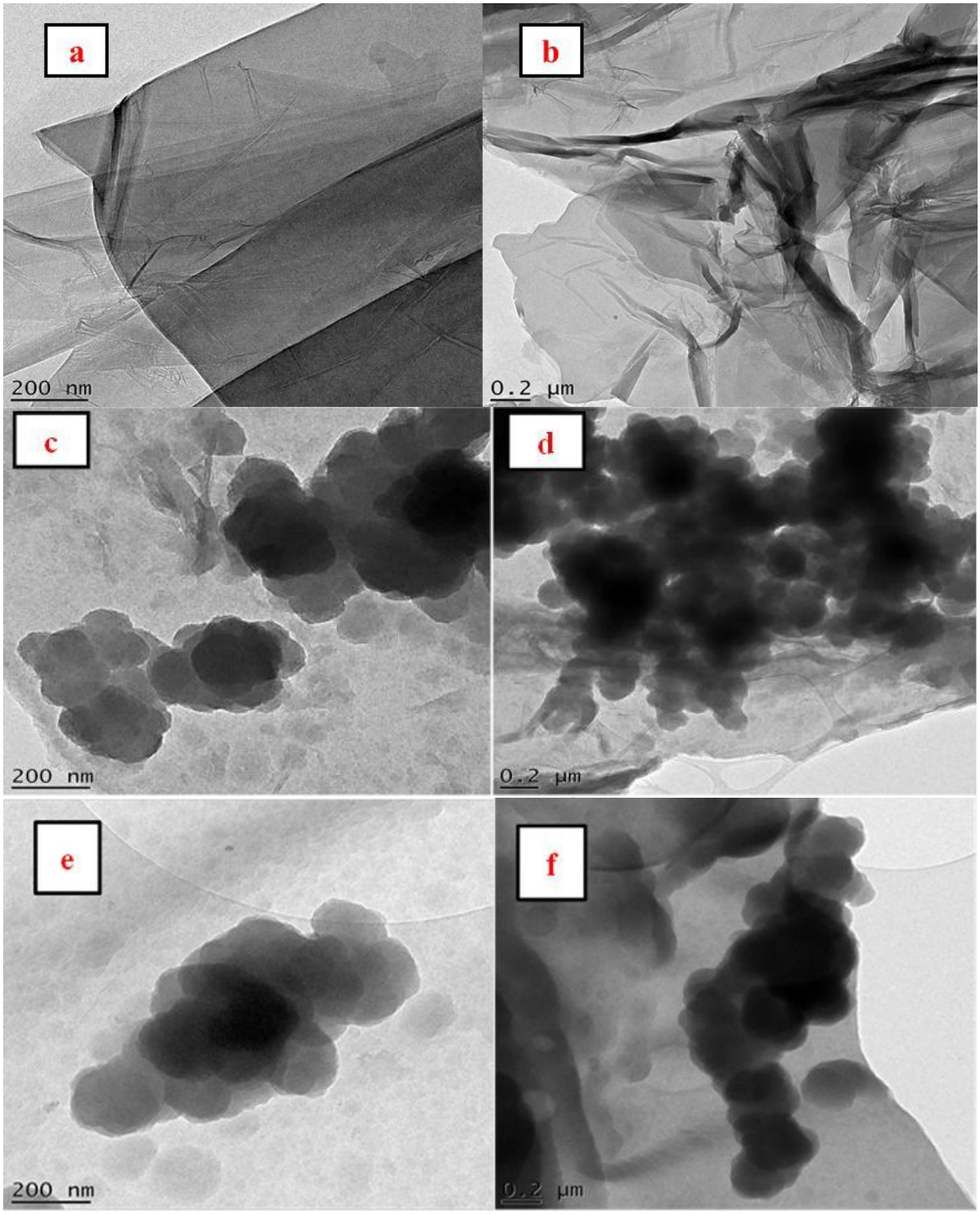

Figures 4.6 HR-TEM images: (a) GO, (b) G1PPI-co-PPy and (c) GO-G1PPI-co-PPy nanocomposites.

4.3- Electrochemical techniques

4.3.1- Electrochemical studies of the platform using cyclic voltammetry (CV)

This section provides the discussion on the electrochemical studies platform which includes; the electrochemical studies of the GO-G1PPI-co-PPy nanocomposite at different scan rate and the CV comparison of bare GCE, G1PPI-co-PPy and GO-G1PPI-co-PPy nanocomposite at the scan rate 50 mV/s. The calculated specific capacitance values for G1PPI-co-PPy and GO-G1PPI-co-PPy nanocomposite is so shown here.

Figure 4.7 (a) shows CV for the electrochemical polymerization from +460 mV to -800 mV of Pyrrole (Py) and GO on the functionalized dendrimer (PPI-2Py) modified GC electrode performed at a scan rate 50 mV/s for 60 cycles in 1 M H_2SO_4 aqueous electrolyte solution. The current increases as number of cycles increases. The anodic peak at around 300 mV indicates that the electrochemical polymerization of Py occurs due to nucleation and self-orientation of PPI-2Py on the electrode surface. The current continues to increase with increase in cycles. Growth of PPy at this step is believed to take place at the α position of the PPI-2Py forming the G1PPI-co-PPy [55]. Due to the abundant negative charges on its surface, GO could serve as a dopant which attracts the Py action radicals during the polymerization process [147]. As a result, G1PPI-co-PPy is formed on the edge and basal planes of GO (Figure 3.1).

Figure 4.7 (b), a shows the results of scan rate as studied (5-100 mV/s) for GO-G1PPI-co-PPy nanocomposite reveals the pseudocapacitance in aqueous 1 M H_2SO_4 electrolyte and the potential range was within -800 mV and +460 mV vs. It has been noted that with the change in voltage sweep rate from 5 mV/s to 100 mV/s the catholic peak at +129 mV shifts

negatively. And the anodic peak shifts towards more positively from +343 to +570 mV The presence of a distinct peak centered at 50 mV corresponds to the oxidation of the GO-G1PPI-co-PPy nanocomposite [24, 144].

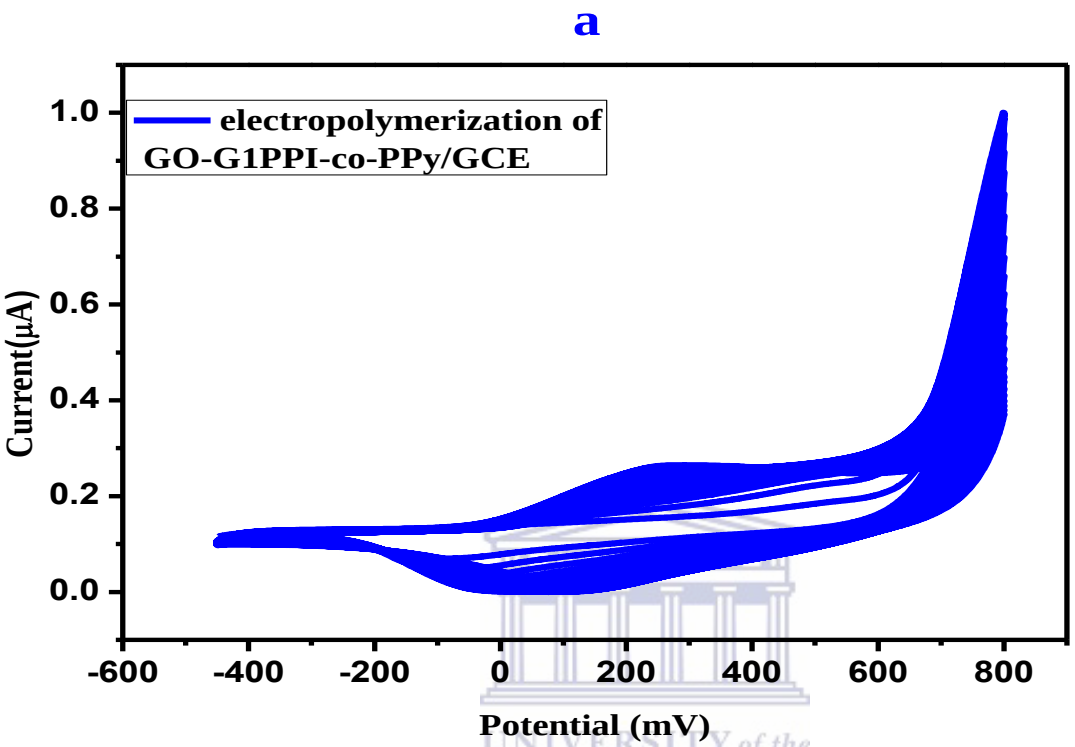

Figure 4.7(a)- Electropolymerization of GO-G1PPI-co-PPy nanocomposite in 1 M H_2SO_4 electrolyte solution at a scan rate of 50 mV/s using GCE.

Figure 4.7 (c) shows a comparative cyclic voltammetric plot of the bare glassy carbon electrode (GCE), G1PPI-co-PPy and GO-G1PPI-co-PPy nanocomposite in 1 M H_2SO_4 electrolyte, at a potential window of +460 mV to -800 mV at 50 mV/s. Compared with G1PPI-co-PPy, GO-G1PPI-co-PPy nanocomposite presents a slight shift peak potentials both cathodic and anodic and an enlarged area implying a good rate performance during charge-discharge process.

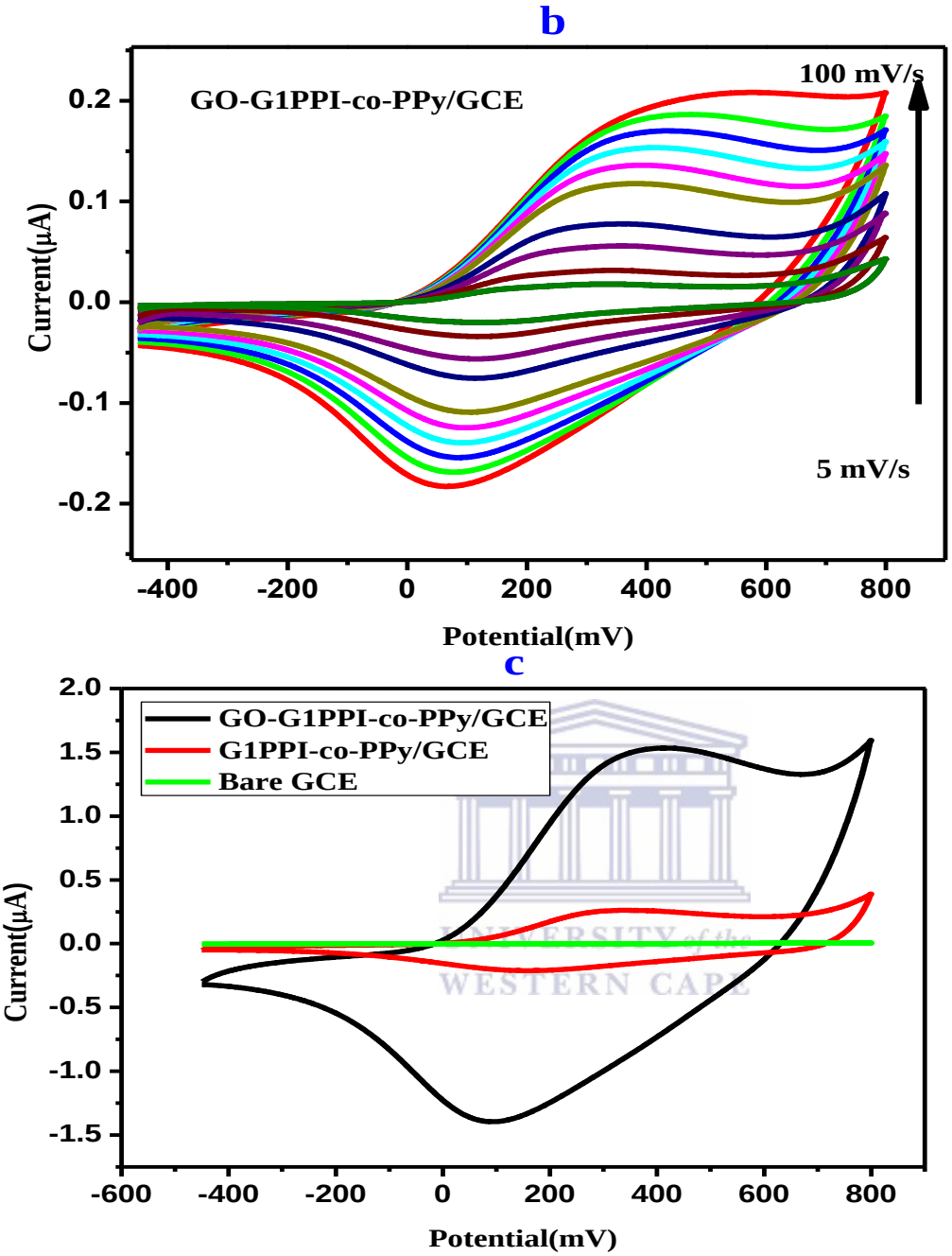

Figures 4.7(b, c)- CV in 1 M H_2SO_4 using GCE (b)-at different scan rates of GO-G1PPI-co-PPy nanocomposites (c) bare GCE, G1PPI-co-PPy and GO-G1PPI-co-PPy nanocomposites at 50 mV/s.

The CV curves for the G1PPI-co-PPy and GO-G1PPI-co-PPy nanocomposites supercapacitor at different scan rates are given in Figure 4.7.c. The specific capacitance of the electrode can be calculated according to the following equation from CV curves.

$$\frac{\quad}{\quad} \tag{4.1}$$

Where I+ and I- are maximum currents in positive and negative voltage scan respectively, C_{sp} is the specific capacitance based on the mass of electroactive materials (F/g), υ is the potential scan rate (mV/s), and m is the mass of the active electrode materials (g) [149].

The variation in the specific capacitance of G1PPI-co-PPy and GO-G1PPI-co-PPy nanocomposites as a function of scan rate is shown in Figure 4.7 d. Specific capacitance values for the GO-G1PPI-co-PPy nanocomposite are 236 and 118 F/g at respective scan rates of 5 and 100 mV/s; in turn, the specific capacitance values of G1PPI-co-PPy are 40 and 25 F/g, respectively, at respective scan rates of 5 and 100 mV/s. The high value of specific capacitance of G1PPI-co-PPy and GO-G1PPI-co-PPy nanocomposites at a lower scan rate is not only due to the oxidation or de oxidation of α–C or β–C atoms, but also the ions get enough time to migrate freely in the PPy matrix [144, 146-147]. However, as compared to the specific capacitances of G1PPI-co-PPy and GO-G1PPI-co-PPy nanocomposites are still high which indicates that the composites have good rate capability. Table 4.1 shows corresponding values of scan rate to the specific capacitance of the different electrodes used.

Table 4.1: Specific capacitances against scan rates of G1PPI-co-PPy/GCE and GO-G1PPI-co-PPy/GCE nanocomposites.

Scan rates (mV/s)	Specific capacitance (F/g) of GO-G1PPI-co-PPy/GCE	Specific capacitance (F/g) of G1PPI-co-PPy/GCE
5	118	40
10	121.5	33
20	125	24
30	125	28
40	132.8	28
50	141.3	27.6
60	156	27.2
70	158	26.2
80	170	25.8
90	203	25.3
100	236	25.1

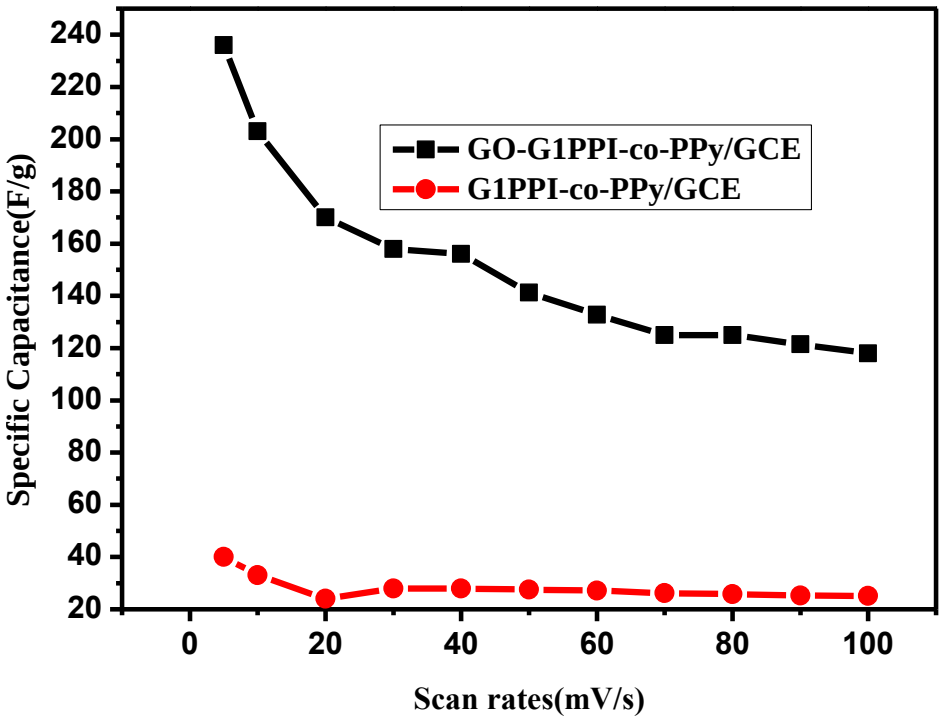

Figure 4.7(d)- Specific capacitance of G1PPI-co-PPy and GO-G1PPI-co-PPy nanocomposites.

4.3.2- Electrochemical impedance spectroscopic studies (EIS)

For the situation of an electrode in contact with electrolyte an equivalent circuit as is illustrated in Figures 4.8, can be impedance parameters.

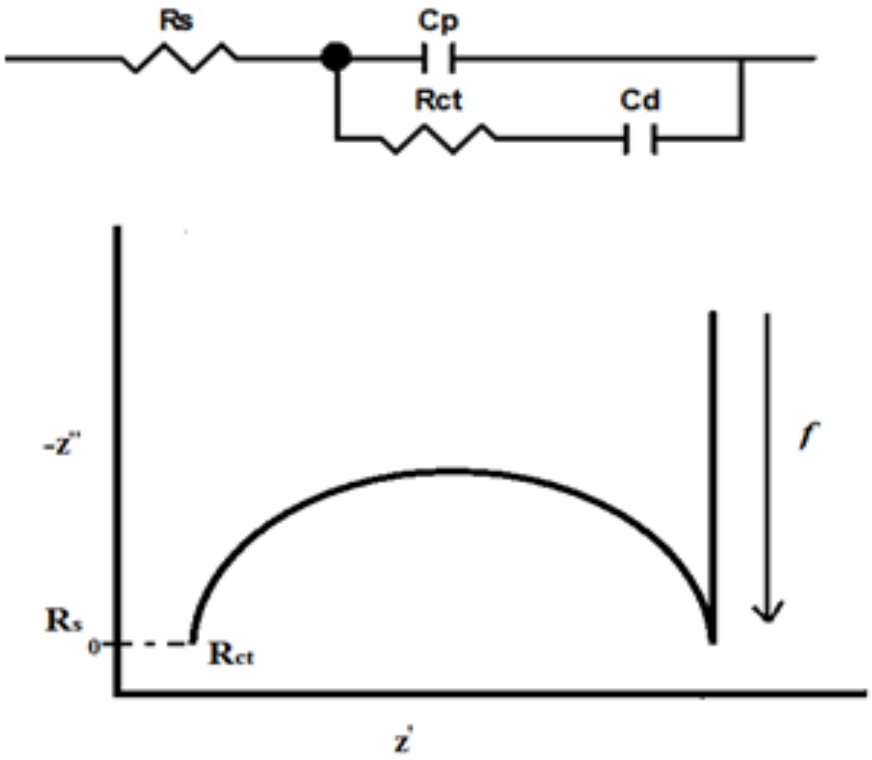

Figure 4.8- Equivalent circuit for an electrode in contact with an electrolyte and corresponding Nyquist plot [152].

Figure 4.8 is the circuit model and the parameters; R_s is the electrolyte resistance in the cell, R_{ct} is the charge transfer resistance, the EDL_s capacitance C_d and the pseudo-capacitive element C_p from the redox process involving the conductive star copolymer [149-151]. R_s, R_{ct} are easily determined from the Nyquist plot. The EDL_s capacitance can be calculated from the frequency at the maximum follower this equation

——— (4.2)

The product of R_{ct} and C_{dl} is often termed the time constant (τ) this can be estimated by equation ($\tau = R_{ct} \times C_{dl}$). The surface coverage $\boldsymbol{\theta}$ of 93.61% was obtained for the GO-G1PPI-co-PPy nanocomposite on the GCE electrode. The value was estimated from the R_{ct} value using the equation (4.3) [155].

$$\theta \qquad \text{———————} \qquad (4.3)$$

Furthermore, since the resistors R_s and R_{ct} are in series in the circuits the combined resistance becomes **($R = R_s + R_{ct}$)** [156].

Thus, a typical variation of the specific capacitance with the inverse of the combined resistance (1/R) as shown in (Table 4.2 below) arises wherein the specific capacitance increases with the reciprocal of the total resistance.

The maximum power density of the supercapacitor has been calculated from the low frequency data of the impedance spectra, according to the equation [15, 153]:

$$\text{——} \qquad (4.4)$$

Where V is the initial voltage, R is the equivalent series resistance and m is the total mass of the system. The ESR has been obtained from the *x*-intercept of the Nyquist plot. For GO-G1PPI-co-PPy electrode, with a cell voltage = 0.09 mV and a total mass = 3.2×10^{-3} g. The following kinetic parameters (Table 4.2 below) were obtained from fitting the EIS plots of the bare GCE, G1PPI-co-PPy and GO-G1PPI-co-PPy nanocomposite.

Table 4.2: Kinetic parameters obtained from the EIS plots of the different electrodes used.

Kinetic parameters	Bare/ GCE	G1PPI-co-PPy/GCE	GO-G1PPI-co-PPy/GCE
R_s (Ω)	58.9	68.63	9.21
C_d (F)	2.5×10^{-7}	1.2×10^{-6}	2.31×10^{-6}
R_{ct} (Ω)	5575	1087	356.6
C_P (F)	7.5×10^{-7}	1.7×10^{-5}	3.7×10^{-5}
ω_{max} (Hz)	719.4	769.2	1213.9
τ (s/rad)	139×10^{-5}	13×10^{-4}	82×10^{-5}
SC_s (F/g)	-	86.5	304
P_{max} (kW/kg)	-	6.5	25

EIS measurements were carried out in the frequency range 100 kHz to 1 Hz in 1 M H_2SO_4 electrolyte modified electrodes scanned at 50 mV/s to understand the frequency response of the bare glassy carbon electrode, G1PPI-co-PPy and GO-G1PPI-co-PPy nanocomposite electrodes super capacitors at room temperature.

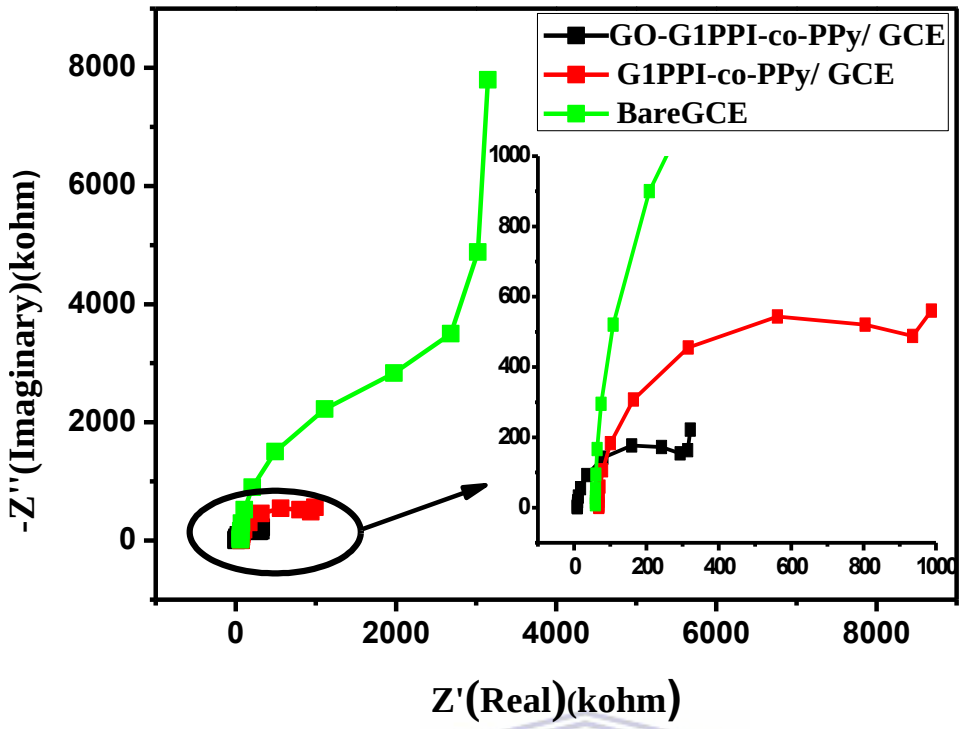

Figure 4.9 Nyquist plots bare GCE, G1PPI-co-PPy and GO-G1PPI-co-PPy nanocomposite electrodes at a frequency range of 0.1 Hz-1000Hz in 1 M H_2SO_4.

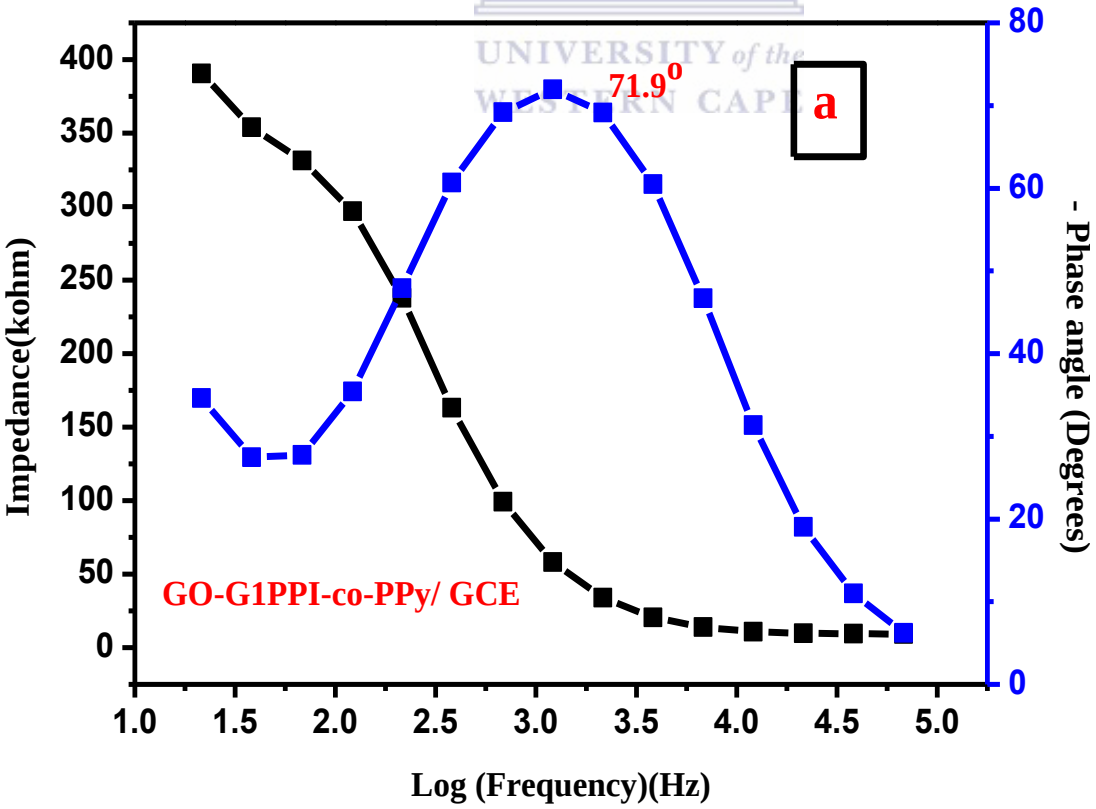

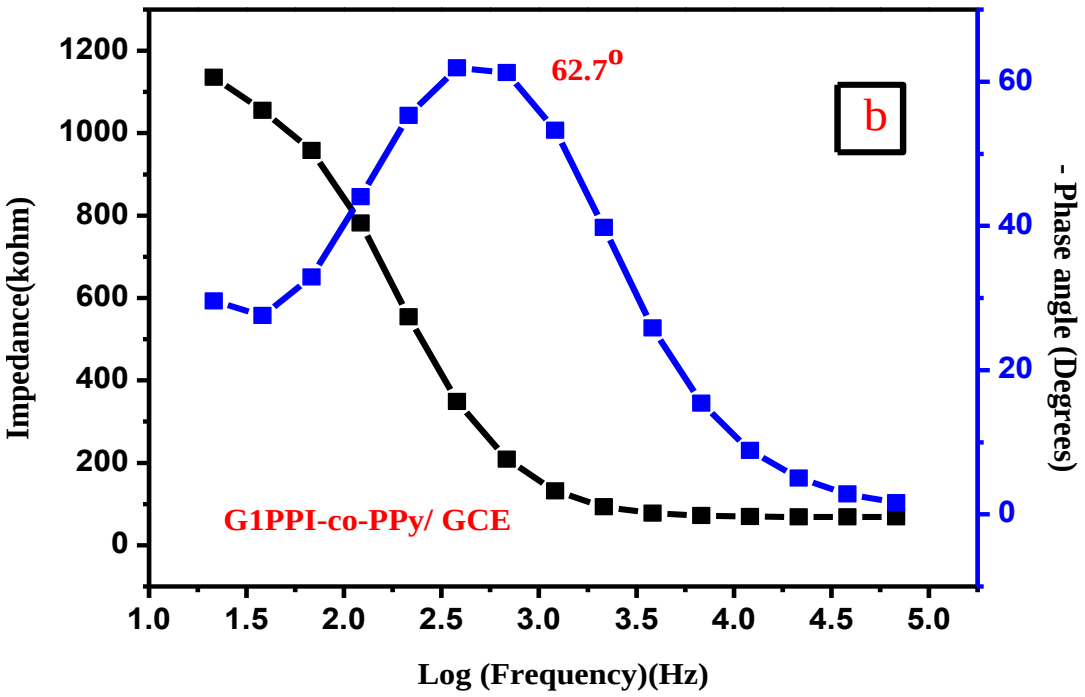

Figures 4.10- Bode plots of nanocomposites: (a) GO-G1PPI-co-PPy and (b) G1PPI-co-PPy.

For the Nyquist plot, the y-axis represents the negative number of the imaginary part of the measured impedance (Z') while the x-axis represents the real part of the measured impedance (Z''). Each data point is at a different frequency with the lower left portion of the curve corresponding to the higher frequencies. Figure 4 9 shown in both the curves displayed (a, b) a near vertical line at the low frequency region, suggesting the low ion diffusion resistance inside the capacitor. The arc shaped parts at the high frequency regions generally represent the resistance generated from the charge carrier transportation or namely R_{ct}. It is notable that the Bare GCE gave an R_{ct} value of 5575 (Ω), the R_{ct} value of G1PPI-co-PPy, was 1087 (Ω) and GO-G1PPI-co-PPy nanocomposite gave R_{ct} 356.6 (Ω). This indicates higher R_{ct} between the electrolyte and the ternary nanocomposite due to the poor conductivity of G1PPI-co-PPy. The binary nanocomposite exhibited the lowest R_{ct} due to the formation of a conductive network between G1PPI-co-PPy and GO within the nanocomposite matrix. It also facilitates

rapid transport of the electrolyte ions in the electrode during charge-discharge processes. Therefore, the composites can greatly reduce the diffusion length, resulting in the improvement of electrochemical properties of GO-G1PPI-co-PPy nanocomposite materials. Figure 4.10 (a) shows the Bode phase angle plot of GO-G1PPI-co-PPy nanocomposite. The phase angle is very close to -71.9° for frequencies up to 3 kHz suggesting the GO-G1PPI-co-PPy super capacitor device behaves as a more like an ideal capacitor [145]. A hypothetical electric circuit consists of parameters with well-defined electrical properties used to describe the EIS response of the GO-G1PPI-co-PPy based supercapacitor.

4.3.3- Performance of supercapacitor cell

The three electrode cell system was used to evaluate the performance of capacitor cell, using the GCE modified. The tester working at the constant charge-discharge mode was used to evaluate the parameters cell specific capacitance, specific energy, specific power and other parameters like the cell stability.

4.3.3.1- Galvanostatic charge-discharge

The galvanostatic charge-discharge measurements of the Bare GCE, G1PPI-co-PPy and GO-G1PPI-co-PPy nanocomposite at current = 30 × 10^{-3}A. Potential range for all electrodes within the potential window of CV (-800 to 460 mV) for about 120 s. Figure 4.11 shows that the GO-G1PPI-co-PPy nanocomposite has a longer and symmetrical charge-discharge curve, although it has lower potential than the bare GCE. Yet the GO-G1PPI-co-PPy nanocomposites achieved higher voltage compared to G1PPI-co-PPy. suggesting that GO-G1PPI-co-PPy has the higher energy storage capability; hence a higher specific capacitance is associated with GO-G1PPI-co-PPy which is the same as observed in the discharge profile

[155-157]. However shows the charge-discharge curves the charging time and discharging times almost constant value between the G1PPI-co-PPy and GO-G1PPI-co-PPy nanocomposite.

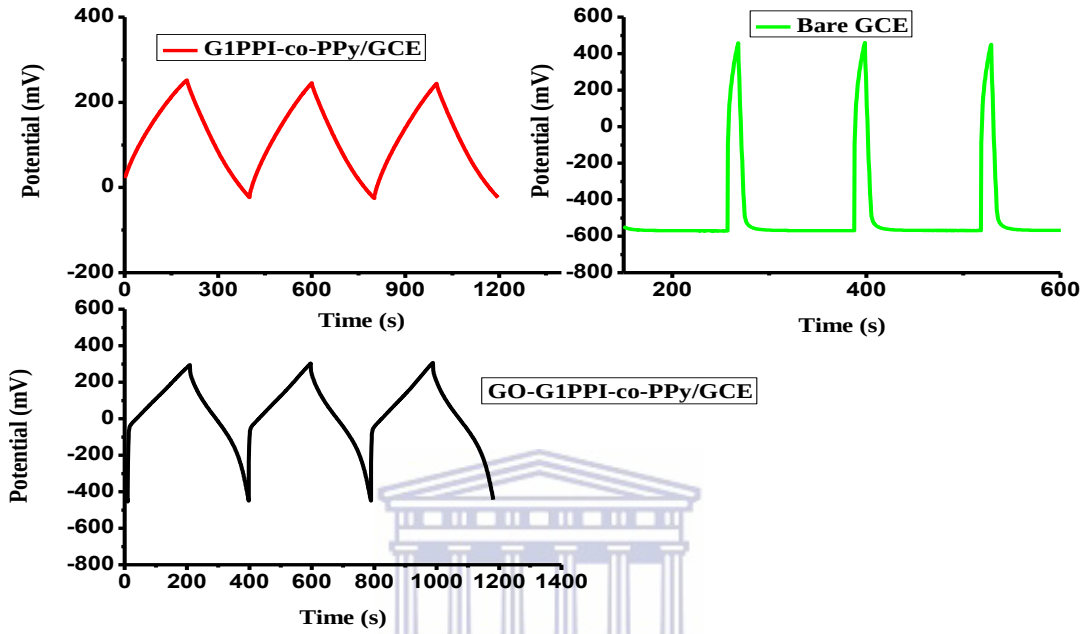

Figures 4.11- Charge-discharge curves: bare GCE, G1PPI-co-PPy and GO-G1PPI-co-PPy nanocomposite at 30 × 10^{-3}A.

The specific capacitance, power density and energy density are calculated based on the galvanic charging-discharging curves using the following equations [157-159]:

—— (4.5)

– (4.6)

(4.7)

where, Cs is the capacitances (F), I is the constant current (A) applied, m is the mass (g) of the electrode material (3.2 × 10^{-3} g) and ΔV is the change in potential energy density Eg

(Wh/kg), power density Pg. (W/kg).

When the same current is used for charging and discharging, the Coulombic efficiency (η) can be determined from the following equation (4.8) [163]:

— (4.8)

where t_D and t_C are the times for galvanostatic discharging and charging, respectively [164]. The Coulombic efficiency has been calculated to be 99.98%.

The above equation (4.5) was used to calculate the specific capacitance using the charging-discharging curve for G1PPI-co-PPy and GO-G1PPI-co-PPy nanocomposites; values were estimated to be 350 F/g and 105 F/g, respectively. The comparison of the specific capacitance of G1PPI-co-PPy and GO-G1PPI-co-PPy was done in 1 M H_2SO_4. In order to estimate the device stability and performance of both electrodes, the cell was run for 100 cycles. Figure 4.12 shows that the capacity was a horizontal line that remained unchanged during the cycle test, suggesting that GO-G1PPI-co-PPy has the specific capacitance possessed high stability for storing the capacitive charges [2, 161]. A slight fluctuation in capacitance for initial cycles was observed, which is attributed to the charge consumption due to some possible faradic reaction (s) with loosely bound surface groups at the electrode electrolyte interfaces.

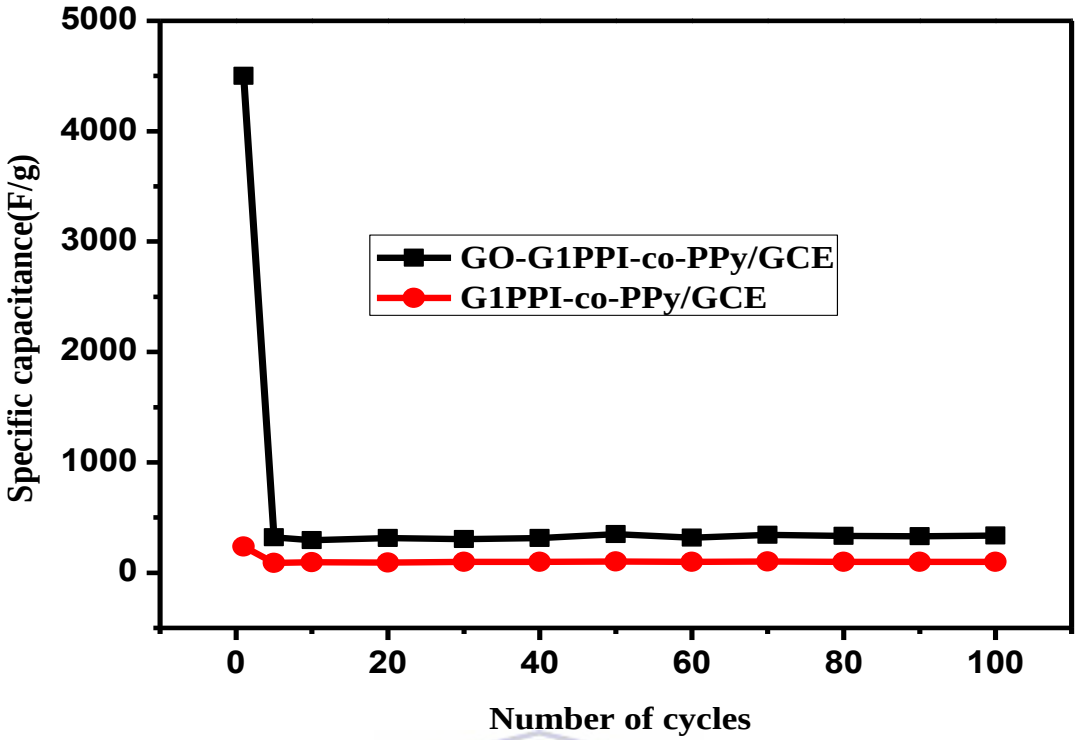

Figure 4.12- The specific capacitance vs. number of cycles for G1PPI-co-PPy and GO-G1PPI-co-PPy nanocomposites.

Energy density and power density have attracted much attention in evaluation of the performance of electrochemical capacitors, especially since such devices are perceived as capable of delivering high power on discharge although intrinsically their energy density is low. An important basis for relating power density to energy density takes the form of graphical presentation by a Ragone plot displayed by Figure 2.2. In evaluating the performance of electrochemical capacitors, as for batteries, characterization of their energy density and power density is one of the most important aspects of rating such electrochemical power devices. In Figure 4.13), the manifest ultrahigh energy density is 40 Wh/kg and power density ~98 KWh/kg for the GO-G1PPI-co-PPy/GCE. The improved of energy and power densities for the G1PPI-co-PPy/GCE after electro polymerization with GO. In addition that the results indicate the GO-G1PPI-co-PPy/GCE nanocomposite has electrochemical stability,

excellent capacitive performance, and the easiness of the preparation method suggests this unique material system is promising for future high performance energy storage applications.

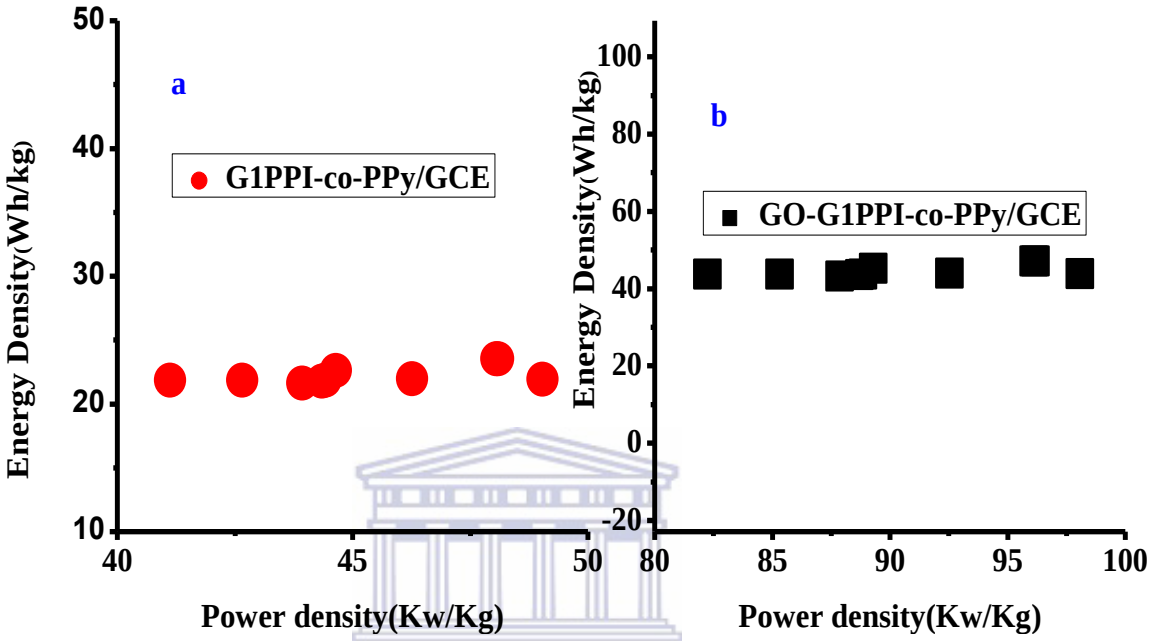

Figure 4.13- Energy density and power density for (a) G1PPI-co-PPy and (b) GO-G1PPI-co-PPy nanocomposites.

The materials are found to be relatively stable over large number of cycle. From the voltage-time profile for GO-G1PP-co-PPy shown in Figure 4.14 the potential remains stable over a large number of cycle meaning that the materials dose not degrade when cycled many times. They have longer cycle life and therefore a high structural integrity under repeated charging and discharging which is a desirable characteristic of supercapacitor materials. Voltage-time profile for the other nanocomposites is given in the appendix.

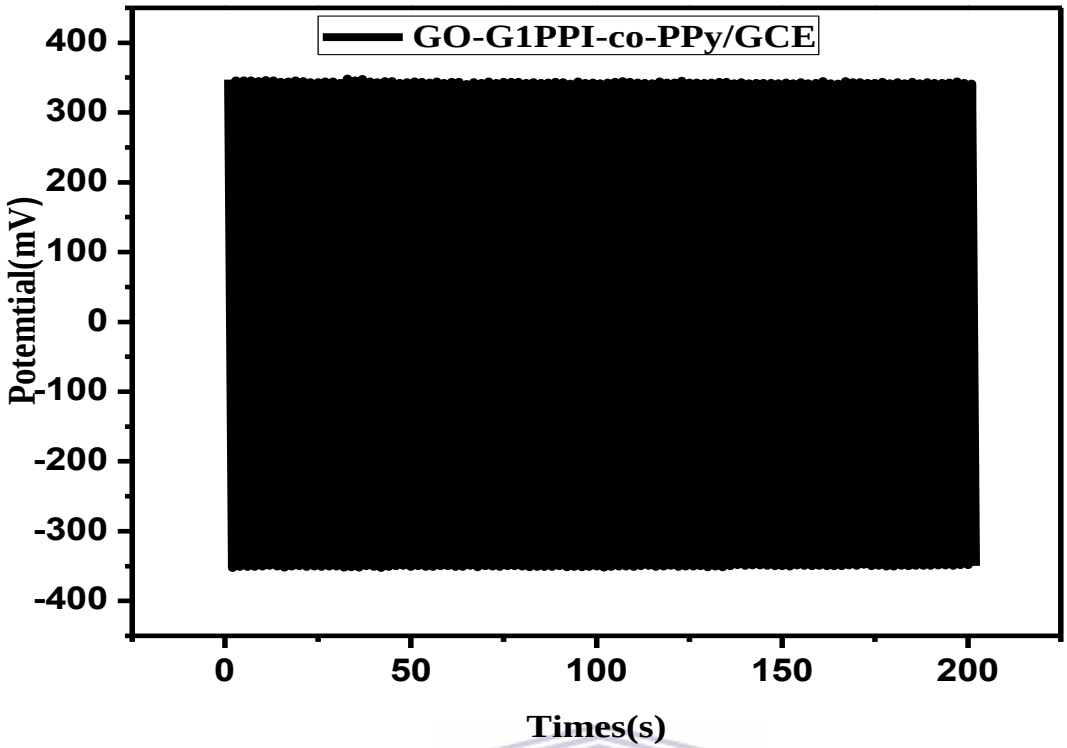

Figure 4.14- Voltage-time profile for GO-G1PP-co-PPy nanocomposites.

The specific capacitance of graphenated-poly (propylene imine)-co-polypyrrole nanocomposite electrode is higher than that of reported values of graphene- conducting polymers composites due to higher electroactivity than other the Conducting polymers. Table 4.3, below shows the specific capacitance for graphene with some conducting polymers composites for supercapacitors.

Table 4.3: Graphene-conducting polymer composites and their specific capacitance.

Composite	Specific capacitance	References
Graphene-poly(3, 4-ethylenedioxythiophene)	154 F/g	[166]
Graphene-polypyrrole	270 F/g	[158]
Graphene-polyaniline	261.4 F/g	[167]
Graphene-polythiophene	154 F/g	[168]
Graphenated-poly (propylene imine)-co-polypyrrole	350 F/g	Our work

CHAPTER FIVE

CONCLUSIONS AND RECOMMENDATIONS

5.1- Summary

This chapter gives brief overview of the main findings of this work which are answers to the questions and the objectives set in this thesis. Some recommendations will also be laid out for future work regarding this topic.

5.2- Conclusions

A graphenated-poly(propylene imine)-co-polypyrrole nanocomposite was successfully synthesized for the first time. Synthesis of this nanocomposite was through electrochemical polymerization reaction between graphene oxide sheet and dendritic conduction star copolymers. The character identification of the nanocomposite was done through HR-SEM. The surface morphology from HR-SEM shows that the nanocomposite has densely scattered florets attached to the

GO surface. This is particularly observed along the edges of the stacked nanosheets with a thickness of several nanometres. It can therefore be suggested that the compatibility between G1PPI-co-PPy and GO is sufficient to obtain nanosized dispersion without an additional surface treatment. The GO-G1PP-co-PPy scattered on the GO surface might be an indication of good capacitive behaviour.

Fourier Transform-Infrared (FT-IR) Spectroscopy also showed strong peak at 1617 cm^{-1} which is due to the downshifted of the carbonyl peak, probably due to the π–π interactions. The GO sheet and aromatic polypyrrole rings from G1PPI-co-PPy, indicating that the

carboxyl groups from GO acted as efficient dopants in the polymerization.

TGA analysis of the synthesized graphenated-poly(propylene imine)-co-polypyrrole shows that the synthesized nanocomposite is stable and can withstand temperature up to 250 °C. The observed major weight loss at 250 °C may be as a result of decomposition of the Py from the composite.

Beside, X-ray diffraction spectra support the complete coating of PPy by the GO. The characteristic diffraction peak of G1PPI-co-PPy is as seen at 24°.The disappeared of GO peak is an illustration of the purity and complete of coating of PPy. There is also good compatibility between G1PPI-co-PPy and GO as confirmed by HR-TEM analysis. An indication of successful polymerization for prepared GO-G1PPI-co-PPy nanocomposites by GO with G1PPI-co-PPy composites.

Alternatively, electrode graphenated-poly(propylene imine)-co-polypyrrole nanocomposite was synthesized electrochemically by copolymerized (7 µL) PPI-2Py with (70 µL) Py monomer and GO (10 g). The synthesized electrode graphenated-poly(propylene imine)-co-polypyrrole nanocomposite was successfully studied on the surface of the glassy carbon microelectrode. The CV analysis shows that peak cathodic at +129 mV and anodic shift +343 to +570 mV and compared with G1PPI-co-PPy, GO-G1PPI-co-PPy nanocomposite presents slight shift peak potentials foe both cathodic and anodic. The enlarged area is an indication of a performance rate during charge-discharge process. This result shows that the synthesized electrode graphenated-poly(propylene imine)-co-polypyrrole nanocomposite has potential application as a stable super capacitor electrode material which has high energy storage capacity and time duration.

Likewise, the Nyquist plots show power behavior of the constructed nanocomposite, GO-G1PPI-co-PPy/GCE such that the impedance increases on the imaginary part (Z'') as the frequency decreases reaching a close to parallel configuration to the imaginary impedance part, with lower R_{ct} around 365.6 Ω for GO-G1PPI-co-PPy than G1PPI-co-PPy. The Bode phase angle plot showed that the phase angle is very close to -71.9^{o} for frequencies up to 3 kHz suggesting the GO-G1PPI-co-PPy super capacitor device behaves as a more like an ideal capacitor. A hypothetical electric circuit consists of parameters with well-defined electrical properties used to describe the EIS response of the GO-G1PPI-co-PPy based supercapacitor. Interestingly, GO-G1PPI-co-PPy/GCE showed ideal capacitive behaviour for application in supercapacitor compared to G1PPI-co-PPy /GCE due to the increased capacitance from 105 F/g of G1PPI-co-PPy /GCE to 350 F/g of the GO-G1PPI-co-PPy /GC electrode. And From the voltage-time profile for GO-G1PP-co-PPy the potential remained stable over a large number of cycle meaning that the materials dose not degrade when cycled many times. They had longer cycle life and therefore a high structural integrity under repeated charging and discharging which is a desirable characteristic of supercapacitor materials. Voltage-time profile for the other nanocomposites is given in the appendix. The properties of nanocomposites show several advantages to be used as the supercapacitor electrode due to the high surface area, large flexibility, high reactivity and shorter ionic diffusion paths. The main advantage of the graphene based nanocomposites material is high conductivity which tailors the electron transport within the electrode material and enhances the cycle life and high rate capability which tailors the electron transport within the electrode material and enhances the cycle life and high rate capability. The GO-Conducting Polymer nanocomposites exhibited good electrochemical properties and cycling performance owing to their synergistic effects. It was taking higher capacitance, lower cost and shorter processing

time into consideration. Also the power density and energy density of these electrodes are compared in Ragone plot with existing commercial supercapacitors and various supercapacitors electrodes reported by other research groups.

5.3- RECOMMENDATIONS

This GO-G1PP-co-PPy nanocomposite material has advantages as a supercapacitor electrode relative to the conventional supercapacitor in the commercial sector. The synthesized nanocomposite is novel and cost effective material. This material is therefore recommended for commercial production and application. It is therefore imperative that the laboratory application of the nanocomposite must be reviewed. A review of other methods as well as + storage and cost. It is also very important to perform the environmental toxicity studies of the synthesized nanocomposite.

REFERENCES

[1] United Nations, *World Economic and Social Survey 2013, Sustainable Development Challenges*, New York, 2013.

[2] M. Hughes, G. Z. Chen, M. S. P. Shaffer, D. J. Fray, and a H. Windle, "Electrochemical capacitance of carbon nanotube-Polypyrrole Composite Films," no. 28, pp. 10, 2000.

[3] N. S. Choi, Z. Chen, S. A. Freunberger, X. Ji, Y. K. Sun, K. Amine, G. Yushin, L. F. Nazar, J. Cho, and P. G. Bruce, "Challenges facing lithium batteries and electrical double-layer capacitors," *Angewandte Chemie-International Edition*, vol. 51, no. 40, pp. 9994-10024, 2012.

[4] J. Keskinen, O. Kaukoniemi, R. Österbacka, F. Pettersson, V. Grönberg, and J. Eriksson, "Printed supercapacitors for energy storage," *Journal of energy*, 2013.

[5] N. Kumar, Y. C. Yu, Y. H. Lu, and T. Y. Tseng, "Fabrication of carbon nanotube/cobalt oxide nanocomposites via electrophoretic deposition for supercapacitor electrodes," *Journal of Materials Science*, vol. 51, no. 5, pp. 2320-2329, 2016.

[6] Z.-S. Wu, K. Parvez, X. Feng, and K. Müllen, "Graphene-based in-plane micro-supercapacitors with high power and energy densities.," *Journal of Alloys and CompoundsNature communications*, vol. 4, pp. 2487, 2013.

[7] W. Weiling, "Development of nanocomposites using Graphene synthesized by solvent exfoliation method," University of Toledo, 2015.

[8] M. Noked, C. Liu, J. Hu, K. Gregorczyk, G. W. Rubloff, and S. B. Lee, "Electrochemical thin layers in nanostructures for energy storage," *Journal of Chemical Research*, vol. 49, no. 10, pp. 2336-2346, 2016.

[9] Y. Xu, C.-Y. Chen, Z. Zhao, Z. Lin, C. Lee, X. Xu, C. Wang, Y. Huang, M. I. Shakir, and X. Duan, "Solution processable holey graphene oxide and its derived macrostructures for high-performance supercapacitors," *Journal of Nano Letters*, vol.

15, no. 7, pp. 4605-4610, 2015.

[10] M. Environmental, "Hybrid nano-structure for enhanced energy storage devices," University of Texas at El Paso, 2015.

[11] G. P. Pandey, S. A. Klankowski, T. Liu, J. Wu, and J. Li, "Toward highly stable solid-state unconventional thin-film battery-supercapacitor hybrid devices: Interfacing vertical core-shell array electrodes with a gel polymer electrolyte," *Journal of Power Sources*, vol. 342, pp. 1006-1016, 2017.

[12] G. Xiong, C. Meng, R. G. Reifenberger, P. P. Irazoqui, and T. S. Fisher, "A review of graphene-based electrochemical microsupercapacitors," *Journal of Electroanalysis*, vol. 26, no. 1, pp. 30-51, 2014.

[13] P. Gregoriou and A. Paraskevi, "Chemical sciences for nanostructures and biological applications magnetism and superconductivity : advanced materials and applications," 2013.

[14] C. Meng, O. Z. Gall, and P. P. Irazoqui, "A flexible super-capacitive solid-state power supply for miniature implantable medical devices," *Biomedical Microdevices*, vol. 15, no. 6, pp. 973-983, 2013.

[15] X. Jian, S. Liu, Y. Gao, W. Tian, Z. Jiang, X. Xiao, H. Tang, and L. Yin, "Carbon-based electrode materials for supercapacitor: progress, challenges and prospective solutions," *Journal of Electrical Engineering*, vol. 4, pp. 75-87, 2016.

[16] A. N. Aphale and P. K. Patra, "Graphene based nanocomposite hybrid electrodes for supercapacitors," University of Bridgeport, 2014.

[17] D. H. Seo, S. Yick, S. Pineda, D. Su, G. Wang, Z. J. Han, and K. Ostrikov, "Single-step, plasma-enabled reforming of natural precursors into vertical graphene electrodes with high areal capacitance," *Journal of ACS Sustainable Chemistry and Engineering*, vol. 3, no. 3, pp. 544-551, 2015.

[18] M. Hughes, G. Z. Chen, M. S. P. Shaffer, D. J. Fray, and a H. Windle, "Electrochemical capacitance of a nanoporous composite of carbon nanotubes and

polypyrrole," *Journal of Chemistry of Materials*, vol. 14, no. 28, pp. 1610-1613, 2002.

[19] M.-M. Titirici, R. J. White, C. Falco, and M. Sevilla, "Black perspectives for a green future: hydrothermal carbons for environment protection and energy storage," *Journal of Energy and Environmental Science*, vol. 5, no. 5, pp. 6796-6822, 2012.

[20] G. Wang, Z. Lei, and Z. Jiujun, "A review of electrode materials for electrochemical supercapacitors," *Journal of Chemical Science*, vol. 41,no. 2, pp. 797, 2012.

[21] C. Zhong, Y. Deng, W. Hu, J. Qiao, L. Zhang, and J. Zhang, "A review of electrolyte materials and compositions for electrochemical supercapacitors.," *Journal of Chemical Society reviews*, vol. 44, no. 21, pp. 7484-7539, 2015.

[22] M. Y. Ho, P. S. Khiew, D. Isa, and T. K. Tan, "A review of metal oxide composite electrode materials for electrochemical capacitors," *Journal of World scientific*, vol. 9, no. 6, pp. 1-25, 2014.

[23] L. L. Zhang, R. Zhou, and X. S. Zhao, "Carbon-based materials as supercapacitor electrodes," *Journal of Chemistry Society Reviews*, vol. 38, no. 29, pp. 2520-2531, 2009.

[24] F. Alvi, "Synthesis and characterization of nanocomposites for electrochemical capacitors," University of South Florida, 2012.

[25] L. Astratine, "Preparation and characterization of conducting polymer materials for electrochromic devices," Dublin Institute of Technology, 2012.

[26] M. D. Stoller, S. Park, Z. Yanwu, J. An, and R. S. Ruoff, "Graphene-based ultracapacitors," *Journal of Nano Letters*, vol. 8, no. 10, pp. 3498-3502, 2008.

[27] T. Kuila, S. Bose, A. K. Mishra, P. Khanra, N. H. Kim, and J. H. Lee, "Chemical functionalization of graphene and its applications," *Journal of Progress in Materials Science*, vol. 57, no. 7, pp. 1061-1105, 2012.

[28] Y. Zhu, S. Murali, W. Cai, X. Li, J. W. Suk, J. R. Potts, and R. S. Ruoff, "Graphene and graphene oxide: Synthesis, properties, and applications," *Journal of Advanced Materials*, vol. 22, no. 35, pp. 3906-3924, 2010.

[29] D. a. C. Brownson, L. J. Munro, D. K. Kampouris, and C. E. Banks, "Electrochemistry of graphene: not such a beneficial electrode material?," *Journal of the Royal Society of Chemistry*, vol. 1, no. 6, pp. 978, 2011.

[30] M. Hernaez, C. R. Zamarreño, S. Melendi-Espina, L. R. Bird, A. G. Mayes, and F. J. Arregui, "Optical fibre sensors using graphene-based materials: a review.," *Journal of Sensors*, vol. 17, no. 1, pp. 155, 2017.

[31] D. Dreyer, "The chemistry of graphene oxide," *Jornal of Chemical Society*, vol. 39, no. 1, pp. 61-95, 2015.

[32] G. Eda and M. Chhowalla, "Chemically derived graphene oxide: towards large-area thin-film electronics and optoelectronics," *Journal of Advanced Materials*, vol. 22, no. 22, pp. 2392-2415, 2010.

[33] A. Tararan, A. Zobelli, A. M. Benito, W. K. Maser, and O. Stéphan, "Revisiting graphene oxide chemistry via spatially-resolved electron energy loss spectroscopy," *Journal of Chemistry of Materials*, vol. 28, no. 11, pp. 3741-3748, 2016.

[34] D. Chen, H. Feng, and J. Li, "Graphene oxide : preparation, functionalization, and electrochemical applications," *Journal of Chemical reviews*, vol. 112,no. 11, pp. 6027-6053, 2012.

[35] I. Latif, T. B. Alwan, and A. H. Al-Dujaili, "Low frequency dielectric study of PAPA-PVA-GR nanocomposites," *Journal of Nanoscience and Nanotechnology*, vol. 2, no. 6, pp. 190-200, 2012.

[36] Y. K. Kim and D. H. Min, "Durable large-area thin films of graphene/carbon nanotube double layers as a transparent electrode," *Journal of Langmuir*, vol. 25, no. 19, pp. 11302-11306, 2009.

[37] and A. Z. D. Pacilé, J. C. Meyer, Ç. Ö. Girit, "The two-dimensional phase of boron nitride: Few-atomic-layer sheets and suspended membranes," *Journal of Applied Physics Letters*, vol. 92, no. 13, pp. 212-214, 2008.

[38] S. N. Alam, N. Sharma, and L. Kumar, "Synthesis of Graphene Oxide (GO) by

modified Hummers method and its thermal reduction to obtain reduced graphene oxide (rGO)," *Journal of Graphene*, vol. 6, no. 1, pp. 1-18, 2017.

[39] L. Shahriary and A. a. Athawale, "Graphene oxide synthesized by using modified Hummers approach," *Journal of Renewable Energy and Environmental Engineering*, vol. 2, no. 1, pp. 58-63, 2014.

[40] D. C. Marcano, D. V Kosynkin, J. M. Berlin, A. Sinitskii, Z. Z. Sun, A. Slesarev, L. B. Alemany, W. Lu, and J. M. Tour, "Improved synthesis of graphene oxide," *Journal of American Chemical Society Nano*, vol. 4, no. 8, pp. 4806-4814, 2010.

[41] W. Ahn, H. S. Song, S.-H. Park, K. B. Kim, K.-H. Shin, S. N. Lim, and S. H. Yeon, "Morphology-controlled graphene nanosheets as anode material for lithium-ion batteries," *Journal of Electrochimica Acta*, vol. 132, pp. 172-179, 2014.

[42] J. Chen, Y. Li, L. Huang, C. Li, and G. Shi, "High-yield preparation of graphene oxide from small graphite flakes via an improved Hummers method with a simple purification process," *Journal of Carbon*, vol. 81, pp. 826-834, 2015.

[43] N. Dubey and M. Leclerc, "Conducting polymers: efficient thermoelectric materials," *Journal of Polymer Science Part B: Polymer Physics*, vol. 49, no. 7, pp. 467-475, 2011.

[44] Q. Wei, M. Mukaida, K. Kirihara, Y. Naitoh, and T. Ishida, "Photoinduced dedoping of conducting polymers: an approach to precise control of the carrier concentration and understanding transport properties," *ACS Applied Materials and Interfaces*, vol. 8, no. 3, pp. 2054-2060, 2016.

[45] H. An, Y. Wang, X. Wang, N. Li, and L. Zheng, "The preparation of PANI/CA composite electrode material for supercapacitors and its electrochemical performance," *Journal of Solid State Electrochemistry*, vol. 14, no. 4, pp. 651-657, 2010.

[46] M. Mastragostino, C. Arbizzani, and F. Soavi, "Polymer-based supercapacitors," *Journal of Power Sources*, vol. 97-98, pp. 812-815, 2001.

[47] and G. C. Gao, Caiyan, "Conducting polymer/carbon particle thermoelectric

composites: Emerging green energy materials," *Journal of Composites Science and Technology*, vol. 124, pp. 52-70, 2016.

[48] Su, Yisong, "Advanced Electrode Materials for Electrochemical Supercapacitors," University of McMaster, 2015.

[49] M. Gerard, M. Gerard, A. Chaubey, and B. D. Malhotra, "Application of conducting polymers to biosensors. biosens bioelectron application of conducting polymers to biosensors," *Journal of Biosensors and Bioelectronics*, vol. 17, no. 5, pp. 345-359, 2002.

[50] W. C. Chen, T. C. Wen, C. C. Hu, and A. Gopalan, "Identification of inductive behavior for polyaniline via electrochemical impedance spectroscopy," *Journal of Electrochimica Acta*, vol. 47, no. 8, pp. 1305-1315, 2002.

[51] C. Guo, L. Zhou, and J. Lv, "Effects of expandable graphite and modified ammonium polyphosphate on the flame-retardant and mechanical properties of wood flour-polypropylene composites," *Journal of polymer and Polymer Composites*, vol. 21, no. 7, pp. 449, 2013.

[52] I. Y. Sapurina and M. a. Shishov, "Oxidative polymerization of aniline: molecular synthesis of polyaniline and the formation of supramolecular structures," INTECH Open Access Publisher, 2012.

[53] Z. Gao, W. Yang, J. Wang, H. Yan, Y. Yao, J. Ma, B. Wang, M. Zhang, and L. Liu, "Electrochemical synthesis of layer-by-layer reduced graphene oxide sheets/polyaniline nanofibers composite and its electrochemical performance," *Journal of Electrochimica Acta*, vol. 91, pp. 185-194, 2013.

[54] R. Kumar, S. Singh, and B. C. Yadav, "Conducting Polymers : Synthesis, Properties and Applications," *Journal of Science*, vol. 2, no. 11, pp. 595-604, 2015.

[55] A. A. A. Baleg, N. M. Jahed, O. A. Arotiba, S. N. Mailu, N. R. Hendricks, P. G. Baker, and E. I. Iwuoha, "Synthesis and characterization of poly(propylene imine) dendrimer-Polypyrrole conducting star copolymer," *Journal of Electroanalytical Chemistry*, vol. 652, no. 1, pp. 18-25, 2011.

[56] and R. D. R. Wang, Fei, "Reflective and conductive star polymers," U.S. Patent No. 6,025,462, 2000.

[57] J. Wan, C. Li, H. Fan, Z. Y. Bu, and B. G. Li, "Elucidating isothermal crystallization behaviors of nylon-11s. Influence of star-chain branching," *Journal of Thermochimica Acta*, vol. 544, pp. 99-104, 2012.

[58] O. Altintas, A. P. Vogt, C. Barner-Kowollik, and U. Tunca, "Constructing star polymers via modular ligation strategies," *Journal of Polymer Chemistry*, vol. 3, no. 1, pp. 34-45, 2012.

[59] E. Poverenov, N. Zamoshchik, A. Patra, Y. Ridelman, and M. Bendikov, "Unusual doping of donor-acceptor-type conjugated polymers using lewis acids," *Journal of the American Chemical Society*, vol. 136, no. 13, pp. 5138-5149, 2014.

[60] S. Bhadra, D. Khastgir, N. K. Singha, and J. H. Lee, "Progress in preparation, processing and applications of polyaniline," *Journal of Polymer Science*, vol. 34, no. 8, pp. 783-810, 2009.

[61] T. Ndlovu, O. a Arotiba, R. W. Krause, and B. B. Mamba, "Electrochemical detection of o-nitrophenol on a Poly(propyleneimine)-gold nanocomposite modified glassy carbon electrode," *Journal of Electrochemical Science*, vol. 5, pp. 1179-1186, 2010.

[62] P. R. L. Malenfant, M. Jayaraman, and J. M. J. Fre, "Dendrimer-supported oligothiophene synthesis: aliphatic ether dendrimers in the Preparation of oligothiophenes with Minimal Substitution," *Journal of the Chemical materials*, vol. 11, no. 12, pp. 3420-3422, 1999.

[63] T. N. Lin, J. C. Huang, J. L. Shen, C. M. Chu, J. M. Yeh, Y. W. Chen-Yang, C. H. Chiu, and H. C. Kuo, "Hybrid dendrimer/semiconductor nanostructures with efficient energy transfer via optical waveguiding," *Journal of Physical Chemistry C*, vol. 119, no. 9, pp. 5107-5112, 2015.

[64] K. S. Novoselov, V. I. Fal, L. Colombo, P. R. Gellert, M. G. Schwab, K. Kim, V. I. F. Ko, L. Colombo, P. R. Gellert, M. G. Schwab, and K. Kim, "A roadmap for graphene," *Journal of Nature*, vol. 490, no. 7419, pp. 192-200, 2013.

[65] J. L. Hedrick, M. Trollsås, C. J. Hawker, B. Atthoff, H. Claesson, A. Heise, and R. D. Miller, "Dendrimer-like Star block and amphiphilic copolymers by combination of ring opening and atom transfer radical polymerization," *Journal of Macromolecules*, vol. 31, pp. 8691-8705, 1998.

[66] R. C. Hedden and B. J. Bauer, "Structure and dimensions of PAMAM/PEG dendrimer-star polymers," *Journal of Macromolecules*, vol. 36, pp. 1829-1835, 2003.

[67] P. L. Golas and K. Matyjaszewski, "Marrying click chemistry with polymerization: expanding the scope of polymeric materials," *Journal of Chemical Society Reviews*, vol. 39, no. 4, pp. 1338-1354, 2010.

[68] Y. Zhao, X. Shuai, C. Chen, and F. Xi, "Synthesis and characterization of star-shaped poly(L-lactide) s initiated with hydroxyl-terminated poly(amidoamine) (PAMAM-OH) dendrimers," *Journal of Chemistry of Materials*, vol. 15, no 14, pp. 2836-2843, 2003.

[69] A. Heise, S. Diamanti, J. L. Hedrick, C. W. Frank, and R. D. Miller, "Investigation of the initiation behavior of a dendritic 12-arm initiator in atom transfer radical polymerization," *Journal of Macromolecules*, vol. 34, no. 11, pp. 3798-3801, 2001.

[70] Q. Zheng and C. Y. Pan, "Preparation and characterization of dendrimer-star PNIPAAM using dithiobenzoate-terminated PPI dendrimer via RAFT polymerization," *Journal of European Polymer*, vol. 42, no. 4, pp. 807-814, 2006.

[71] Q. Zheng and C. Y. Pan, "Synthesis and characterization of dendrimer-star polymer using dithiobenzoate-terminated poly(propylene imine) dendrimer via reversible addition-fragmentation transfer polymerization," *Journal of Macromolecules*, vol. 38, no. 16, pp. 6841-6848, 2005.

[72] J. Wang, M. Jiang, A. Fortes, and B. Mukherjee, "New label-free DNA recognition based on doping nucleic-acid probes within conducting polymer films," *Journal of Analytica Chimica Acta*, vol. 402, no. 1, pp. 7-12, 1999.

[73] T. M. Miller, T. X. Neenan, E. W. Kwock, and S. M. Stein, ""Dendritic analogs of engineering plastics: a general one-step synthesis of dendritic polyaryl ethers," *Journal of the American Chemical Society*, vol. 115,no.1, pp. 356-357, 1993.

[74] L. L. Miller, R. G. Duan, D. C. Tully, and D. A. Tomalia, “Electrically conducting dendrimers,” *Journal of the American Chemical Society*, vol. 119, no. 5, pp. 1005-1010, 1997.

[75] S. Balurkar, R. S. Pentewar, M. Bhange, P. Bhosle, and A. Jadhav, “Dendrimers: a novel approach for drug delivery,” *Journal of Pharmaceutical Research*, vol. 5, no. 9, pp. 2231-6876, 2015.

[76] R. Esfand and D. a. Tomalia, “Poly(amidoamine) (PAMAM) dendrimers : from biomimicry to drug delivery and biomedical applications,” *Journal of Drug Discovery Today*, vol. 6, no. 8, pp. 427-436, 2001.

[77] S. Watanabe and S. L. Regen, “Dendrimers as Building Blocks for Multilayer Construction,” *Journal of the American Chemical Society*, vol. 116, no. 19, pp. 8855-8856, 1994.

[78] A. Sharma, F. Haque, F. Pi, L. S. Shlyakhtenko, B. M. Evers, and P. Guo, “Controllable self-assembly of RNA dendrimers,” *Journal of Nanomedicine: Nanotechnology, Biology and Medicine*, vol. 12, no. 3, pp. 835-844, 2016.

[79] P. Kesharwani, V. Mishra, and N. K. Jain, “Generation dependent hemolytic profile of folate engineered poly(propyleneimine) dendrimer,” *Journal of Drug Delivery Science and Technology*, vol. 28, pp. 1-6, 2015.

[80] E. K. Woller and M. J. Cloninger, “Mannose functionalization of a sixth generation dendrimer,” *Journal of Biomacromolecules*, vol. 2, no. 3, pp. 1052-1054, 2001.

[81] Huck, Wilhelm TS, Frank CJM van Veggel and David N. Reinhoudt, “‘Controlled assembly of nanosized metallodendrimers.,’” *Journal of Angewandte Chemie International Edition in English*, vol. 35.11, pp. 1213-1215, 1996.

[82] X. Cao, Y. Shi, X. Wang, R. W. Graff, and H. Gao, “Design a Highly Reactive trifunctional core molecule to obtain hyperbranched polymers with over a million molecular weight in one-pot click polymerization,” *Journal of Macromolecules*, vol. 49, no. 3, pp. 760-766, 2016.

[83] J.-P. Korb and R. G. Bryant, "Magnetic field dependence of proton spin-lattice relaxation times.," *Journal of the Society of Magnetic Resonance*, vol. 48, pp. 21-26, 2002.

[84] M. J. Joralemon, R. K. O'Reilly, J. B. Matson, A. K. Nugent, C. J. Hawker, and K. L. Wooley, "Dendrimers clicked together divergently," *Journal of Macromolecules*, vol. 38, no. 13, pp. 5436-5443, 2005.

[85] A. S. Chauhan, "Dendrimer nanotechnology for enhanced formulation and controlled delivery of resveratrol," *Annals of the New York Academy of Sciences*, vol. 1348, no. 1, pp. 134-140, 2015.

[86] M. J. Taylor, S. Tanna, and T. Sahota, "In vivo study of a polymeric glucose-sensitive insulin delivery system using a rat model.," *Journal of pharmaceutical sciences*, vol. 99, no. 10, pp. 4215-4227, 2010.

[87] R. G. Duan, L. L. Miller, D. A. Tomalia, I. West, and S. Andrews, "An electrically conducting dendrimer," *Journal of the American Chemical Society*, vol. 117, no. 43, pp. 10783-10784, 1995.

[88] C. J. Hawker, E. E. Malmstrom, C. W. Frank, and J. P. Kampf, "Exact linear analogs of dendritic polyether macromolecules: Design, synthesis, and unique properties," *Journal of the American Chemical Society*, vol. 119, no. 41, pp. 9903-9904, 1997.

[89] A. Almonam, A. Alsalam, and E. I. Iwuoha, "Synthesis and electrochemistry of novel conducting dendrimeric star copolymers on poly(propylene imine) dendrimer," University of the Western Cape, 2011.

[90] S. E. Stiriba, H. Frey, and R. Haag, "Dendritic polymers in biomedical applications: From potential to clinical use in diagnostics and therapy," *Journal of Angewandte Chemie-International Edition*, vol. 41, no. 8, pp. 1329-1334, 2002.

[91] J. W. F. To, J. He, J. Mei, R. Haghpanah, Z. Chen, T. Kurosawa, S. Chen, W.-G. Bae, L. Pan, and J. B.-H. Tok, "Hierarchical N-doped carbon as CO_2 adsorbent with high CO_2 selectivity from rationally designed polypyrrole precursor," *Journal of the American Chemical Society*, vol. 138, no. 3, pp. 1001-1009, 2016.

[92] A. Razaq, M. Strømme, L. Nyholm, and A. Mihranyan, "Ultrafast all-polymer paper-based," *Journal of Nano letters*, vol. 9, no. 10, pp. 3635-3639, 2009.

[93] P. Camurlu, "Polypyrrole derivatives for electrochromic applications," *Journal of RSC Advances*, vol. 4, no. 99, pp. 55832-55845, 2014.

[94] J. H. Chen, Z. P. Huang, D. Z. Wang, S. X. Yang, W. Z. Li, J. G. Wen, and Z. F. Ren, "Electrochemical synthesis of polypyrrole films over each of well-aligned carbon nanotubes," *Journal of Synthetic Metals*, vol. 125,no. 3, pp. 289-294, 2001.

[95] J. Xu, D. Wang, Y. Yuan, W. Wei, L. Duan, L. Wang, H. Bao, and W. Xu, "Polypyrrole/reduced graphene oxide coated fabric electrodes for supercapacitor application," *Journal of Organic Electronics: physics*, vol. 24, pp. 153-159, 2015.

[96] J. Wu and J. Pawliszyn, "Preparation and applications of polypyrrole films in solid-phase microextraction," *Journal of Chromatography A*, vol. 909, pp. 37-52, 2001.

[97] K. Liu, Y. Li, G. Zhang, X. Lv, and M. Yang, "The effect of humidity on the electrical behavior of a cationic conjugated polyelectrolyte based on poly(phenylene vinylene)," *journal of Sensors and Actuators, B: Chemical*, vol. 135, no. 2, pp. 597-602, 2009.

[98] F. Ahmed, B. S. Lalia, V. Kochkodan, N. Hilal, and R. Hashaikeh, "Electrically conductive polymeric membranes for fouling prevention and detection: A review," *Journal of Desalination*, vol. 391, pp. 1-15, 2016.

[99] A. Cirpan, S. Alkan, L. Toppare, Y. Hepuzer, and Y. Yagci, "Immobilization of invertase in conducting copolymers of 3-methylthienyl methacrylate," *Jornal of Bioelectrochemistry*, vol. 59, no. 1-2, pp. 29-33, 2003.

[100] J. Pellegrino, "The use of conducting polymers in membrane-based separations: A review and recent developments," *Annals of the New York Academy of Sciences*, vol. 984, no. 1, pp. 289-305, 2003.

[101] R. Kiefer, S. Y. Chu, P. A. Kilmartin, G. A. Bowmaker, R. P. Cooney, and J. Travas-Sejdic, "Mixed-ion linear actuation behaviour of polypyrrole," *Journal of Electrochimica Acta*, vol. 52, no. 7, pp. 2386-2391, 2007.

[102] K. M. Molapo, P. M. Ndangili, R. F. Ajayi, G. Mbambisa, S. M. Mailu, N. Njomo, M. Masikini, P. Baker, and E. Iwuoha, "Electronics of conjugated polymers (I): polyaniline," *Journal of Electrochemical Science*, vol. 7, pp. 11859-11875, 2012.

[103] P. M. George, A. W. Lyckman, D. A. Lavan, A. Hegde, Y. Leung, R. Avasare, C. Testa, P. M. Alexander, R. Langer, and M. Sur, "Fabrication and biocompatibility of polypyrrole implants suitable for neural prosthetics," *Biomaterials*, vol. 26, no. 17, pp. 3511-3519, 2005.

[104] A. H. Nashat, and R. Langer, "Temporal characteristics of activation, deactivation, and restimulation of signal transduction following depolarization in the pheochromocytoma cell line PC12" *Journal of Molecular and cellular biology*, vol. 23, no. 14, pp. 4788-4795, 2003.

[105] A. N. Zelikin, D. M. Lynn, J. Farhadi, I. Martin, V. Shastri, and R. Langer, "Erodible conducting polymers for potential biomedical applications," *Journal of Angewandte Chemie-International Edition*, vol. 41, no. 1, pp. 141-144, 2002.

[106] Y. Liu, T. Cui, and K. Varahramyan, "All-polymer capacitor fabricated with inkjet printing technique," *Journal of Solid-State Electronics*, vol. 47, no. 9, pp. 1543-1548, 2003.

[107] H. Yoon, "Current trends in sensors based on conducting polymer nanomaterials," *Journal of Nanomaterials*, vol. 3, no. 3, pp. 524-549, 2013.

[108] P. Somani and S. Radhakrishnan, "Effect of dye aggregation on the photosensitization effect of conducting polypyrrole sensitized with Prussian Blue," *Journal of Materials Chemistry and Physics*, vol. 70, no. 2, pp. 150-155, 2001.

[109] T. Uyar, L. Toppare, and J. Hacaloğlu, "Pyrolysis mass spectrometric analysis of poly(pyrrole-g-(2-(N-pyrrolyl)ethylvinylether)," *Journal of Analytical and Applied Pyrolysis*, vol. 68-69, pp. 15-24, 2003.

[110] J. Zhao, H. Li, G. Cheng, and Y. Cai, "On predicting the effective elastic properties of polymer nanocomposites by novel numerical implementation of asymptotic homogenization method," *Journal of Composite Structures*, vol. 135, pp. 297-305,

2016.

[111] H. Kim, A. A. Abdala, and C. W. MacOsko, "Graphene/polymer nanocomposites," *Journal of Macromolecules*, vol. 43, no. 16, pp. 6515-6530, 2010.

[112] F. Kim, L. J. Cote, and J. Huang, "Graphene oxide: Surface activity and two-dimensional assembly," *Journal of Advanced Materials*, vol. 22, no. 17, pp. 1954-1958, 2010.

[113] S. Bose, T. Kuila, M. E. Uddin, N. H. Kim, A. K. T. Lau, and J. H. Lee, "In-situ synthesis and characterization of electrically conductive polypyrrole/graphene nanocomposites," *Journal of Polymer*, vol. 51, no. 25, pp. 5921-5928, 2010.

[114] A. A. Balandin, "Thermal properties of graphene and nanostructured carbon materials," *Journal of Nature. Materials*, vol. 10, no. 8, pp. 569, 2011.

[115] Y. S. Lim, Y. P. Tan, H. N. Lim, W. T. Tan, M. A. Mahnaz, Z. A. Talib, N. M. Huang, A. Kassim, and M. A. Yarmo, "Polypyrrole/graphene composite films synthesized via potentiostatic deposition," *Journal of Applied Polymer Science*, vol. 128, no. 1, pp. 224-229, 2013.

[116] Y. Cui, S. I. Kundalwal, and S. Kumar, "Gas barrier performance of graphene/ polymer nanocomposites," *Journal of Carbon*, vol. 98, pp. 313-333, 2016.

[117] J. Seyyed Monfared Zanjani, B. Saner Okan, and Y. Menceloglu, "Manufacturing of multilayer graphene oxide/poly(ethylene terephthalate) nanocomposites with tunable crystallinity, chain orientations and thermal transitions," *Journal of Materials Chemistry and Physics*, vol. 176, no. 8, pp. 58-67, 2016.

[118] S. Stankovich, D. A. Dikin, G. H. B. Dommett, K. M. Kohlhaas, E. J. Zimney, E. A. Stach, R. D. Piner, S. T. Nguyen, and R. S. Ruoff, "Graphene-based composite materials," *Journal of Nature*, vol. 442, no. 7100, pp. 282-286, 2006.

[119] Q. Guan, J. Cheng, B. Wang, W. Ni, G. Gu, X. Li, L. Huang, G. Yang, and F. Nie, "Needle-like Co_3O_4 Anchored on the Graphene with Enhanced Electrochemical Performance for Aqueous Supercapacitors," *ACS Applied Materials and Interfaces*,

vol. 6, no. 10, pp. 7626-7632, 2014.

[120] H. Zou, S. Wu, and J. Shen, "Polymer-Grpahene nanocomposites: preparation, characterization, properties, and applications," *Journal of Chemical reviews*, vol. 108, no. 9, pp. 3893-957, 2008.

[121] W. Wang, "Development of nanocomposites using graphene synthesized by solvent exfoliation method," University of Toledo, 2014.

[122] T. Kuilla, S. Bhadra, D. H. Yao, N. H. Kim, S. Bose, and J. H. Lee, "Recent advances in graphene based polymer composites," *Journal of Polymer Science*, vol. 35, no. 11, pp. 1350-1375, 2010.

[123] W. Cui, Q. Jiao, Y. Zhao, H. Li, H. Liu, and M. Zhou, "Preparation of poly(ethylene terephthalate)/layered double hydroxide nanocomposites by in-situ polymerization and their thermal property," *Express Polymer Letters*, vol. 6, no. 6, pp. 485-493, 2012.

[124] M. M. Gudarzi and F. Sharif, "Enhancement of dispersion and bonding of graphene-polymer through wet transfer of functionalized graphene oxide," *Express Polymer Letters*, vol. 6, no. 12, pp. 1017-1031, 2012.

[125] D. Verma, P. C. Gope, A. Shandilya, and A. Gupta, "Mechanical-Thermal-Electrical and Morphological Properties of Graphene Reinforced Polymer Composites: A Review," *Journal of Transactions of the Indian Institute of Metals*, vol. 67,no. 6, pp. 803-816, 2014.

[126] J. R. Potts, D. R. Dreyer, C. W. Bielawski, and R. S. Ruoff, "Graphene-based polymer nanocomposites," *Journal of Polymer*, vol. 52, no. 1, pp. 5-25, 2011.

[127] D. Galpaya, "Recent Advances in Fabrication and characterization of graphene-polymer nanocomposites," *Journal of Graphene*, vol. 1, no. 2, pp. 30-49, 2012.

[128] R. Atif and F. Inam, "Reasons and remedies for the agglomeration of multilayered graphene and carbon nanotubes in polymers," *Journal of Nanotechnology*, vol. 7, no. 1, pp. 1174-1196, 2016.

[129] G. Armstrong, "An introduction to polymer nanocomposites," *Journal of Physics*, vol.

36, no. 6, pp. 63001, 2015.

[130] L. Mészáros and J. Szakács, "Elastic recovery at graphene reinforced PA 6 nanocompostes," *Journal of Nanocon Conference*, pp. 51-55, 2014.

[131] S. M. Park and D. S. Kim, "Preparation and physical properties of polypropylene nanocomposites with dodecylated graphene nanoplatelets," *Journal of Composite Interfaces*, vol. 24, no. 4, pp. 335-345, 2017.

[132] D. Yang, A. Velamakanni, G. Bozoklu, S. Park, M. Stoller, R. D. Piner, S. Stankovich, I. Jung, D. A. Field, C. A. Ventrice, and R. S. Ruoff, "Chemical analysis of graphene oxide films after heat and chemical treatments by X-ray photoelectron and Micro-Raman spectroscopy," *Journal of Carbon*, vol. 47, no. 1, pp. 145-152, 2009.

[133] G. Smith, R. Chen, and S. Mapolie, "The synthesis and catalytic activity of a first-generation poly(propylene imine) pyridylimine palladium metallodendrimer," *Journal of Organometallic Chemistry*, vol. 673, no. 1, pp. 111-115, 2003.

[134] A. V. Cunha, A. S. Bondarenko, and T. L. C. Jansen, "Assessing spectral simulation protocols for the amide i band of proteins," *Journal of Chemical Theory and Computation*, vol. 12, no. 8, pp. 3982-3992, 2016.

[135] R. Goenka, P. Parthasarathy, N. K. Gupta, N. K. Biyahut, and S. Narayanan, "Kinetic analysis of biomass and comparison of its chemical compositions by thermogravimetry, wet and experimental furnace methods," *Jornal of Waste and Biomass Valorization*, vol. 6, no. 6, pp. 989-1002, 2015.

[136] A. A. McMath, J. Van Drunen, J. Kim, and G. Jerkiewicz, "Identification and analysis of electrochemical instrumentation limitations through the study of platinum surface oxide formation and reduction," *Journal of Analytical Chemistry*, vol. 88, no. 6, pp. 3136-3143, 2016.

[137] M. M. Ndipingwi, "Designing next generation high energy density lithium- ion battery with manganese orthosilicate-capped alumina nanofilm," University of the Western Cape, no. 12, 2015.

[138] H. Luo, C. Dong, K. Xiao, and X. Li, "The passive behaviour of ferritic stainless steel containing alloyed tin in acidic media," *RSC Advances*, vol. 6, no. 12, pp. 9940-9949, 2016.

[139] M. Conte, "Supercapacitors technical requirements for new applications," *Journal of Fuel Cells*, vol. 10, no. 5, pp. 806, 2011.

[140] E. Chappa, Sankararao, "Change in the affinity of ethylene glycol methacrylate phosphate monomer and its polymer anchored on a graphene oxide platform toward Uranium(VI) and Plutonium(IV) Ions," *Journal of Physical Chemistry B*, vol. 120, no. 11, pp. 2942-2950, 2016.

[141] S. Konwer, R. Boruah, and S. K. Dolui, "Studies on conducting polypyrrole/graphene oxide composites as supercapacitor electrode," *Journal of Electronic Materials*, vol. 40, no. 11, pp. 2248-2255, 2011.

[142] C. Zhu, J. Zhai, D. Wen, and S. Dong, "Graphene oxide/polypyrrole nanocomposites: one-step electrochemical doping, coating and synergistic effect for energy storage," *Journal of Materials Chemistry*, vol. 22, no. 13, pp. 6300-6306, 2012.

[143] A. Ganguly, S. Sharma, P. Papakonstantinou, and J. Hamilton, "Probing the thermal deoxygenation of graphene oxide using high resolution in situ X-Ray based spectroscopies," *Journal of Physical Chemistry*, pp. 17009-17019, 2011.

[144] W.-C. Oh and F.-J. Zhang, "Preparation and Characterization of Graphene Oxide Reduced From a Mild Chemical Method," *Journal of Chemistry*, vol. 23, no. 2, pp. 875, 2011.

[145] J. Wang, Y. Xu, J. Zhu, and P. Ren, "Electrochemical in situ polymerization of reduced graphene oxide/polypyrrole composite with high power density," *Journal of Power Sources*, vol. 208, pp. 138-143, 2012.

[146] N. Dywili, "Polyanilino-graphene oxide intercalated with platinum group metal nanocomposites, for application as novel supercapacitor materials nomxolisi dywili," University of The Western Cape, 2014.

[147] P. Si, H. Chen, P. Kannan, and D.-H. Kim, "Selective and sensitive determination of dopamine by composites of polypyrrole and graphene modified electrodes," *Journal of Analyst*, vol. 136, no. 24, pp. 5134-5138, 2011.

[148] S. Bose, N. H. Kim, T. Kuila, K. Lau, and J. H. Lee, "Electrochemical performance of a graphene-polypyrrole nanocomposite as a supercapacitor electrode," *Journal of Nanotechnology*, vol. 22, pp. 9, 2011.

[149] S. Sahoo, S. Dhibar, G. Hatui, P. Bhattacharya, and C. K. Das, "Graphene/polypyrrole nanofiber nanocomposite as electrode material for electrochemical supercapacitor," *Journal of Polymer*, vol. 54, no. 3, pp. 1033-1042, 2013.

[150] J. Xu, D. Wang, L. Fan, Y. Yuan, W. Wei, R. Liu, S. Gu, and W. Xu, "Fabric electrodes coated with polypyrrole nanorods for flexible supercapacitor application prepared via a reactive self-degraded template," *Journal of Organic Electronics*, vol. 26, pp. 292-299, 2015.

[151] J. Li, H. Xie, and Y. Li, "Fabrication of graphene oxide/polypyrrole nanowire composite for high performance supercapacitor electrodes," *Journal of Power Sources*, vol. 241, pp. 388-395, 2013.

[152] P. E. I. I. Ngqongwa, Lundi Vincent, Dr. Tesfaye T. Waryo and Prof. Priscilla G.L. Baker, "Potential application as dielectric materials in sulfonated-Polyaniline-based Supercapacitors," University of the Western Cape, 2010.

[153] S. Biswas and L. T. Drzal, "Multilayered nanoarchitecture of graphene nanosheets and polypyrrole nanowires for high performance supercapacitor electrodes," *Journal of Chemistry of Materials*, vol. 22, no. 20, pp. 5667-5671, 2010.

[154] S. Li, C. Zhao, K. Shu, C. Wang, Z. Guo, G. G. Wallace, and H. Liu, "Mechanically strong high performance layered polypyrrole nano fibre/graphene film for flexible solid state supercapacitor," *Journal of Carbon*, vol. 79, no. 1, pp. 554-562, 2014.

[155] M. Gholami, P. M. Nia, and Y. Alias, "Morphology and electrical properties of electrochemically synthesized pyrrole-formyl pyrrole copolymer," *Journal of Applied Surface Science*, vol. 357, pp. 806-813, 2015.

[156] R. Ramya, R. Sivasubramanian, and M. V. Sangaranarayanan, "Conducting polymers-based electrochemical supercapacitors-Progress and prospects," *Journal of Electrochimica Acta*, vol. 101, pp. 109-129, 2013.

[157] F. B. E. Frackowiak, "Carbon materials for the electrochemical storage of energy in capacitors," *Journal of Carbon*, vol. 39, pp. 937-950, 2001.

[158] P. A. Basnayaka, M. K. Ram, L. Stefanakos, and A. Kumar, "Graphene/Polypyrrole nanocomposite as electrochemical supercapacitor electrode: electrochemical impedance studies," *Journal of Graphene*, vol. 2, no. 2, pp. 81-87, 2013.

[159] V. P, Bolisetty, "Novel approach of using polyvinylidene fluoride langmuir-schaefer film on Graphene-Polyaniline nanocomposite for supercapacitor applications," University of South Florida, 2013.

[160] Y. Zou, Q. Wang, C. Xiang, Z. She, H. Chu, S. Qiu, F. Xu, S. Liu, C. Tang, and L. Sun, "One-pot synthesis of ternary polypyrrole-Prussian-blue-graphene-oxide hybrid composite as electrode material for high-performance supercapacitors," *Journal of Electrochimica Acta*, vol. 188, no. 1, pp. 126-134, 2016.

[161] X. M. Liu and X. G. Zhang, "NiO-based composite electrode with RuO2 for electrochemical capacitors," *Journal of Electrochimica Acta*, vol. 49, no. 2, pp. 229-232, 2004.

[162] K. C. Tsay, L. Zhang, and J. Zhang, "Effects of electrode layer composition/thickness and electrolyte concentration on both specific capacitance and energy density of supercapacitor," *Journal of Electrochimica Acta*, vol. 60, pp. 428-436, 2012.

[163] G. P. a Changzhou Yuan a, c, Longhai Zhang a, Linrui Hou a, Jingdong Lin b and A, "Green interfacial synthesis of two-dimensional poly(2, 5-dimethoxyaniline) nanosheets as a promising electrode for high performance electrochemical capacitors," *Journal of Royal Society of Chemistry*, vol. *4*, no. 47, pp. 24773-24776, 2014.

[164] P. E. I. I. Ngqongwa, Lundi Vincent, Dr. Tesfaye T. Waryo and Prof. Priscilla G.L. Baker, "potential application as dielectric materials in sulfonated-polyaniline- based supercapacitors," University of the Western Cape, 2010.

[165] G. Zhang, Y. Song, H. Zhang, J. Xu, H. Duan, and J. Liu, "Radially aligned porous carbon nanotube arrays on carbon fibers: A hierarchical 3D carbon nanostructure for high-performance capacitive energy storage," *Advanced Functional Materials*, vol. 26, no. 18, pp. 3012-3020, 2016.

[166] S. Lee, M. S. Cho, H. Lee, J.-D. Nam, and Y. Lee, "A facile synthetic route for well defined multilayer films of graphene and PEDOT via an electrochemical method," *Journal of Materials Chemistry*, vol. 22, no. 5, pp. 1899-1903, 2012.

[167] X. Li, H. Song, Y. Zhang, H. Wang, K. Du, H. Li, Y. Yuan, and J. Huang, "Enhanced electrochemical capacitance of graphene nanosheets coating with polyaniline for supercapacitors," *Journal of Electrochemical Science*, vol. 7, no. 6, pp. 5163-5171, 2012.

[168] F. Alvi, P. A. Basnayaka, M. K. Ram, H. Gomez, E. Stefanako, Y. Goswami, and A. Kumar, "Graphene-polythiophene nanocomposite as novel supercapacitor electrode material," *Journal of New Materials for Electrochemical Systems*, vol. 15, no. 2, pp. 89-95, 2011.